

✓ T
D-68
CHA

ANALYSIS OF PLATE BENDING BY FINITE ELEMENT
(DISPLACEMENT) METHOD

by

Subrata Chakrabarti

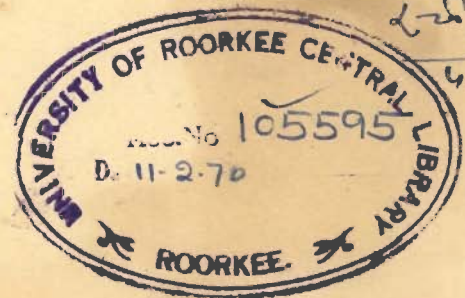
Thesis submitted in fulfilment of the requirements

for the degree of

DOCTOR OF PHILOSOPHY

in

CIVIL ENGINEERING



DEPARTMENT OF CIVIL ENGINEERING

UNIVERSITY OF ROORKEE

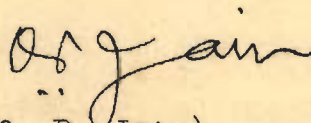
ROORKEE

1968

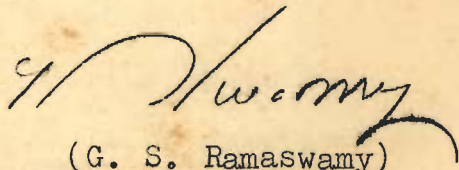
CERTIFICATE

Certified that the thesis entitled
"ANALYSIS OF PLATE BENDING BY FINITE ELEMENT
(DISPLACEMENT) METHOD" which is being submitted by
Mr. Subrata Chakrabarti in fulfilment of the
requirements for the award of the degree of Doctor
of Philosophy in Civil Engineering of the
University of Roorkee is a record of student's own
work carried out by him under our supervision and
guidance. The matter embodied in this thesis
has not been submitted for award of any other Degree.

This is to further certify that he has
worked for a period of two years and 8 months from
January 1966 to August 1968 for preparing this thesis.



(O. P. Jain)
Head, Department of
Civil Engineering,
University of Roorkee,
Roorkee, U.P.



(G. S. Ramaswamy)
Director, Structural
Engineering Research
Centre,
Roorkee, U.P.

Roorkee

Dated September 2, 1968

ACKNOWLEDGEMENTS

The author wishes to express his sincere gratitude to his thesis supervisors Professor O.P. Jain and Professor G.S. Ramaswamy for their encouragement and advice during the entire period of study.

The author is grateful to Professor G.S. Ramaswamy for providing the author with a Senior Research Fellowship at the Structural Engineering Research Centre, Roorkee, and all the facilities of research.

Thanks are due to the staff members of the Computer Centre of the Structural Engineering Research Centre for their assistance. The author is thankful to Mr. N.V. Raman, Head, Computer Centre for his kind co-operation. The author also wishes to thank Mr. R.K. Vaish for his help and suggestions in programming. The assistance of Mr. R. Narayanan in running the programs is gratefully acknowledged.

Sincere thanks are also due to the staff of the Drawing Office for their unfailing help in the preparation of the figures and drawings and in putting the thesis in its final form.

A special note of appreciation is due to all friends and colleagues for their interest, co-operation and encouragements.

The author thanks Mr. R.K. Sood for neatly typing the thesis.

ABSTRACT

ANALYSIS OF PLATE BENDING BY FINITE ELEMENT (DISPLACEMENT) METHOD

A study of bending of plates for small deformations by applying the finite element method is presented in this thesis.

This thesis is mainly concerned with the development of new displacement functions for rectangular and triangular elements. For rectangular elements, a method has been proposed for selecting displacement functions in which trigonometric expression that had apparently failed to give satisfactory results in earlier attempts, can be used along with polynomial terms. The method leads to conforming displacement functions which satisfy the convergence criteria. Not many suitable conforming functions have been reported so far. But, the method developed here for rectangular elements shows how many more new displacement functions can be found, all of them satisfying the convergence criteria. In fact, the number of such functions is almost unlimited.

A conforming displacement function has been suggested for triangular elements by using simple polynomial expressions. Continuity of normal slopes have been achieved by forcing them to vary linearly along the element boundaries. To accomplish this, additional correction functions have been used.

Several plate bending problems have been solved using an IBM 1620 Model I computer. Results are presented for four different displacement functions; three are for rectangular elements and one for triangular elements.

All the functions converge towards the true answers with successive refinements in the sub-division analysis. The convergence is monotonic in all cases.

CONTENTS

Notations

CHAPTER-1:	INTRODUCTION	1 - 7
1.1	Introduction	1
1.2	Brief description of the Finite Element Method	4
1.3	Scope	7
CHAPTER-2:	THE FINITE ELEMENT METHOD	8 - 41
	DISPLACEMENT APPROACH	
2.1	General remarks	8
2.2	Displacement approach	9
2.3	Convergence requirements	10
2.4	Conforming and non-conforming functions	11
2.5	Selecting a displacement function	13
2.6	Element stiffness matrix	22
2.7	Analysis of the assemblage	27
2.8	Finite element method as a special form of Rayleigh-Ritz method	38
CHAPTER-3:	NEW DISPLACEMENT FUNCTIONS	42- 68
3.1	Purpose	42
3.2	Rectangular elements	42
3.3	Triangular elements	54

CHAPTER-4:	EXAMPLES AND DISCUSSION ON RESULTS	69- 96
4.1	Introduction	69
4.2	Displacement functions tested	69
4.3	Examples worked out	71
4.4	Brief description of computer work on IBM 1620	75
4.5	Tables of results	79
4.6	Discussion on results	90
CHAPTER-5:	APPLICATION OF THE METHOD TO SHELL STRUCTURES	97-100
5.1	Introduction	97
5.2	Analysis by the finite element method	97
CHAPTER-6:	CONCLUSIONS	101-102
	REFERENCES	103-113
	APPENDIX-1	

Notations

The list below contains the important symbols used in this thesis. All these symbols are defined as they arise in the text.

a, b	dimensions of rectangular elements
D	$\frac{Eh^3}{12(1-\mu^2)}$, flexural rigidity of plate, element
E	modulus of elasticity, correction functions
F	nodal force vector of an element
h	thickness of plate, element
I	identity matrix
k	stiffness matrix of an element
K	stiffness matrix of an assemblage
L	plate dimension
M_x	moments in planes parallel to xoz plane
M_y	moments in planes parallel to yoz plane
P	concentrated load
q	uniformly distributed load
r	joint displacement vector of an assemblage
R	applied joint load vector of an assemblage
T	transformation matrix
u	nodal displacement vector of an element
w	deflection of plate, element normal to middle plane
w_x	$\partial w / \partial x$, slope in plate, element
w_y	$\partial w / \partial y$, slope in plate, element

w_n	$\partial w / \partial n$, slope in normal direction
w_t	$\partial w / \partial t$, slope in tangential direction
w_{xx}	$\partial^2 w / \partial y^2$, curvature in plate, element
w_{yy}	$\partial^2 w / \partial y^2$, curvature in plate, element
w_{xy}	$\partial^2 w / \partial x \partial y$, twist in plate, element
x, y, z	
$\bar{x}, \bar{y}, \bar{z}$	cartesian co-ordinate systems
x_0, y_0, z_0	
α	coefficient in displacement expressions
β_x, β_y	coefficients in M_x and M_y expressions
e	strain
μ	poisson's ratio
δ	increment
$[\]$	matrix
$\{ \}$	column matrix

CHAPTER ONE

INTRODUCTION

1.1 INTRODUCTION

Bending of a thin laterally loaded plate is governed by Lagrange's equation when deflections w are small compared to the plate thickness. This equation is (1)

$$\nabla^4 w = \frac{q(x,y)}{D} \quad (1.1)$$

where, $q(x,y)$ is the intensity of lateral loading and D is the flexural rigidity of the plate. The derivation of this equation is based on the assumptions that there is no straining of the middle plane of the plate, the plane section remains plane before and after bending and the normal stresses in the transverse direction can be ignored. Thus the mathematical analysis of a plate problem reduces itself to finding a solution of the above equation satisfying the prescribed boundary conditions.

It may be observed that this approach becomes difficult for a vast majority of practical situations, especially due to the complexities at the boundaries. Besides this, the method cannot be applied easily if, the domain contains arbitrary openings. These difficulties have led to the development of several approximate methods and they possess various degrees of accuracy depending on the nature of approximation introduced.

Three approaches based on variational principles have wide applications. Each one of them involves the selection of a suitable shape function for the bent plate in terms of unknown parameters, which need satisfy only the geometric boundary conditions. The function may be taken as

$$w = a_1 f_1(x) \cdot f_1(y) + a_2 f_2(x) \cdot f_2(y) + \dots + a_n f_n(x) \cdot f_n(y) \quad (1.2)$$

In the well known Rayleigh-Ritz method (2), these unknown parameters are determined by minimising the total potential energy of the system for each of the modes of deformations associated with them. Since the state of minimum potential is also the state of complete equilibrium, an exact solution is possible by taking infinite number of such parameters. The second approach is due to Galerkin (2). In this method, the unknown parameters are determined by minimising an error. This is done by equating the work done by the actual loads and the indirect loading from the equation (1.1), for each of the assumed shape functions, during a virtual displacement. The third is the method of Kantorovich (2). Here, a part of the shape function say $f(x)$, is selected by satisfying the boundary conditions in one direction. The parameters are then obtained by solving the equation (1.1) to satisfy the remaining boundary conditions.

The method of finite difference (2,3) is another powerful approximate approach in which, the

the governing differential equation is approximated by a system of linear simultaneous equations. These equations express the values of the function at certain selected points in the domain. The method has been applied to analyse several problems of plate bending, but it encounters difficulty in treating certain boundaries. In many situations, the convergence is neither fast nor satisfactory.

Several practical problems have been analysed by collocation methods. These can be formulated in two ways. One approach consists in selecting a function with unknown parameters, which satisfies only the governing differential equation. The unknown parameters are then obtained by satisfying the conditions at certain selected points on the boundary. In the other approach the function satisfies the boundary conditions and the parameters are determined to satisfy the differential equation at some selected points in the domain.

Hrennikoff's framework analogy (4,5) is an example of the discretisation technique for the analysis of the problems in elasticity. The method employs the concept of replacing the continuum by a discrete system having finite degrees of freedom. This idealised system is composed of analogous framework molecules which are three dimensional pin-connected structures. The bar areas of the mathematical model are determined from the condition of equal

deformability of the actual plate structure and the and the analogous model under the action of uniform stress. The stiffness matrix of the molecule is then determined by the principles of frame analysis.

The advent of high speed electronic digital computers and their availability at most centres of study have revolutionized the approach to structural analysis. As a consequence, the older methods have been reoriented to make them suitable for machine computation. In addition, new methods which are particularly suitable for computers are being developed. The wide use of matrix methods may be cited as an example.

In recent years, a new technique known as the Finite Element Method has successfully been applied to the solution of a large class of problems in elasticity. The origin of this method may be traced to the approach suggested by Hrennikoff employing the concept of replacing a continuum by a discrete system. In this study the method has been applied to the analysis of thin plates in bending within the framework of the limitations stated earlier.

1.2 BRIEF DESCRIPTION OF THE FINITE ELEMENT METHOD

The finite element method was originally developed in the aircraft industry. The earliest contribution was by Argyris (6,7,8). Clough (9,10) demonstrated the possibility of applying it to several problems of structural engineering.

The most attractive feature of the method is its extreme versatility and the potential it has for handling problems for which solutions are not now available. This is evident from the wide range of applications attempted since its inception. To-day, the method covers problems relating to two and three dimensional continuum (11,12). The problems may be structural (13,14,15) or non-structural, for example, seepage flow and heat conduction (39).

The basic philosophy of the finite element method consists in regarding the continuum as an assemblage of finite number of elements interconnected at a discrete number of points called nodes. Figure 1.1 shows a possible idealisation of a plate structure in bending. The behaviour of the actual structure is predicted from the analysis of this idealised system. The choice of elements to obtain the idealised system depends on the nature of the analysis to be performed. For example, in two dimensional plane stress problems two dimensional elements are the answer. The same elements again find use in problems of bending of plates and shells. Intuitively, it is possible to think in terms of three dimensional elements, such as tetrahedrons, while treating the problems of solids. Once the idealised system is finalised, the analysis of the continuum reduces to a series of standard matrix operations as in one dimensional systems such as frames.

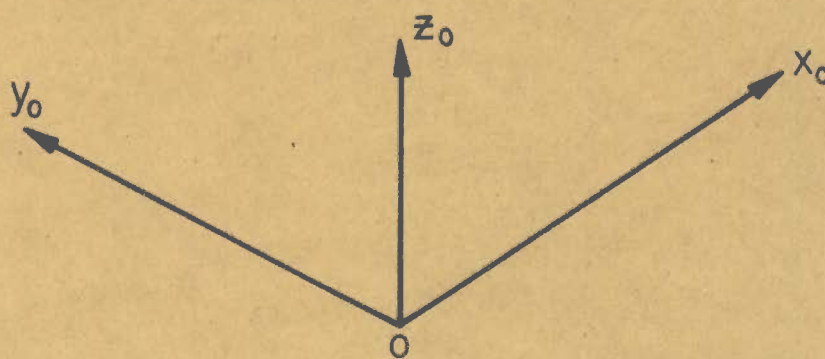
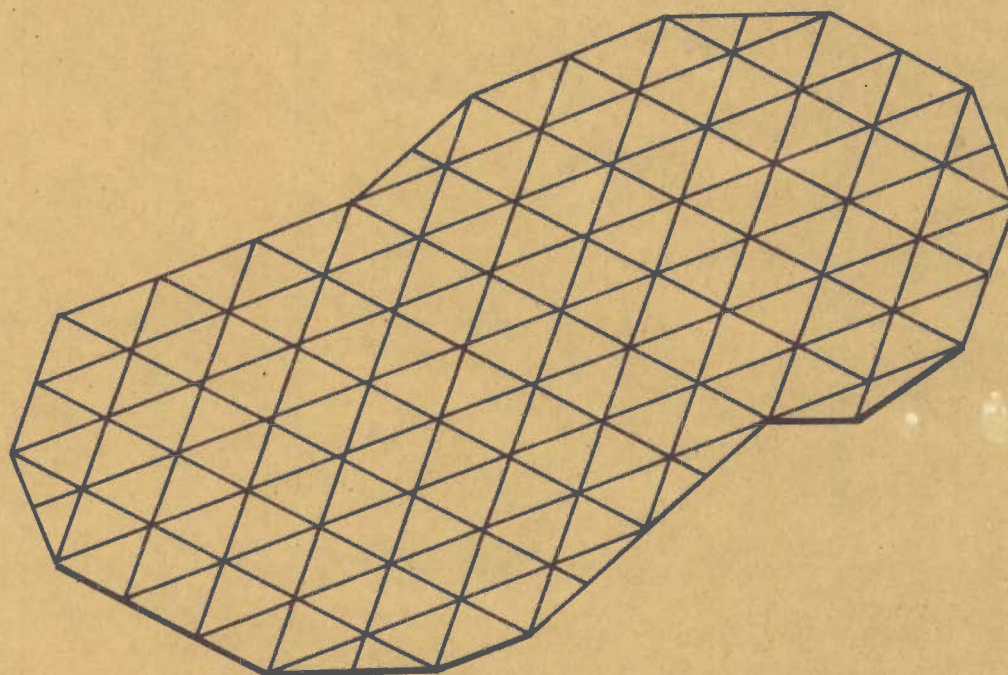


FIG. 1.1 AN IDEALISED PLATE STRUCTURE

The formulation of the method can be based on two distinct approaches. They are the well known force and displacement methods. Depending on the type of approach, the nodal force - displacement relationships can be expressed as, either element flexibility or stiffness matrices. In this dissertation the formulation is based on the displacement approach. The corresponding element property is, therefore, its stiffness matrix.

The analytical procedure involved in the finite element method can be explained very conveniently through the following steps:

- (i) Visualisation of the continuum as an assemblage of finite number of elements interconnected at suitable nodes, Figure 1.1. For plate bending problems, the elements are flat plate elements. They are the actual representation of the area they cover in the continuum, retaining all the associated properties.
- (ii) Evaluation of element stiffness matrix, $[k]$. This requires the knowledge of stress - strain relations.
- (iii) Appropriate summation of the individual element stiffness, applying proper co-ordinate transformations, if necessary, to generate the overall stiffness matrix $[K]$, of the entire assemblage. This involves the consideration of equilibrium of forces and continuity of displacements at all nodes.

- (iv) Computation of nodal displacements, r , due to applied forces, R , from

$$\{r\} = [K]^{-1} \{R\} \quad (1.3)$$

after incorporating the boundary conditions.

- (v) Determination of element forces due to the nodal deformations, from their individual analysis.

1.3 SCOPE

The scope of this dissertation is limited to the analytical study of the bending of plates using the finite element method. The aim is to explore the possibilities of new displacement functions and study their behaviour and usefulness in solving plate bending problems.

Various functions have been proposed (22), from time to time, to determine the element stiffness matrices. Their performance has been studied by comparison with the available results obtained by other methods. Some of them converge while others diverge; the convergence being either monotonic or oscillating (39).

The type of functions proposed in this dissertation is different from those already investigated. The behaviour of these functions have been studied with an open mind to assess their usefulness in the analysis of bending of plates. This has been accomplished by comparing the results of the analysis of some selected plate bending problems for which either exact or acceptable approximate results are available. The functions reported in this thesis show monotonic convergence.

CHAPTER TWO

THE FINITE ELEMENT METHOD

DISPLACEMENT APPROACH

2.1 GENERAL REMARKS

From the description of the finite element method, it is clear that the most vital part in the entire analysis is the derivation of the element stiffness matrices. They decide the stiffness of the entire assemblage and consequently the quality of the final results. This part, therefore, needs utmost skill and care.

A direct formulation of these matrices, using the method adopted for one dimensional elements, for example beams, (16,17) is almost impracticable. Nevertheless, an alternative method can be devised which is approximate, but simple and elegant. The approach consists in assigning a suitable strain distribution over the element and deriving the corresponding stiffness relations from the principle of virtual work (18). This approach known as displacement method, has been adopted in this dissertation.

The alternative formulation that results in element flexibility relations is called the force method. Here, the selection is of a suitable stress field (18). This approach has been successfully applied to the plane stress problems (19,20).

On the other hand, the study of plate bending problems by the finite element method is almost restricted to the use of the displacement approach. This is because of the difficulty in selecting a suitable stress field for the plate elements in bending.

2.2 DISPLACEMENT APPROACH

The strain in a plate in bending is completely defined by its deflection normal to the middle plane. Therefore, the approach here reduces itself to the selection of a suitable displacement function for the element which can be a rectangle, triangle or any other polygon. It is obvious that at a node where several elements of the assemblage meet, continuity of displacements should exist. If at such nodes only the deflections are matched, the structure will develop kinks. To avoid this, the associated slopes must also be made continuous. For this purpose slopes along any two perpendicular directions, for example w_x and w_y are considered. Thus at any node, continuity of these three quantities has to be established. The number of equilibrium conditions thereby becomes three.

The overall state of deformation of an element can be uniquely defined by selecting its displacement pattern in terms of its nodal displacements. If this is done, an element will have three degrees of freedom at each node. Hence, the total degrees of freedom of the element become three times the number

of its nodes. A rectangular or quadrilateral element will have twelve and a triangle nine degrees of freedom, if their corners are selected as nodes. Thus, the infinite degrees of freedom of a continuum is reduced to a finite number in the finite element method. Therefore, it is reasonable to expect that by increasing the number of elements convergence should result.

In general, convergence to the exact results will never be possible, because the idealised system, Figure 1.1, can never have infinite degrees of freedom. Mathematically speaking, this happens only in the limit, when the element dimensions become microscopic. In all practical problems, reasonable accuracy is sufficient. This can be achieved, provided the results tend to converge. Any displacement function, selected at random, may not lead to convergence. For this purpose they must satisfy certain requirements (21,39).

2.3 CONVERGENCE REQUIREMENTS

In order to achieve convergence, the selected displacement function must be able to represent

- i) all rigid body motions of the element without self straining, and
- ii) the state of constant strain.

The first criterion follows from the reasoning that the elements should be able to accommodate all possible states of deformations while representing the

continuum. Strain in an element develops from the relative displacements at its nodes. The elements of continuum, in general, will travel some distance as rigid bodies before developing strains. These movements do not induce any strain in the elements. For plate bending, three types of such movements are possible - one translation and two rotations about two perpendicular axes. As the strains here are the three curvatures, the requirement means that the displacement function should reduce to a first degree expression in the co-ordinates when the nodal displacements conform to the rigid body movements.

The second condition is essential for convergence. With successive subdivision, the strain, in the limit, will tend to become constant in the elements. If the elements are incapable of representing this state, convergence will not be possible, no matter how fine the subdivision is. The selected displacement function must be tested to make sure that it does satisfy this criterion. In mathematical terms, this means that the displacement function for a plate element in bending should reduce to a general quadratic expression, when the nodal displacements conform to the condition of constant strain. This implies that if for any reason, this condition is violated, the solution will diverge (22).

2.4 CONFORMING AND NON-CONFORMING FUNCTIONS

The displacements at a node in the assemblage

are unique because continuity is established at these points. This nodal continuity may not lead to their continuity all along a boundary where two elements meet. Generally, it is observed that the continuity of the slope in the direction normal to such a boundary is violated. However, the deflection and its associated slope in the vertical plane containing the element boundary remain continuous. A displacement function of this type is called a non-conforming function. The use of such functions results in the idealised structure becoming too stiff or too flexible. In principle, there is no objection to their use as long as they satisfy the two requirements for convergence already stated. Several authors have used such functions successfully (39). The strain energy in such a case is contributed by the elements individually due to the absence of complete interaction between the elements along their boundaries. Results oscillate above and below the exact answer depending on whether the resulting assemblage is too stiff or too flexible at the various stages of the analysis.

Convergence is possible even if complete continuity is not ensured. But monotonic convergence demands complete continuity. If the displacement function assumed results in complete continuity the structure will consistently be overstiff. That is, its strain energy will always be below the minimum. With successive subdivision the structure will progressively become less and less stiff and approach

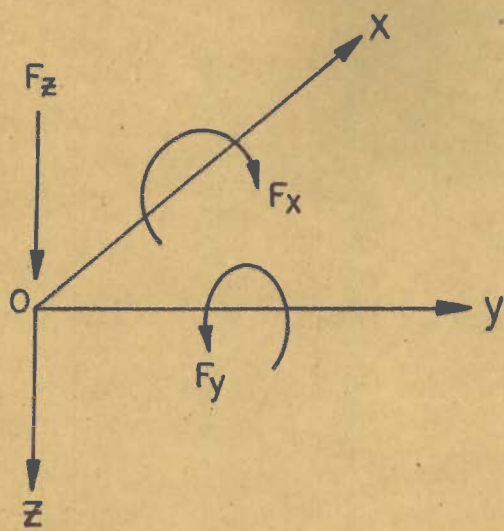
the actual stiffness, while at the same time strain energy will approach the true level as a lower bound.

2.5 SELECTING A DISPLACEMENT FUNCTION

The choice of functions to represent the element deformation is unlimited. In principle, any function that satisfies the above requirements is acceptable. As already stated, the method allows the use of any shape of elements such as rectangle, triangle or any other polygon. For rectangular boundaries elements of the same shape become the automatic choice. Other shapes, for example, triangle or quadrilateral, can be employed to approximate a curved boundary. Parallelogram elements have been used for skew plates.

The first step in selecting a displacement function is to decide on the position of the nodes of the element. For this purpose the corners of an element boundary are suitable. Thus, the shape of an element itself decides the number and positions of its nodes. The selection of the displacement function can be made in several different ways once the nodes are located.

In the simplest approach, the displacement pattern of an element is considered as a combination of several independent modes of deformations of unknown amplitudes. According to this, the function for a rectangular element of Figure 2.1 can be expressed by simple polynomial as



NODAL FORCES

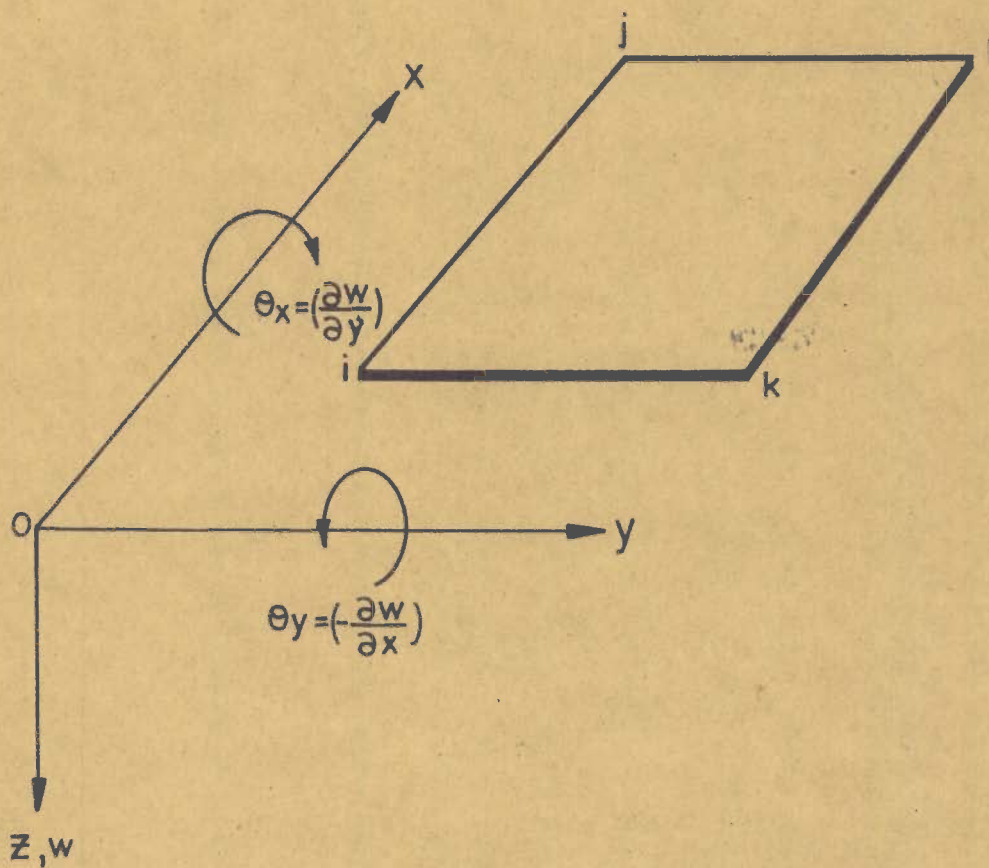


FIG. 2.1 A RECTANGULAR ELEMENT

$$w = A_1 + A_2x + A_3y + A_4x^2 + A_5xy + A_6y^2 + A_7x^3 + A_8y^3 + A_9x^2y + A_{10}xy^2 + A_{11}x^3y + A_{12}xy^3 \quad (2.1)$$

This function has been used by Clough (22) and Zienkiewicz (23). The number of independent modes have been kept equal to the number of total degrees of freedom of the element. Thus the amplitude coefficients are uniquely determined in terms of the nodal displacements of the element. It is observed that the function reduces to a cubic expression along lines $x = \text{constant}$ and $y = \text{constant}$. This is an advantage because a cubic function is completely defined by four constants. These four constants are uniquely defined in terms of deflection and the slope in the same vertical plane at the two nodes joining a boundary. Therefore, the equality of the nodal displacements leads to identical expressions for the deflections along the common boundaries for the elements lying on either side. Thus in the entire assemblage, along all the boundaries where two elements meet, the deflections and slopes in the corresponding vertical planes are continuous. Along these boundaries there is one more slope in the normal directions. Here the expressions for these normal slopes are also cubic. This leads to the discontinuity of the normal slopes along the common faces of the elements because they are equal only at two points on a boundary. Thus this particular displacement function

is of the non - conforming type. It is one of the few such functions which have proved to be extremely suitable for a large class of problems. This very function after suitable transformation into skew co-ordinates has been used by West (24) and Ramstad (25,26) for parallelogram elements. For the same rectangular elements, Melosh (27,28) has suggested two different function in two different ways. The deflection function becomes a cubic expression in both the cases along the element boundaries. The continuity of normal slope is again violated.

The displacement function for parallelogram and rectangular elements can also be obtained in a different manner. This is done by assuming that the complete deformation of an element consists of a set of rigid body motions and those producing uniform strains. As already stated, three types of rigid body motions are possible in plate bending. Therefore, the method proceeds by forming mathematical expressions for each of these motions and those resulting in uniform strains and, finally adding up these expressions to obtain the total displacement function. This approach is due to Argyris (29). Here also the normal slopes are discontinuous along the common boundaries. Results of several examples demonstrate the inherent merit of the technique.

A conforming function for a rectangular element may be selected in a very simple and elegant

manner as follows. The first step here is to clamp all the nodes excepting one. Then at this node, unit deflection w and unit slopes w_x and w_y are applied one at a time, Figure 2.2. For each of these nodal displacements the corresponding mathematical expressions for the deformed shape of the plate element is now written. This process is repeated in turn at all the nodes. The complete displacement function is then obtained by combining all these expressions. As an example, the expression for unit deflection at the node 1 of a rectangular element is shown in Figure 2.3. This method was attempted by Papenfuss (30), but the selected function has not led to satisfactory results because of its inability to represent uniform twist. The successful use of this method is due to Butlin (31,32) and Hansteen (33). Both of them proposed the same function independently. Continuity of twist w_{xy} has been considered additionally, to overcome the deficiency in the approach of the earlier investigator. The other conforming function for rectangular elements is due to Schmit et al (34). The function has been derived by using the Hermitian interpolation formulae. Here also, the continuity of w_{xy} has been considered in addition to w , w_x and w_y .

The displacement function for a triangular element can also be taken as a simple polynomial expression. A triangle has nine degrees of freedom and the complete cubic expression contains ten terms

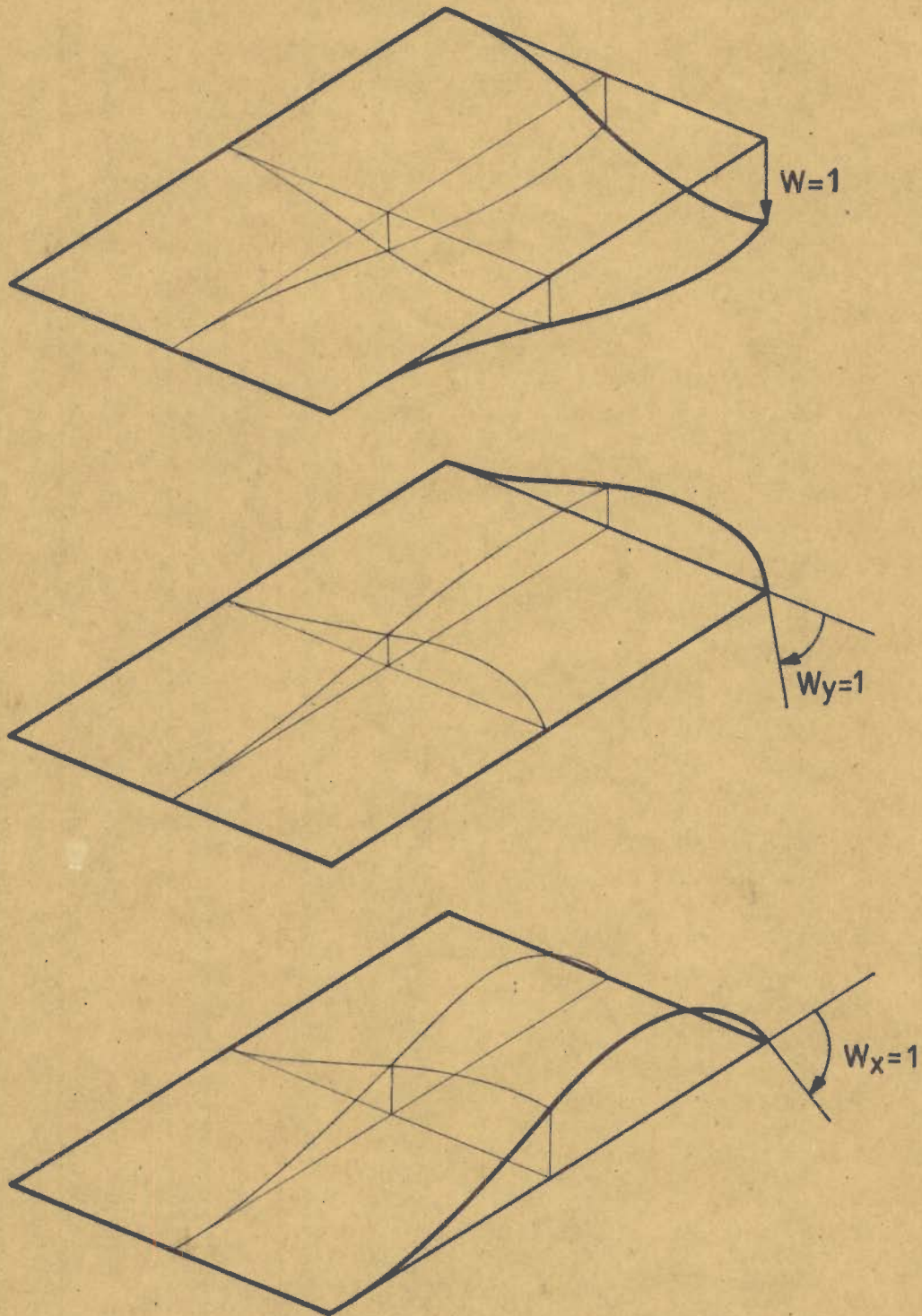


FIG. 2.2 APPLICATION OF UNIT NODAL DISPLACEMENTS.

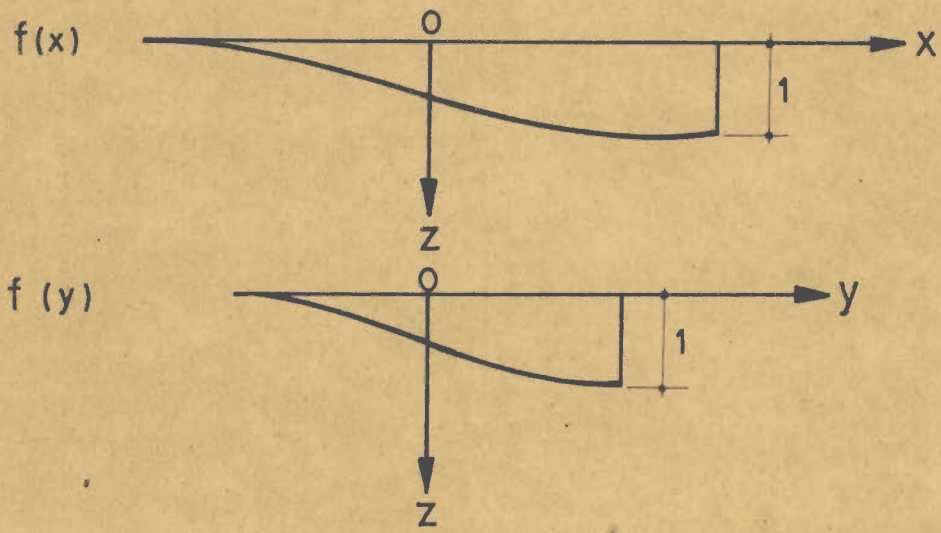
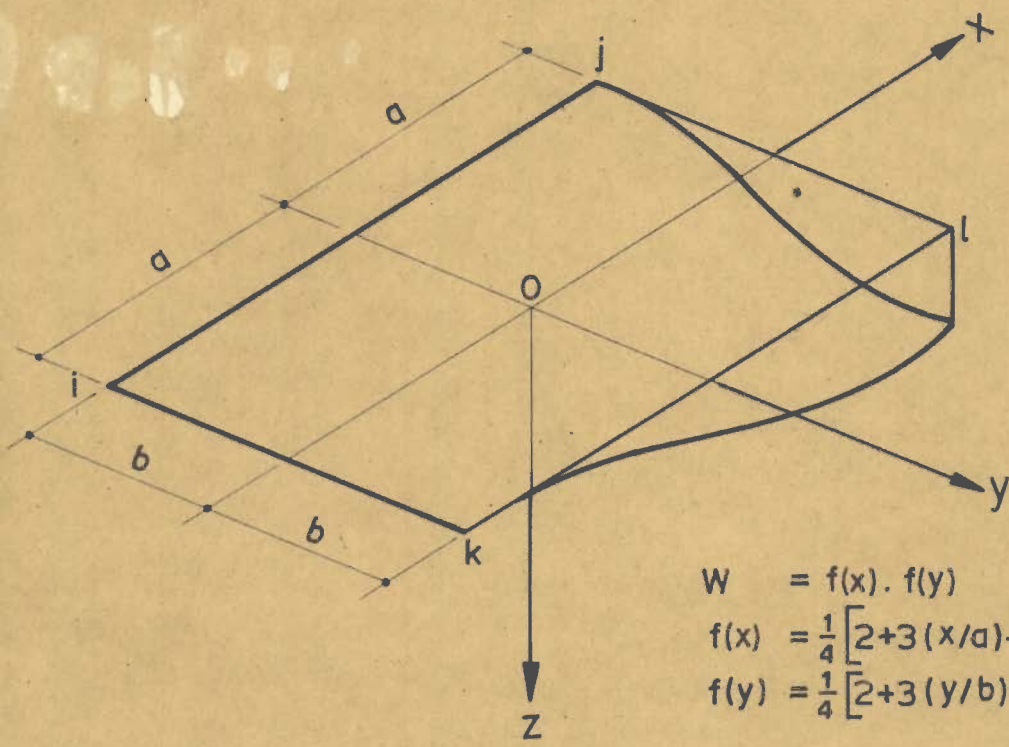


FIG. 2.3 EXPRESSION FOR UNIT DEFLECTION AT A NODE.

(Eq. 2.1). Clearly, it is necessary to drop one of them. This can be done in several ways. But none of the resulting functions is reported to have led to satisfactory results (22). Adini (35) excluded the uniform twist term xy from the complete cubic expression (Eq. 2.1); hence his solution does not converge. Tocher (36) tried two different functions, one by combining the higher twist terms x^2y and xy^2 and next, the complete cubic expression. In both these methods total ten terms are involved but the functions do not provide satisfactory convergence (22). Moreover, the second function leads to a singular characteristic for certain orientation of the sides of the triangle, for example, when two sides are parallel to x and y co-ordinate axes (39). Nevertheless, these pioneering contributions have helped later investigators in their search for better displacement functions.

The successful use of the polynomial function for triangular elements has been achieved by Clough et al (22) through a very elegant approach which has the merit that it leads to complete continuity of the displacements. The triangle is first divided into three sub-elements by joining the three corners and its centre of gravity, Figure 2.4. Then for each of these sub-elements an independent cubic displacement function of nine terms is selected with reference to their independent local co-ordinate systems $(\bar{x}, \bar{y}, \bar{z})$.

Z AXIS UPWARD

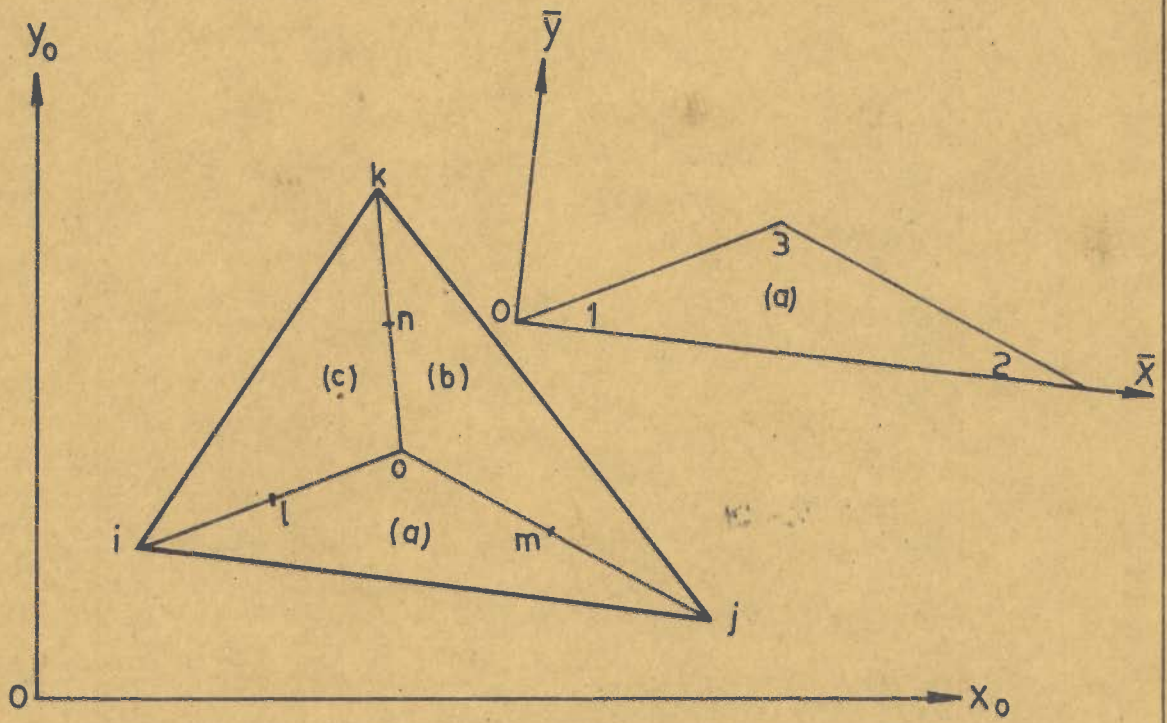


FIG. 2.4 DIVISION INTO SUB-ELEMENTS

These functions are such that they provide a linear variation of normal slopes along the exterior boundaries of the sub-elements. The normal slope varies parabolically along the interior boundaries because of selecting a cubic displacement function. In all, twenty seven constants are involved and these are determined from the solution of an equal number of simultaneous equations. Nine of these equations express the nodal displacements of the original undivided triangle, fifteen the continuity of displacements at the nodes i , j , k and o , and the remaining three are obtained by equating the normal slopes at the mid-points l , m and n for the corresponding elements. These last three conditions lead to conforming behaviour. This is possible because the normal slopes have parabolic variations along these internal boundaries and a parabola is uniquely defined through three points.

A significant contribution in the methods of selecting a displacement function for a triangular element is due to Zienkiewicz et al (37). This has been achieved by using the area co-ordinates which was independently suggested earlier by Irons (38). The method leads to a cubic displacement function which is of the non-conforming type. A recent publication by Zienkiewicz (39) provides information on this technique. This displacement function can be transformed into a conforming function by using additional correction functions as suggested by

Beseley et al (40). The use of correction function leads to the linear variation of normal slopes along the boundaries of the element. This displacement function has given excellent results when applied to several problems.

The task of selecting a displacement function for an arbitrary quadrilateral element is extremely difficult. Though an arbitrary quadrilateral has the same number of nodes as a rectangle, the polynomial function selected for the rectangular element (Eq. 2.1) is not suitable here. Excepting the lines $x = \text{constant}$ and $y = \text{constant}$ the displacement function of equation (2.1), reduces to a fourth degree expression. For a unique definition of such an expression five conditions are necessary. Thus the deflection and the slope in the corresponding vertical plane can remain continuous along a common boundary provided five conditions are available on these boundaries. This is not available here and, therefore, for a quadrilateral, the use of equation (2.1) leads to complete discontinuity of all the displacements along the common boundaries in the assemblage. The simplest approach seems to be to divide a quadrilateral into two or four arbitrary triangles and obtain the stiffness matrix using suitable functions for these sub-elements. Sander and Veubeke (39) have suggested a method using three separate displacement functions with a total of sixteen constants. The continuity of normal slopes has been achieved by selecting four mid-point

nodes at the boundaries. At these nodes, the normal slopes have been taken as extra degrees of freedom. Thus the approach involves the use of two types of nodes, the corners, where all the three displacements are specified and the mid-point nodes for the normal slopes. The interested reader may obtain the details from the original publications (41,42).

So far only the use of polynomial expressions has been discussed. For plate bending analysis one basic reason for adopting these functions, in addition to their simplicity, is the ease with which they may be made to satisfy the convergence requirements. In principle, any other function such as trigonometric expressions can also be used. But unfortunately the experience with these functions so far has not been rewarding and very few investigators have reported the use of such functions. Butlin (32) observed that the displacement function of this type for a rectangular element failed to represent the rigid body motions without self-straining. The results became poor with successive sub-divisions and ultimately diverged. Henshell et al (43) report a similar experience for rectangular elements. They felt that "the reason for this divergence is that with trigonometric shape functions, unlike polynomial types, the deflected form of one large finite element cannot be represented with a large number of small finite elements". A careful study shows that the reason given cannot account for the unsatisfactory performance of trigonometric

type of functions. In fact the selected displacement function does not satisfy the requirements of convergence and this is really responsible for the reported behaviour.

The main difficulty which precludes the use of such functions for representing element displacements lies in satisfying the convergence requirements. This thesis has mainly been concerned with the search for new displacement functions. After several initial failures, the author has at last developed a means of employing functions hitherto considered unsuitable. The number of suitable functions is rather limited. But the method developed in this thesis for rectangular elements enables many new displacement functions to be used successfully. The technique employed is set out in detail in the next chapter.

Another problem studied in this dissertation is the triangular element using the polynomial displacement function. Such a function has been successfully employed only by Clough (22). The technique adopted in this study is a variation of the method used by Clough. The triangle is first divided into three sub-elements by joining the three corners and its centre of gravity. For each one of these sub-elements a conforming type of displacement function has been derived using additional correction functions which are also simple polynomial expressions. The method differs in two ways when compared with Clough's approach. First additional

correction functions have been used. Secondly, the normal slopes vary linearly instead of parabolically along the inner boundaries of the sub-elements. The approach is presented in detail in the next chapter.

2.6 ELEMENT STIFFNESS MATRIX

The stiffness matrix of an element is derived from the principle of virtual displacements using the selected displacement function. A typical rectangular element with its co-ordinate system is shown in Figure 2.1. Here the entire process of obtaining the stiffness matrix for this element is illustrated with the help of few steps which are applicable to all other shapes.

(i) Let the element displacement field be

$$w = \sum_i^n a_i M_i (x,y) \quad (2.2)$$

where $M_i (x,y)$ are the assumed modes of deformations with unknown amplitudes a_i .

In matrix notation this is written as (omitting the brackets).

$$w = Ma \quad (2.3)$$

where, M and a , are row and column matrices respectively.

The number of constants a , are taken equal to the total degrees of freedom of an element as stated earlier. Thus, a rectangular element involves the

use of twelve of them. At a node, displacements consist of the deflection and two slopes. The displacement vector u_i at the node i of the element is

$$u_i = \begin{Bmatrix} \theta_x \\ \theta_y \\ w \end{Bmatrix}_i = \begin{Bmatrix} \partial w / \partial y \\ -\partial w / \partial x \\ w \end{Bmatrix}_i \quad (2.4)$$

The complete displacement vector u of the element is given by the displacements of all the nodes. Therefore,

$$u = \begin{Bmatrix} u_i \\ u_j \\ u_k \\ u_l \end{Bmatrix} \quad (2.5)$$

(ii) The constants a are evaluated by writing the equations of nodal displacements and solving them simultaneously. Let these equations be

$$u = Ca \quad (2.6)$$

The matrix C involves the co-ordinates of the nodes.

By inversion,

$$a = C^{-1}u \quad (2.7)$$

(iii) Strains e at a point in the plate element are given by the curvatures when the deformations are small (1). These are w_{xx} , w_{yy} and w_{xy} . Therefore,

$$e = \begin{Bmatrix} -w_{xx} \\ -w_{yy} \\ +w_{xy} \end{Bmatrix} \quad (2.8)$$

These are obtained by appropriate partial differentiations of equation (2.2). This leads to

$$e = Ba \quad (2.9)$$

The elements of B matrix are in terms of x and y.

Using relations (2.7),

$$e = BC^{-1}u \quad (2.10)$$

(iv) Stress resultants σ , i.e., the moments are given by the relations (1)

$$\begin{aligned} M_x &= -D (w_{xx} + \mu w_{yy}) \\ M_y &= -D (\mu w_{xx} + w_{yy}) \\ M_{xy} &= D (1-\mu) w_{xy} \end{aligned} \quad (2.11)$$

where,

$$D = \frac{Eh^3}{12(1-\mu^2)}$$

Hence,

$$\sigma = \begin{Bmatrix} M_x \\ M_y \\ M_{xy} \end{Bmatrix} = D \begin{bmatrix} 1 & \mu & 0 \\ \mu & 1 & 0 \\ 0 & 0 & (1-\mu) \end{bmatrix} \begin{Bmatrix} -w_{xx} \\ -w_{yy} \\ w_{xy} \end{Bmatrix} \quad (2.12)$$

$$\text{or, } \sigma = \bar{D} e \quad (2.13)$$

From equation (2.10)

$$\sigma = \bar{D}BC^{-1}u \quad (2.14)$$

(v) Strain energy in the volume dv of the element is

$$dU = e^T \sigma dv \quad (2.15)$$

where, e^T is the transpose of e .

Since there are two twisting couples, and their contributions in the energy are equal, the matrix \bar{D} of the equation (2.12) is modified to

$$\bar{D} = \begin{bmatrix} 1 & \mu & 0 \\ \mu & 1 & 0 \\ 0 & 0 & 2(1-\mu) \end{bmatrix} \quad (2.16)$$

The internal work done in the volume dv of the element during a virtual displacement is the product of the actual stresses $\bar{\sigma}$ and the strains \bar{e} due to such displacement. Therefore,

$$dW_i = \bar{e}^T \bar{\sigma} dv \quad (2.17)$$

Using equation (2.10)

$$\bar{e} = BC^{-1} \int u \quad (2.18)$$

where, $\int u$ denotes the virtual nodal displacements.

These virtual displacements can be selected as unit nodal displacements. If only one is applied at a time, keeping all the remaining displacements equal to zero, $\int u$ can be taken as a unit matrix, I .

Then,

$$\bar{e} = BC^{-1} \int u = BC^{-1} I = BC^{-1} \quad (2.19)$$

Therefore, the total virtual work done by the internal stresses become

$$W_i = \int \left[(BC^{-1})^T \bar{D} BC^{-1} u \right] dv \quad (2.20)$$

$$\text{or, } W_i = (C^{-1})^T \left[\int_{\text{vol}} B^T \bar{D} B dv \right] C^{-1} u \quad (2.21)$$

Only B matrix involves x and y and therefore, it is kept inside the brackets.

(vi) Work done by the nodal forces are now calculated for the same virtual displacements. At a node three forces are present.

They are, one vertical force F_z and two couples F_x and F_y . The vector for the node i is

$$F_i = \begin{Bmatrix} F_{xi} \\ F_{yi} \\ F_{zi} \end{Bmatrix} \quad (2.22)$$

and, for the element it is

$$F = \begin{Bmatrix} F_i \\ F_j \\ F_k \\ F_l \end{Bmatrix} \quad (2.23)$$

The total virtual work done by the nodal forces is

$$W_e = (\delta u)^T F = \delta F = F \quad (2.24)$$

Equating $W_e = W_i$

$$F = (C^{-1})^T \int_{vol} [(B^T DB) dv] C^{-1} u \quad (2.25)$$

This equation represents the relations between the nodal forces and displacements. Thus, these are the required stiffness relations which may be written as

$$\{F\} = [k] \{u\} \quad (2.26)$$

Here,

$$k = (C^{-1})^T \int_{\text{vol}} \left[(B^T \bar{D} B) dv \right] (C^{-1}) \quad (2.27)$$

and, it is the stiffness matrix of the element.

2.7 ANALYSIS OF THE ASSEMBLAGE

Analysis of the idealised system requires the formulation of the stiffness matrix $[K]$ of the entire assemblage to start with. It states the relations between the forces and the displacements at the nodes of the entire structure. The next phase consists in calculating the deformations at these nodes due to the applied loading. Once the nodal deflections become known the deformations of the individual elements are easily obtained. The corresponding internal forces developing in the elements are finally determined from their individual analysis.

(a) Stiffness of the assemblage

The stiffness matrix $[K]$, of the entire assemblage is obtained by summing up the individual element stiffness matrices in a suitable manner. This summing up actually involves the setting up of the equations of equilibrium at all the nodes of the structure. For this purpose, one important point has to be recognised. A node of the structure connects the elements around it. Thus, these connected elements have identical displacements at such points. Generally, the individual element stiffness matrices are expressed

in terms of their independent local co-ordinate systems. These co-ordinates may differ amongst themselves and at the same time from the co-ordinate system of the entire structure which may be designated as global co-ordinates. The stiffness matrix $[K]$ is formulated with respect to this global system. Hence, appropriate co-ordinate transformations become necessary to write the equations of equilibrium.

The steps involved in deriving the stiffness matrix are best illustrated by means of an example. Here, an assembly of four elements as shown in Figure 2.5, is considered. In this particular example, the local co-ordinates of the elements are parallel to the global system. Therefore, the necessity of co-ordinate transformations does not arise. However, this particular aspect is discussed at a later stage.

The stiffness matrices of the individual elements of the assemblage are

$$\left\{ F^{(x)} \right\} = \left[k^{(x)} \right] \left\{ u^{(x)} \right\} \quad (2.28)$$

$x = 1, 2, 3 \dots$

This matrix can be expanded as

$$\begin{pmatrix} F_i \\ F_j \\ F_k \\ F_l \end{pmatrix}^{(x)} = \begin{bmatrix} k_{ii} & k_{ij} & k_{ik} & k_{il} \\ k_{ji} & k_{jj} & k_{jk} & k_{jl} \\ k_{ki} & k_{kj} & k_{kk} & k_{kl} \\ k_{li} & k_{lj} & k_{lk} & k_{ll} \end{bmatrix} \begin{pmatrix} u_i \\ u_j \\ u_k \\ u_l \end{pmatrix}^{(x)} \quad (2.29)$$

$$x = 1, 2, 3 \dots$$

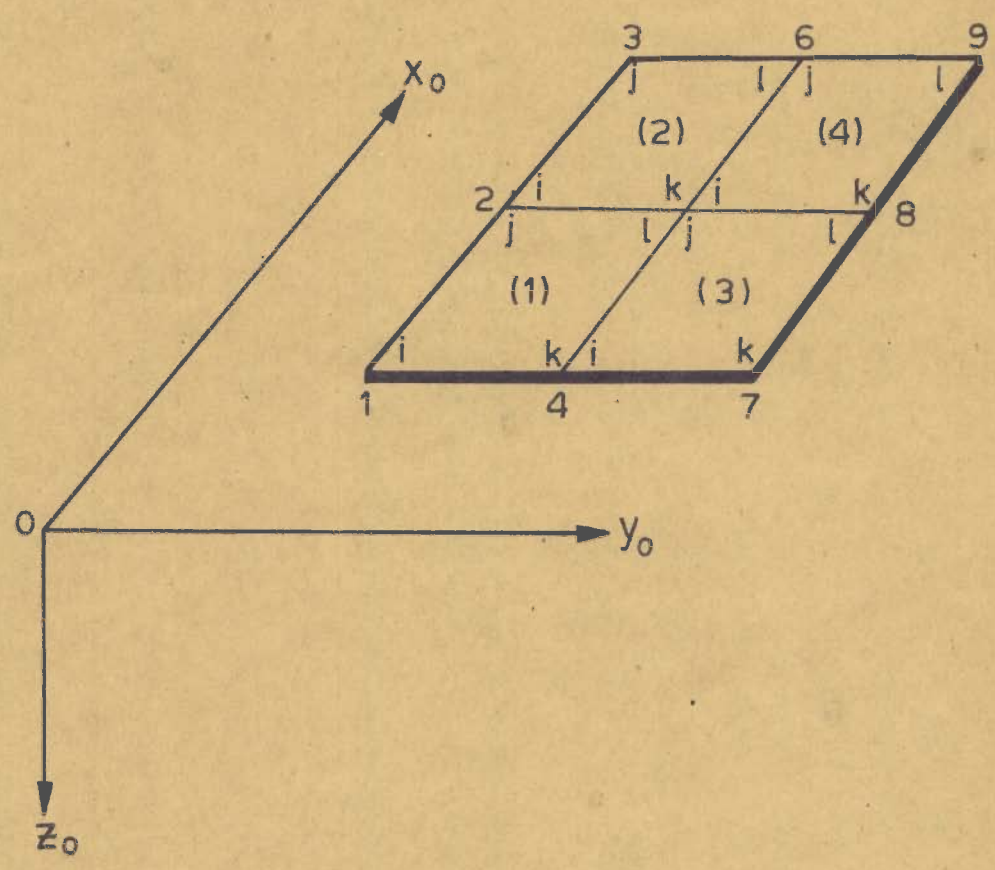
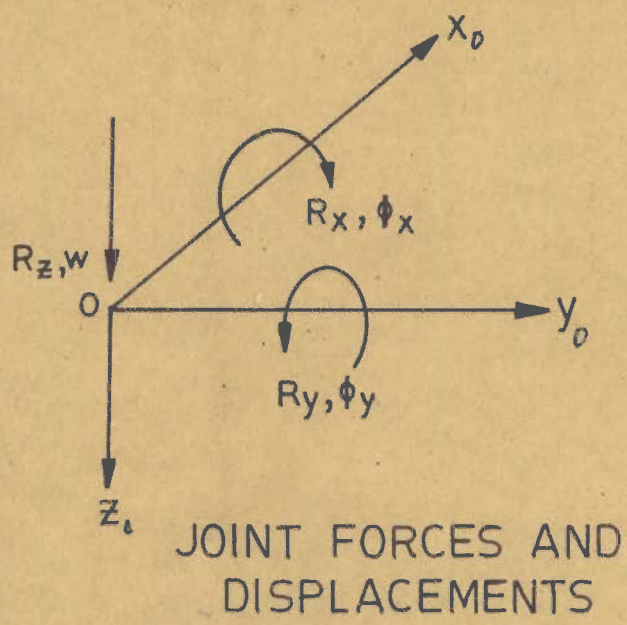


FIG. 2.5 AN ASSEMBLAGE OF RECTANGULAR
ELEMENTS

F_i, F_j, \dots and u_i, u_j, \dots are the corner forces and displacements of any element as already explained in section 2.6. k_{ij} are the 3×3 sub-matrices of the element stiffness matrix.

For equilibrium at a node of the structure, the applied forces at this point must be equal and opposite to the internal forces developed at that point within the connected elements. The general form of the equations of equilibrium at a node i is

$$R_i = \sum k_{ij}^{(x)}, \quad x = 1, 2, 3, \dots \quad (2.30)$$

Here, R represents the applied forces at any node i of the assemblage, which is

$$R_i = \begin{Bmatrix} R_x \\ R_y \\ R_z \end{Bmatrix} \quad (2.31)$$

i

For the particular problem selected here, the equations of equilibrium are

$$\begin{aligned} R_1 &= F_i^{(1)} \\ R_2 &= F_j^{(1)} + F_i^{(2)} \\ R_3 &= F_j^{(2)} \\ &\cdot \\ &\cdot \\ &\cdot \end{aligned} \quad (2.32)$$

$$R_8 = F_1^{(3)} + F_k^{(4)}$$

$$R_9 = F_1^{(4)}$$

The displacements r at the nodes of the entire structure are defined as

$$r = \left\{ \begin{array}{c} r_1 \\ r_2 \\ r_3 \\ \vdots \\ \cdot \end{array} \right\} \quad (2.33)$$

where, $r_1, r_2, r_3 \dots$ are the displacements at joints $1, 2, 3, \dots$ of the structure. At a joint i , r_i is defined as

$$r_i = \left\{ \begin{array}{c} \phi_x \\ \phi_y \\ w \end{array} \right\}_i \quad (2.34)$$

The corner displacements of the connected elements at a joint of the structure can be easily obtained from the considerations of continuity. This is done by observing that at a node i , the displacements of all the connected elements are equal to r_i . Thus, in the present example the following relations are valid,

$$\begin{aligned}
 u_i^{(1)} &= r_1 \\
 u_j^{(1)} &= u_i^{(2)} = r_2 \text{ etc.}
 \end{aligned}
 \tag{2.35}$$

These relations can be easily incorporated in the equations of equilibrium of this example. Using relations of the type (2.29) and (2.35), equations (2.32) become

$$\begin{aligned}
 R_1 &= k_{ii}^{(1)} r_1 + k_{ij}^{(1)} r_2 + k_{ik}^{(1)} r_4 + k_{il}^{(1)} r_5 \\
 R_2 &= k_{ji}^{(1)} r_1 + (k_{jj}^{(1)} + k_{ii}^{(2)}) r_2 + k_{ij}^{(2)} r_3 \\
 &\quad + k_{ik}^{(1)} r_4 + (k_{jl}^{(1)} + k_{ik}^{(2)}) r_5 \\
 &\quad + k_{il}^{(2)} r_6
 \end{aligned}
 \tag{2.36}$$

.
 .
 .

and so on.

These equations are now written as

$$\begin{Bmatrix} R_1 \\ R_2 \\ \cdot \\ \cdot \\ \cdot \\ R_9 \end{Bmatrix} = \begin{bmatrix} k_{ii}^{(1)} & k_{ij}^{(1)} & \cdot & \cdot & \cdot \\ k_{ji}^{(1)} & (k_{jj}^{(1)} + k_{ii}^{(2)}) & \cdot & \cdot & \cdot \\ \cdot & \cdot & \cdot & \cdot & \cdot \\ \cdot & \cdot & \cdot & \cdot & \cdot \end{bmatrix} \begin{Bmatrix} r_1 \\ r_2 \\ \cdot \\ \cdot \\ \cdot \\ r_9 \end{Bmatrix}
 \tag{2.37}$$

Equations (2.37) state the relations between the forces and displacements at the nodes of the structure considered here. Thus, the matrix within the square bracket is the stiffness matrix of the structure. The same approach, results in a similar set of equations if applied for any other arbitrary geometry. Only difference will be in the sizes of the matrices which are governed by the number of joints and degrees of freedom at the connections.

Equations (2.37) can be abbreviated as:

$$\{ R \} = [K] \{ r \} \quad (2.38)$$

where, $[K]$ is the stiffness matrix of the structure.

It is observed that only the surrounding nodes of the structure contribute their effects to the equations of equilibrium at a point. This makes the resulting $[K]$ matrix well conditioned. Generation of this matrix while using a digital computer presents no problems. This is explained in the appendix.

If the independent co-ordinate systems of the elements have different orientations, their stiffness matrices are first transferred to the global system. When this is done, the formulation of equations of equilibrium using these transformed stiffness matrices follows the usual steps. Let, the x co-ordinate axis of an element be inclined at an angle β with respect to the \bar{x} axis of a system $(\bar{x}, \bar{y}, \bar{z})$ taken parallel to the global system of the

entire structure, Figure 2.6. All the directions of the forces and displacements are also indicated.

At any point i , the displacements with respect to the element co-ordinate system can be expressed in terms of the displacements of the auxiliary system

$(\bar{x}, \bar{y}, \bar{z})$ as:

$$\begin{Bmatrix} \theta_x \\ \theta_y \\ w \end{Bmatrix}_i = \begin{bmatrix} \cos\beta & \sin\beta & 0 \\ -\sin\beta & \cos\beta & 0 \\ 0 & 0 & 1 \end{bmatrix} \begin{Bmatrix} \bar{\theta}_x \\ \bar{\theta}_y \\ \bar{w} \end{Bmatrix}_i \quad (2.39)$$

or

$$\{u_i\} = [T] \{\bar{u}_i\} \quad (2.40)$$

where, u_i and \bar{u}_i are the displacements of the (x, y, z) and $(\bar{x}, \bar{y}, \bar{z})$ co-ordinate systems

respectively. T is the transformation matrix.

Now, expressing the forces in $(\bar{x}, \bar{y}, \bar{z})$ co-ordinate system with respect to those belonging to the element co-ordinate system (x, y, z) , at the same point i , one obtains,

$$\{\bar{F}_i\} = [T]^T \{F_i\} \quad (2.41)$$

where, \bar{F}_i and F_i are the forces with respect to

$(\bar{x}, \bar{y}, \bar{z})$ and (x, y, z) systems respectively. T^T

is the tranpose of T .

A similar set of equations result if the displacements and forces at all the nodes of the element are considered one at a time. They can be combined as

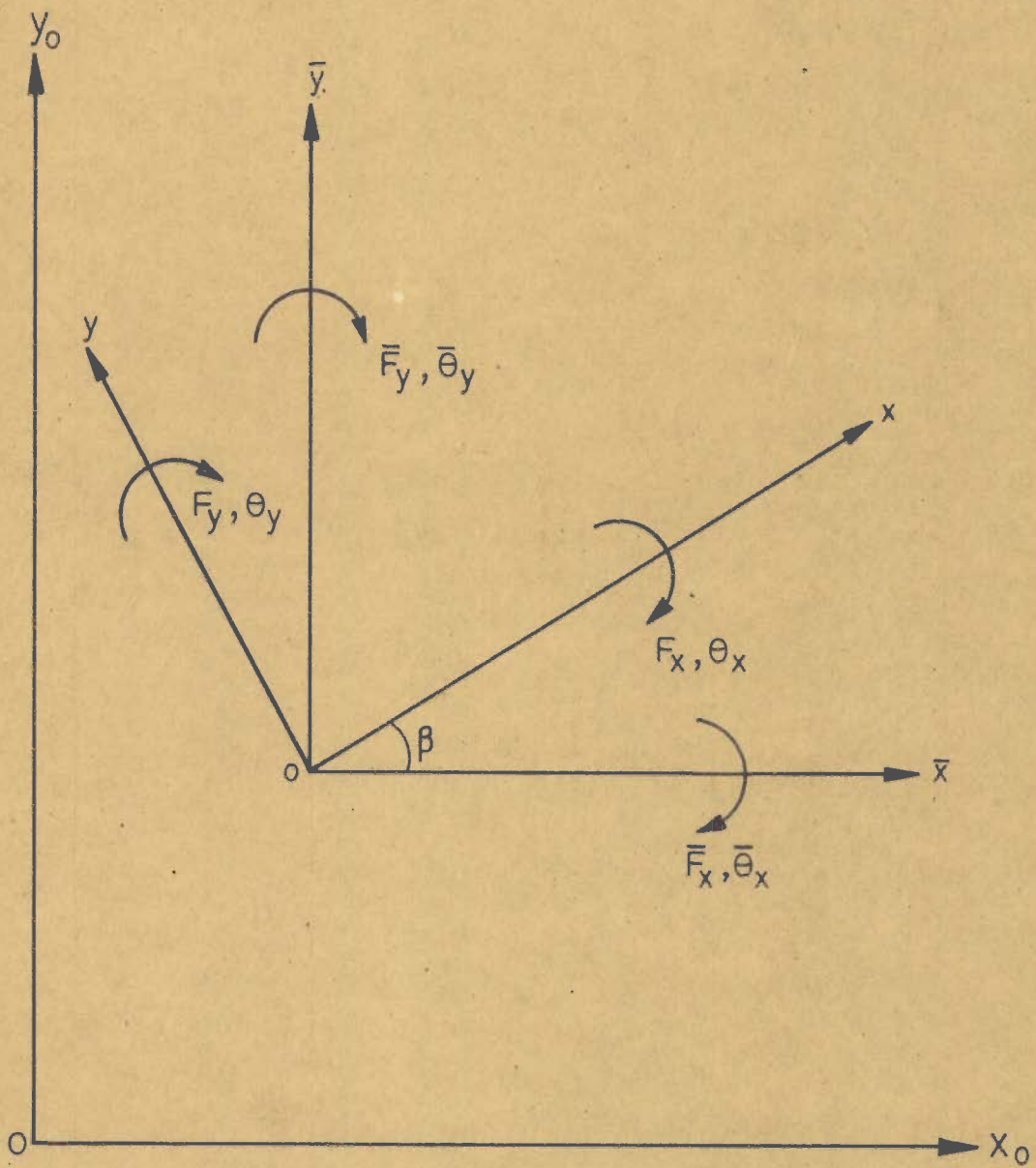


FIG. 2.6 ROTATION OF CO-ORDINATES

$$\begin{Bmatrix} \bar{F}_i \\ \bar{F}_j \\ \cdot \\ \cdot \end{Bmatrix} = \begin{bmatrix} [T]^T & & & \\ & [T]^T & & \\ & & \cdot & \\ & & & \cdot \end{bmatrix} \begin{Bmatrix} F_i \\ F_j \\ \cdot \\ \cdot \end{Bmatrix} \quad (2.42)$$

or, $\{\bar{F}\} = [T_e]^T \{F\}$ (2.43)

and

$$\begin{Bmatrix} u_i \\ u_j \\ \cdot \\ \cdot \end{Bmatrix} = \begin{bmatrix} [T] & & & \\ & [T] & & \\ & & \cdot & \\ & & & \cdot \end{bmatrix} \begin{Bmatrix} \bar{u}_i \\ \bar{u}_j \\ \cdot \\ \cdot \end{Bmatrix} \quad (2.44)$$

or,

$$\{u\} = [T_e] \{\bar{u}\} \quad (2.45)$$

Here, i, j, \dots refer to the nodes of the element.

T_e is the transformation matrix for the element. T_e^T is the transpose of T_e .

The element stiffness relations expressed in terms of its own co-ordinate system is (Eq. 2.26)

$$\{F\} = [k] \{u\}$$

Using equations (2.43) and (2.45)

$$\{\bar{F}\} = [T_e]^T [k] [T_e] \{\bar{u}\} \quad (2.46)$$

This equation expresses the stiffness relations of the element with respect to the global system and the transformed stiffness matrix $[\bar{k}]$ is

$$[\bar{k}] = [T_e]^T [k] [T_e] \quad (2.47)$$

When several elements with their independent orientations $\beta_1, \beta_2 \dots$ are involved, individual transformation matrices can be formed simply by inserting their respective angles in place of β in equation (2.39).

The transformed stiffness matrices for the elements of the structure can now be expressed as

$$\left\{ \bar{F} \right\}^{(x)} = [\bar{k}]^{(x)} \left\{ \bar{u} \right\}^{(x)} \quad (2.48)$$

$x = 1, 2, 3 \dots$

Thus, this becomes the starting point for the formulation of the equations of equilibrium. From this stage onward the formulation of the stiffness matrix $[K]$ proceeds as indicated earlier.

(b) Nodal deflections

For a set of applied loads, the deformations at the nodes of the structure are easily obtained from an equation of the type (2.38). Generally, the structures have certain restrictions of movements depending on the manner in which they are supported. These are the boundary conditions. Thus, for example, if the idealized plate of Figure 2.5 is clamped along the edge 123, all the deformations at joints 1-3 should vanish. This means that

$$r_1 = r_2 = r_3 = 0 \quad (2.49)$$

It is also obvious that the effect of the external forces applied at these points on the overall

deformations of the structure is zero. Therefore, the stiffness matrix $[K]$ may be modified taking these into account. It is clear that these forces and the displacements can be left out in the formulation of the stiffness matrix. This means that the effective size of the $[K]$ matrix is reduced. The reduction in size is carried out in two stages. The first step consists in wiping out the rows and columns of the unwanted forces and displacements respectively and keeping these places blank. After this, the matrix is condensed by omitting all these blank spaces so that its size is reduced. This reduced stiffness matrix may be termed $[\bar{K}]$. Therefore, the relations (2.38) are now written as,

$$\{R\} = [\bar{K}] \{r\} \quad (2.50)$$

The joint displacements, due to the forces applied at such points are obtained from

$$\{r\} = [\bar{K}]^{-1} \{R\} \quad (2.51)$$

(c) Joint loads

The derivation as such allows the application of concentrated forces only. On many occasions the applied forces consist of distributed loads of uniform or varying intensity. These forces have to be represented by a set of concentrated nodal forces. This can be done in two ways. The simplest way is to assign simple concentrated loads at the nodes on the basis of the area that they command.

This solution is suitable for most cases and with the increase in the number of elements the associated errors get reduced.

In the second approach, equivalent nodal forces are calculated from the principle of virtual work. A set of nodal forces for which the work done during a virtual displacement becomes equal to that due to the actual distributed forces is taken as the equivalent loading. These equivalent forces are calculated for the individual elements.

Let, the actual distributed force on an element be $q(x,y)$ and its equivalent forces P_E . The work done during the virtual displacement δu by nodal forces P_E is

$$W_p = (\delta u)^T P_E = I P_E = P_E \quad (2.52)$$

Here the virtual displacement has been considered in the way stated in section 2.6.

For the same displacements, the work done by the distributed forces is

$$W_D = \iint (\delta w)^T q(x,y) dx dy \quad (2.53)$$

From equations (2.3) and (2.7)

$$w = Ma = MC^{-1}u \quad (2.54)$$

$$\therefore \delta w = MC^{-1}\delta u = MC^{-1} \quad (2.55)$$

Equating $W_p = W_D$

$$P_E = \iint (MC^{-1})^T q(x,y) dx dy \quad (2.56)$$

The vector P_E will have couples in addition to the vertical forces. When more than one element meets at a node, contribution of each of them are to be considered to calculate the joint loads.

(d) Calculation of element forces

The nodal displacements of an element become known once the solution of equations (2.51) is obtained. Using them, the internal forces are obtained from the equation (2.14).

$$\sigma = (\bar{D}BC^{-1}) u$$

When several elements meet at a node of the structure, only the deflection and its first derivations^{ve} are equal for each of these elements at that point. This leads to discontinuity of corner forces. Therefore, for design purpose the average magnitudes of the respective forces are to be considered. However, these forces can be calculated at some interior point, say, the centre of gravity of the elements. This avoids the calculation of average values.

2.8 FINITE ELEMENT METHOD AS A SPECIAL FORM OF RAYLEIGH - RITZ METHOD

The description of the finite element method developed so far helps one to visualise that a plate structure is divided into a large number of small elements interconnected at certain selected points;

such a picture is certainly useful in gaining a physical insight into the process. Variational principles may be employed to provide a much deeper understanding of the method. That the finite element method is a special form of the well known Rayleigh - Ritz method has been fully realised only of late.

According to this new line of thinking, a plate structure need not be considered as divided into small elements physically separated from each other along their common boundaries in the domain; instead, the domain may be visualised as divided into a number of zones by drawing a set of imaginary lines. The displacement function selected for a typical element, according to this concept, becomes a representation of the deformations assumed in a typical zone bound by a set of imaginary lines.

In the Rayleigh - Ritz method, the selected displacement function is valid for the entire structure. The function assumed in terms of some undetermined parameters, satisfies the prescribed boundary conditions of a particular situation. The parameters are determined by minimising the total potential energy of the system for each of the modes of deformations associated with them. As more parameters are considered, the approximations in defining the deformations of the structure approach more closely the actual deformations and the results converge towards the true answers with the total potential energy approaching the true minimum.

This entire process is achieved in the finite element method, but this fact remains obscure. Here the deformations of the entire structure are visualised from the displacement functions selected for the restricted zones. A function for a divided zone involves a fixed number of parameters, and as a result, the deformations are poorly represented if the division is coarse. Increasing the number of zones improves the representation and indirectly increases the number of parameters.

However, a subtle difference exists between the two methods in respect of determining the parameters. In the finite element method, unlike in the Rayleigh - Ritz method, the parameters are determined by forming equations of equilibrium at the nodes (using the principle of virtual displacements) which can be expressed in the form of a stiffness matrix. So far as the results are concerned, it makes no difference whether one elects to use the principle of virtual displacement or the minimum potential, because they are the two different forms of the same principle. Thus the true level of minimum potential energy is reached when the zones become microscopic.

The advantage of this new concept over the classical approach of Rayleigh - Ritz method is in the extreme generality in the formulation. A function of a divided zone is designed to accept all possible boundary conditions. The additional feature of the method is the convergence criteria.

They are necessary due to the discretisation introduced. In the Rayleigh - Ritz method, the selected displacement function provides complete continuity of both displacements and the stress resultants over the entire domain. Here the overall stiffness of the structure will be consistently higher than its actual stiffness. On the other hand, in the finite element method, the stress resultants are usually discontinuous across the boundaries of the divided zones. The displacements may or may not be continuous across these boundaries. When the displacements are continuous, the overall stiffness of the structure exhibits a behaviour similar to that observed in the Rayleigh - Ritz method. But if the displacements are discontinuous, the overall stiffness of the structure oscillates about its true value depending on whether the resulting assemblage is too stiff or too flexible at the various stages of sub-divisions assumed. However, as the number of sub-divisions is increased, the strains, in the limit, tend to become uniform over the restricted zones. This finally leads to the continuity of the stress resultants. Thus ultimately complete continuity and equilibrium are achieved throughout the entire domain. Herein, the convergence criteria play a vital role.

CHAPTER THREE

NEW DISPLACEMENT FUNCTIONS

3.1 PURPOSE

The displacement functions proposed in this dissertation are derived in this chapter. Two shapes of elements have been adopted; one is rectangular and the other triangular. The former is most suitable for rectangular plate problems and the latter any arbitrary shape. For both these shapes, the functions derived are of the conforming type.

3.2 RECTANGULAR ELEMENT

Figure 3.1 shows a rectangular element with its four nodes i, j, k and l. The element is in the x - y plane and the z - axis is taken vertically downward. For this element, the displacement function has been obtained by deriving the expressions for the deformed shape of the plate element due to the application of unit displacements at its nodes. In this derivation, the following relations have been used throughout:

$$\begin{aligned} X_m &= 1 - \frac{X}{a} \\ Y_m &= 1 - \frac{Y}{b} \\ X_p &= 1 + \frac{X}{a} \\ Y_p &= 1 + \frac{Y}{b} \end{aligned} \tag{3.1}$$

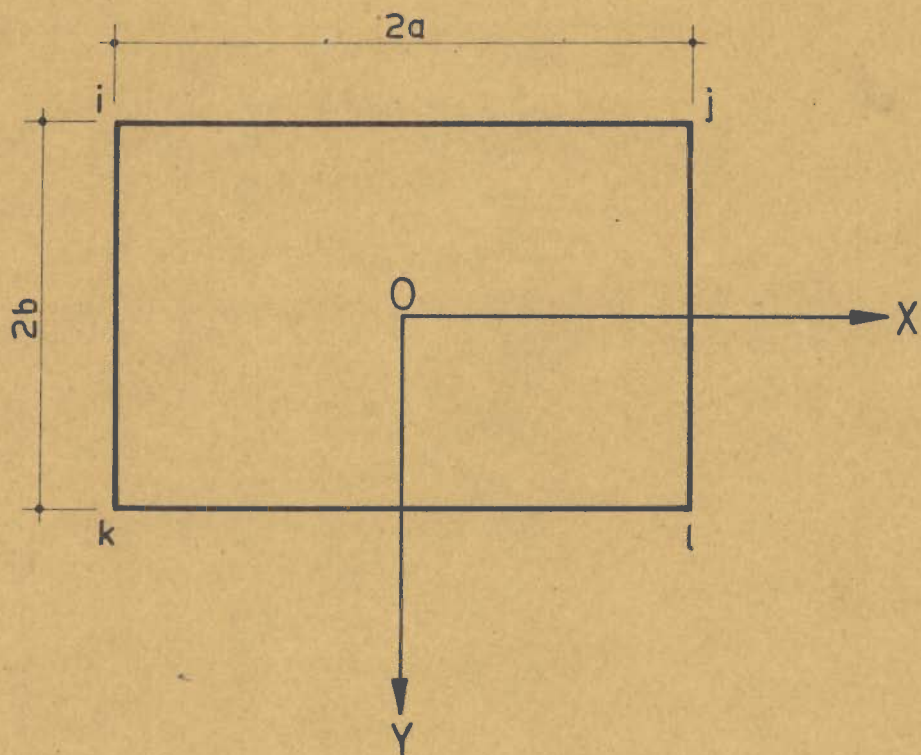


FIG. 3.1 A RECTANGULAR ELEMENT

(a) Shape Functions for the deflections at the nodes

(i) Node i

In order to derive the expression for unit deflection at this node, the shape function is taken as

$$w = \frac{X_m Y_m}{4} \quad (3.2)$$

Equation (3.2) results in unit deflection at the node i, and the deflection varies linearly along $x = -a$ and $y = -b$ as shown in Figure 3.2.

From equation (3.2) the slopes are

$$\begin{aligned} w_x &= -\frac{1}{a} \frac{Y_m}{4} \\ w_y &= -\frac{1}{b} \frac{X_m}{4} \end{aligned} \quad (3.3)$$

Since the expression to be obtained is for unit deflection at the node i, these slopes should be made zero at all the nodes. This can be very easily achieved by eliminating the normal slopes along the element boundaries.

It is observed that w_x is independent of the x - co-ordinate and varies linearly along the y - axis. That is, w_x is constant for a particular value of the y co-ordinate. A similar behaviour is noticed for w_y with respect to y and x co-ordinates.

Along $x = -a$, (Eq. 3.3)

$$a w_x = -\frac{Y_m}{4} \quad (3.4)$$

In order to make w_x vanish along these edges a correction function is required which will produce equal and opposite w_x along these very edges, without

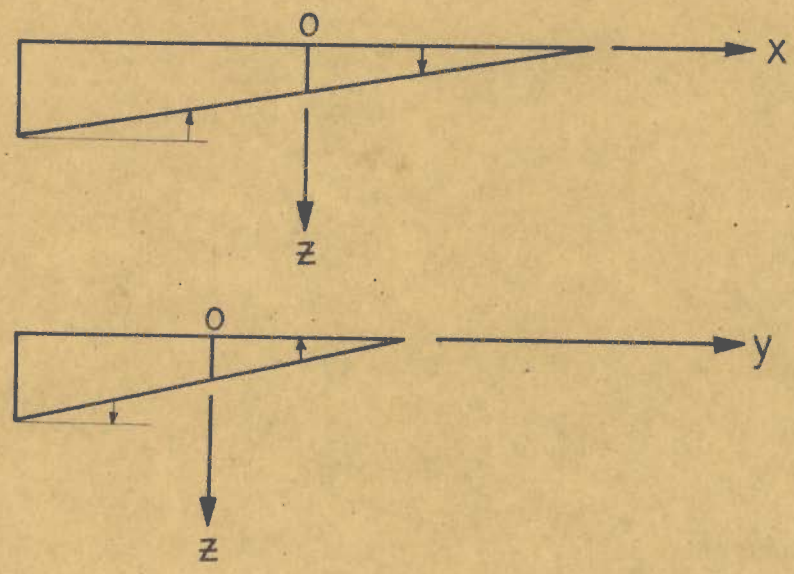
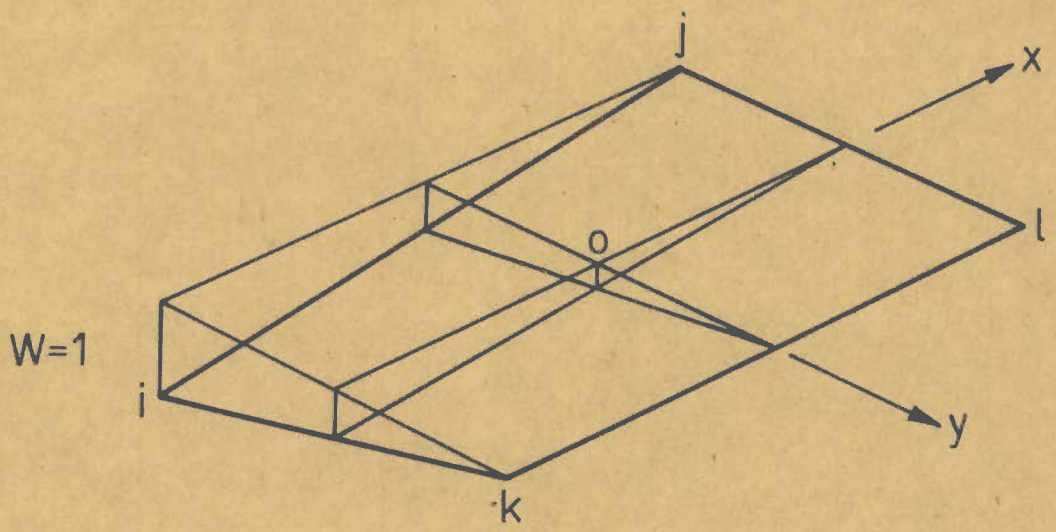


FIG. 3.2 LINEAR EDGE DISPLACEMENTS FOR UNIT DEFLECTION AT NODE i

altering the existing values of nodal deflections. Obviously, the function should give zero deflection along $x = \pm a$ for this purpose. From equation (3.4) it is seen that the normal slopes, i.e., w_x are the same in magnitude and direction at $x = \pm a$ for a particular value of y . Therefore, a function in x alone can be used for eliminating w_x at the edges mentioned above. Let this be any function $f(x)$.

This function $f(x)$ is taken such that it produces $w_x = 1/a$, but zero deflection at $x = \pm a$. Assuming for the time being, that such a function $f(x)$ exists, the required correction is

$$\phi_1 = \frac{Y_m}{4} \left[f(x) \right] \quad (3.5)$$

Introducing this in equation (3.2) the deflection equation becomes

$$w = \frac{X_m Y_m}{4} + \frac{Y_m}{4} \left[f(x) \right] \quad (3.6)$$

Now the slope w_y is

$$w_y = -\frac{1}{b} \left[\frac{X_m}{4} + \frac{1}{4} f(x) \right] \quad (3.7)$$

Here, w_y is constant for all y and is same in magnitude and direction at $y = \pm b$ for a particular value of x . To eliminate w_y at $y = \pm b$, a function $f(y)$ with similar properties as that of $f(x)$ is required. That means $f(y)$ should produce $w_y = 1/b$, but no deflection at $y = \pm b$. Thus, the correction required to eliminate w_y along these particular edges

$$\text{is } \phi_2 = \left[\frac{X_m}{4} + \frac{1}{4} f(x) \right] \left[f(y) \right] \quad (3.8)$$

Therefore, the shape function for unit deflection at the node i, becomes

$$w = \frac{X_m Y_m}{4} + \frac{Y_m}{4} \left[f(x) \right] + \frac{1}{4} \left[X_m + f(x) \right] \left[f(y) \right] \quad (3.9)$$

In this equation (3.9), the slopes w_x and w_y are eliminated at all the nodes and along all the edges the normal slopes are zero. If, w_i is applied at node i instead of unit deflection, the equation (3.9) after simplification can be written as

$$w = \frac{w_i}{4} \left[X_m + f(x) \right] \left[Y_m + f(y) \right] \quad (3.10)$$

The expressions for deflections at the remaining nodes are obtained in the same way as outlined above. They are, for

(ii) Node j

$$w = \frac{w_j}{4} \left[X_p - f(x) \right] \left[Y_m + f(y) \right] \quad (3.11)$$

(iii) Node k

$$w = \frac{w_k}{4} \left[X_m + f(x) \right] \left[Y_p - f(y) \right] \quad (3.12)$$

(iv) Node l

$$w = \frac{w_l}{4} \left[X_p - f(x) \right] \left[Y_p - f(y) \right] \quad (3.13)$$

(b) Shape functions for the slopes

The derivation of the expressions for the deformed shape of the element due to the application of unit nodal slopes involves a little more trial and manipulation. Since the functions $f(x)$ and $f(y)$

have already been used in the expressions for the nodal deflections, they cannot be left out here. It is difficult to fulfil the convergence requirements, if they are omitted. Thus, the process actually reduces to adjusting the functions $f(x)$ and $f(y)$ with the help of certain other suitable expressions, so that the derived shape functions ultimately satisfy the requirements of convergence.

Node i

Following the above reasoning, the expression for the deformed shape of the element due to unit slope w_x applied at node i, is taken as

$$\psi_1 = \frac{a}{4} \left[f(x) + \frac{X_m X_p}{2} \right] \left[Y_m + f(y) \right] \quad (3.14)$$

and, for unit slope w_y applied at the same node i, as

$$\psi_2 = \frac{b}{4} \left[f(y) + \frac{Y_m Y_p}{2} \right] \left[X_m + f(x) \right] \quad (3.15)$$

Applying θ_{xi} and θ_{yi} instead of unit slopes, the respective expressions are modified as

$$\psi_1 = \frac{a \theta_{xi}}{4} \left[f(x) + \frac{X_m X_p}{2} \right] \left[Y_m + f(y) \right] \quad (3.16)$$

$$\psi_2 = \frac{b \theta_{yi}}{4} \left[f(y) + \frac{Y_m Y_p}{2} \right] \left[X_m + f(x) \right] \quad (3.17)$$

The steps involved in deriving these functions are quite simple. Here these are explained only with

reference to ψ_1 ; similar steps are used for arriving at ψ_2 .

First, a function is selected to satisfy following conditions:

$$\begin{aligned} \text{at } x = +a, \quad w = 0, \quad w_x = 0 \\ \text{at } x = -a, \quad w = 0, \quad w_x = \frac{1}{a} \end{aligned} \quad (3.18)$$

These are satisfied by

$$\phi(x) = \frac{1}{2} \left[f(x) + \frac{x_m x_p}{2} \right] \quad (3.19)$$

where, $f(x)$ is as already defined. The function ψ_1

is then taken as

$$\psi_1 = a \phi(x) \cdot \phi(y) \quad (3.20)$$

The function $\phi(y)$ is selected such that it satisfies the following conditions

$$\begin{aligned} \text{at } y = -b, \quad w = 1 \quad w_y = 0 \\ \text{at } y = +b, \quad w = 0 \quad w_y = 0 \end{aligned} \quad (3.21)$$

These are satisfied by

$$\phi(y) = \frac{1}{2} \left[Y_m + f(y) \right] \quad (3.22)$$

already used in equation (3.10). Several functions satisfy the conditions of equations (3.18) and (3.21).

If these functions $\phi(x)$ and $\phi(y)$ are selected only on the basis of these conditions, the resulting function may not satisfy the requirements of convergence. These expressions were finalized after several trials remembering the conditions of convergence, especially the requirements relating

to rigid body motions at this stage. Considering the remaining nodes, one at a time, the corresponding functions are derived on similar lines. They are,

for

(ii) Node j

$$\psi_3 = \frac{a\theta_{xj}}{4} \left[f(x) - \frac{X_m X_p}{2} \right] \left[Y_m + f(y) \right] \quad (3.23)$$

$$\psi_4 = \frac{b\theta_{yj}}{4} \left[f(y) + \frac{Y_m Y_p}{2} \right] \left[X_p - f(x) \right] \quad (3.24)$$

(iii) Node k

$$\psi_5 = \frac{a\theta_{xk}}{4} \left[f(x) + \frac{X_m X_p}{2} \right] \left[Y_p - f(y) \right] \quad (3.25)$$

$$\psi_6 = \frac{b\theta_{yk}}{4} \left[f(y) - \frac{Y_m Y_p}{2} \right] \left[X_m + f(x) \right] \quad (3.26)$$

(iv) Node l

$$\psi_7 = \frac{a\theta_{xl}}{4} \left[f(x) - \frac{X_m X_p}{2} \right] \left[Y_p - f(y) \right] \quad (3.27)$$

$$\psi_8 = \frac{b\theta_{yl}}{4} \left[f(y) - \frac{Y_m Y_p}{2} \right] \left[X_p - f(x) \right] \quad (3.28)$$

(c) Complete displacement function for a rectangular element

The complete displacement function is obtained by adding up the expressions for the nodal displacements derived above.

Let,

$$\begin{aligned} F_1(x) &= \frac{1}{2} \left[X_m + f(x) \right] \\ F_2(x) &= \frac{1}{2} \left[X_p - f(x) \right] \\ F_3(x) &= \frac{1}{2} \left[f(x) + \frac{X_m X_p}{2} \right] \end{aligned}$$

$$\begin{aligned}
 F_4(x) &= \frac{1}{2} \left[f(x) - \frac{X_m X_p}{2} \right] \\
 F_1(y) &= \frac{1}{2} \left[Y_m + f(y) \right] \\
 F_2(y) &= \frac{1}{2} \left[Y_p - f(y) \right] \\
 F_3(y) &= \frac{1}{2} \left[f(y) + \frac{Y_m Y_p}{2} \right] \\
 F_4(y) &= \frac{1}{2} \left[f(y) - \frac{Y_m Y_p}{2} \right]
 \end{aligned} \tag{3.29}$$

In these expressions $f(x)$ and $f(y)$ are not yet defined. But the requirements which these functions have to satisfy have been already stated. These functions will be discussed in detail at a later stage. Using these above definitions, the complete displacement function for the rectangular element is written as:

$$\begin{aligned}
 w = & w_i F_1(x) \cdot F_1(y) + a \theta_{xi} F_3(x) \cdot F_1(y) \\
 & + b \theta_{yi} F_1(x) \cdot F_3(y) + w_j F_2(x) \cdot F_1(y) \\
 & + a \theta_{xj} F_4(x) \cdot F_1(y) + b \theta_{yj} F_2(x) \cdot F_3(y) \\
 & + w_k F_1(x) \cdot F_2(y) + a \theta_{xk} F_3(x) \cdot F_2(y) \\
 & + b \theta_{yk} F_1(x) \cdot F_4(y) + w_l F_2(x) \cdot F_2(y) \\
 & + a \theta_{xl} F_4(x) \cdot F_2(y) + b \theta_{yl} F_2(x) \cdot F_4(y) \\
 & \dots \tag{3.30}
 \end{aligned}$$

The resulting displacement function written above satisfies fully the requirements of rigid body motions. It is also capable of representing the state of uniform moments in x and y directions, but unfortunately fails to represent the condition of

uniform twist. Examination of this function reveals that the quantity w_{xy} or the twist is zero at all the nodes. To make w_{xy} non-zero at the nodes, it is taken as an additional degree of freedom at the nodes. The shape functions giving twist are taken as,

$$\begin{aligned}
 \text{at node } i, \quad w &= ab \theta_{xyi} F_3(x) \cdot F_3(y) \\
 \text{at node } j, \quad w &= ab \theta_{xyj} F_4(x) \cdot F_3(y) \\
 \text{at node } k, \quad w &= ab \theta_{xyk} F_3(x) \cdot F_4(y) \\
 \text{at node } l, \quad w &= ab \theta_{xyl} F_4(x) \cdot F_4(y)
 \end{aligned} \tag{3.31}$$

These expressions are added to the function of equation (3.30) to arrive at the final displacement function.

$$\begin{aligned}
 w &= F_1(x) \cdot F_1(y) w_i + aF_3(x) \cdot F_1(y) \theta_{xi} + bF_1(x) \cdot F_3(y) \theta_{yi} \\
 &+ abF_3(x) \cdot F_3(y) \theta_{xyi} + F_2(x) F_1(y) w_j \\
 &+ aF_4(x) F_1(y) \theta_{xj} + bF_2(x) F_3(y) \theta_{yj} + \\
 &+ abF_4(x) F_3(y) \theta_{xyj} + F_1(x) F_2(y) w_k + aF_3(x) F_2(y) \theta_{xk} \\
 &+ bF_1(x) F_4(y) \theta_{yk} + abF_3(x) F_4(y) \theta_{xyk} \\
 &+ F_2(x) F_2(y) w_l + aF_4(x) F_2(y) \theta_{xl} \\
 &+ bF_2(x) F_4(y) \theta_{yl} + abF_4(x) F_4(y) \theta_{xyl}
 \end{aligned} \tag{3.32}$$



The displacement function with these additional degrees of freedom now satisfies all the requirements of convergence. That the function is of the conforming type is obvious from the approach outlined,

and it is interesting to note that the $f(x)$ and $f(y)$ have not yet been derived explicitly. This part will be taken up now.

(d) Function $f(x)$ and $f(y)$

So far it has been assumed in the derivation that it is possible to find functions $f(x)$ and $f(y)$. Nothing has been stated explicitly about their forms excepting the conditions that they are to satisfy. These conditions are

$$f(x) = 0, f'(x) = \frac{1}{a} \text{ at } x = \pm a \quad (3.33)$$

for the function $f(x)$, and

$$f(y) = 0, f'(y) = \frac{1}{b} \text{ at } y = \pm b \quad (3.34)$$

for the function $f(y)$, where, $f'(x)$ and $f'(y)$ are the respective first derivatives.

If the shape is now drawn for any one of them with respect to the element co-ordinate system, an anti-symmetric function is obtained as shown in Figure 3.3. Two approaches, with a subtle difference, are available to determine the mathematical expression for the shape; one is by physical intuition and the other by solving equations of boundary conditions. If we opt for the latter, the simplest procedure is to assume a cubic expression with four constants. Therefore, let

$$f(x) = A_1 + A_2 \left(\frac{x}{a}\right) + A_3 \left(\frac{x}{a}\right)^2 + A_4 \left(\frac{x}{a}\right)^3 \quad (3.35)$$

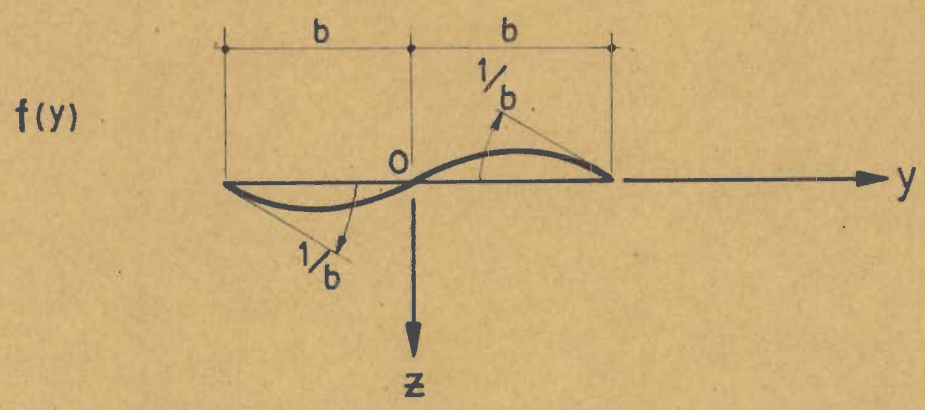
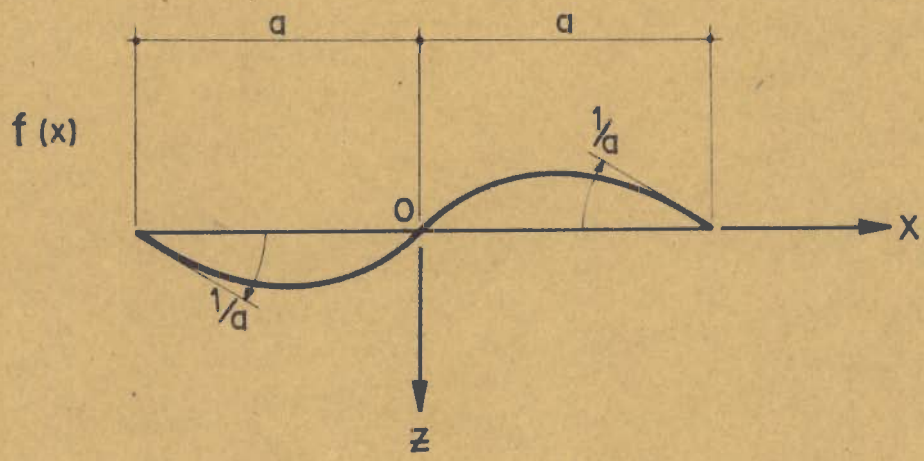


FIG. 3.3 FUNCTIONS $f(x)$ AND $f(y)$

These four constants are then solved for the boundary conditions stated in equations (3.33). The simplified form of the functions with known constants is

$$f(x) = \frac{1}{2} \left(\frac{x}{a}\right) \left[\left(\frac{x}{a}\right)^2 - 1 \right] \quad (3.36)$$

A similar expression in y is selected for $f(y)$.

Now the explicit forms of the relations defined in equations (3.29) are easily obtained using the expressions for $f(x)$ and $f(y)$. If the relations of the type of equation (3.36) are used, the final displacement function arrived at is the same as the one suggested by Butlin (31,32) and Hansteen (33). The results given by this function are extremely satisfactory as reported in the above publications. This function, therefore, has not been discussed further in this study. No other variation is possible with simple polynomial expressions. Partial fractions can be tried, but integration becomes complicated. Care is required in such a case to make sure that the function does not possess singularity within the domain.

The physical approach on the other hand proves to be extremely convenient; the most important feature of this approach being that the use of trigonometric functions becomes possible. Such functions, as already stated, did not lead to convergence on previous attempts (32,43). But the method outlined in this section clearly indicates that trigonometric functions can be easily used to define functions $f(x)$ and $f(y)$.

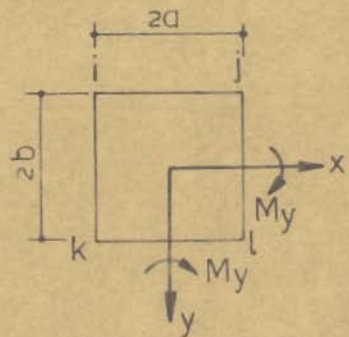
Since the resulting displacement function (Equation 3.32) satisfies all the requirements, the results of the analysis will show convergence. Moreover, convergence is bound to be monotonic because the displacement function is of the conforming type.

A sine function is an anti-symmetric function with reference to the selected co-ordinate system shown in Figure 3.1. Thus, the following expressions are selected for the function $f(x)$ shown in Figure 3.3:

$$\begin{aligned} \text{(i)} \quad f(x) &= -\frac{1}{\pi} \sin\left(\frac{\pi x}{a}\right) \\ \text{(ii)} \quad f(x) &= \left[\left(\frac{x}{a}\right) - \sin\frac{\pi x}{2a} \right] \\ \text{(iii)} \quad f(x) &= \frac{1}{3} \left[\left(\frac{x}{a}\right)^3 - \sin\frac{\pi x}{2a} \right] \quad (3.37) \\ \text{(iv)} \quad f(x) &= \frac{1}{3} \left[2\left(\frac{x}{a}\right)^3 - 3\left(\frac{x}{a}\right) + \sin\frac{\pi x}{2a} \right] \\ \text{(v)} \quad f(x) &= -\frac{2}{\pi} \left[\left(\frac{x}{a}\right) \cos\frac{\pi x}{2a} \right] \end{aligned}$$

The functions $f(y)$ are obtained simply by replacing x by y in the above expressions. All these expressions satisfy the conditions of equations (3.33) and (3.34), and it is obvious that these are by no means the only functions that are possible. In fact, the number of such functions is endless. This derivation, therefore, clearly demonstrates the possibility of employing a large class of suitable displacement functions (Eq. 3.32).

V_i^a	K_{11}	Symmetrical												$\frac{w_i}{d}$					
M_x^i	K_{21}	K_{22}											w_{xi}						
M_y^i	K_{31}	K_{32}	K_{33}									w_{yi}							
$T \frac{y}{d}$	K_{41}	K_{42}	K_{43}	K_{44}								$d w_{xy}^i$							
V_j^d	K_{51}	K_{52}	K_{53}	K_{54}	K_{11}							$\frac{w_j}{d}$							
M_x^j	$-K_{52}$	K_{62}	K_{63}	K_{64}	$-K_{21}$	K_{22}					w_{xi}								
M_y^j	K_{53}	$-K_{63}$	K_{73}	K_{74}	K_{31}	$-K_{32}$	K_{33}				w_{yi}								
$T \frac{y}{d}$	$-K_{54}$	K_{64}	$-K_{74}$	K_{84}	$-K_{41}$	K_{42}	$-K_{43}$	K_{44}				$d w_{xy}^j$							
V_k^d	K_{91}	K_{92}	K_{93}	K_{94}	K_{131}	$-K_{132}$	K_{133}	$-K_{134}$	K_{11}				$\frac{w_k}{d}$						
M_x^k	K_{92}	K_{102}	K_{103}	K_{104}	$-K_{141}$	K_{142}	$-K_{143}$	K_{144}	K_{21}	K_{22}			w_{xk}						
M_y^k	$-K_{93}$	$-K_{103}$	K_{113}	K_{114}	K_{151}	$-K_{152}$	K_{153}	$-K_{154}$	$-K_{31}$	$-K_{32}$	K_{33}			w_{yk}					
$T \frac{y}{d}$	$-K_{94}$	$-K_{104}$	K_{114}	K_{124}	$-K_{161}$	K_{162}	$-K_{163}$	K_{164}	$-K_{41}$	$-K_{42}$	K_{43}	K_{44}			$d w_{xy}^k$				
V_l^d	K_{131}	K_{132}	K_{133}	K_{134}	K_{91}	$-K_{92}$	K_{93}	$-K_{94}$	K_{51}	K_{52}	$-K_{53}$	$-K_{54}$	K_{11}			$\frac{w_l}{d}$			
M_x^l	$-K_{132}$	K_{142}	K_{143}	K_{144}	$-K_{101}$	K_{102}	$-K_{103}$	K_{104}	K_{61}	K_{62}	$-K_{63}$	$-K_{64}$	$-K_{21}$	K_{22}			w_{xl}		
M_y^l	$-K_{133}$	K_{143}	K_{153}	K_{154}	K_{111}	$-K_{112}$	K_{113}	$-K_{114}$	$-K_{71}$	$-K_{72}$	K_{73}	K_{74}	$-K_{31}$	K_{32}	K_{33}			w_{yl}	
$T \frac{y}{d}$	K_{134}	$-K_{144}$	$-K_{154}$	K_{164}	$-K_{121}$	K_{122}	$-K_{123}$	K_{124}	$-K_{81}$	$-K_{82}$	K_{83}	K_{84}	K_{41}	$-K_{42}$	$-K_{43}$	K_{44}			$d w_{xy}^l$



Z AXIS DOWNWARD

TABLE 3.1 STIFFNESS MATRIX [k]

The displacement function for rectangular element derived as described above is used to obtain the stiffness matrix as outlined in the section 2.6. An explicit form of the stiffness matrix, unlike in the case of simple polynomials, is more involved when trigonometric functions are used. Therefore, the stiffness matrix was generated in the machine for which a separate programme has been written. The size of this matrix is 16 x 16 because of the assignment of four degrees of freedom at a node. The extra degree of freedom is the twist w_{xy} , corresponding to which an extra force is obtained at each node. This force is a fictitious couple. Since the boundary conditions involve the specification of known displacements only, for a fixed edge, the displacement w_{xy} is taken as zero. For other conditions such as free or simply supported edges, this is not zero. Table 3.1 shows the form of the stiffness matrix.

3.3 TRIANGULAR ELEMENT

A displacement function for a triangular element derived by using simple polynomial expressions is presented in this section. The method adopted is a variation of the technique employed by Clough (22), discussed earlier. Figure 3.4 shows a triangular element which has been divided into three sub-elements by joining the three corners and its centre of gravity.

z_0 AXIS UPWARD

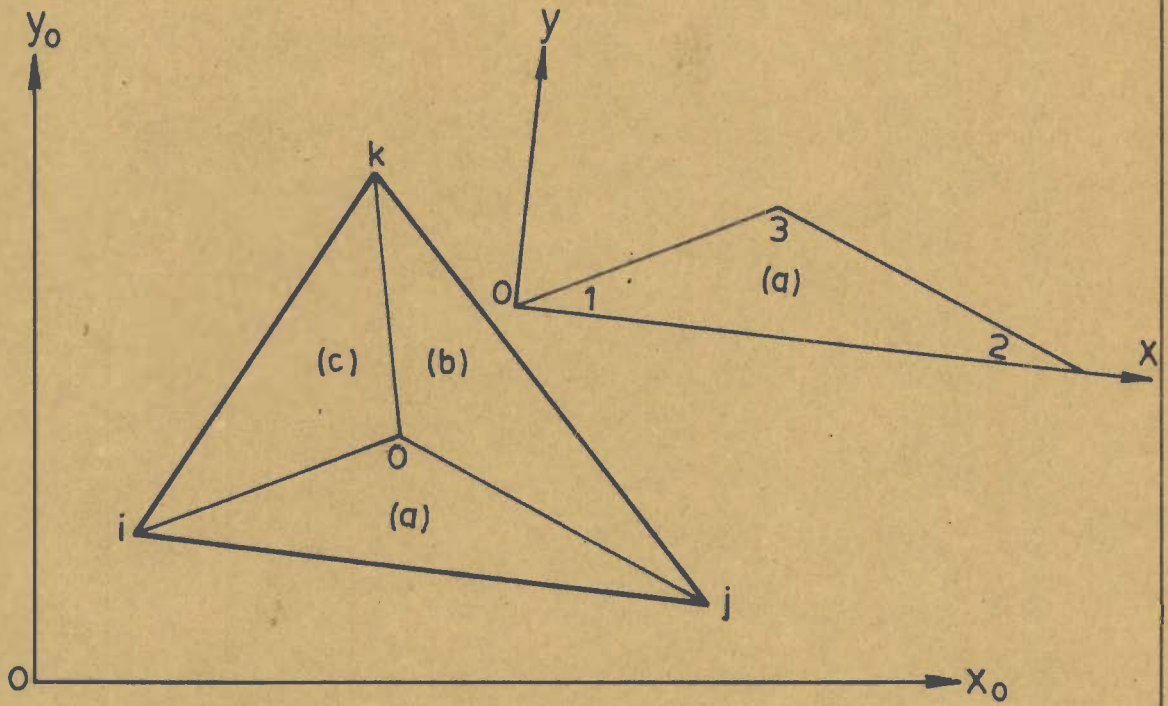


FIG. 3.4 DIVISION INTO SUB-ELEMENTS

The element is in the $x_0 - y_0$ plane and the z_0 axis is directed upward. An independent polynomial displacement function of nine terms is selected for each of these sub-elements with respect to their local co-ordinates (x, y, z) . The function for the element a , for example, is taken as

$$\begin{aligned} w^{(a)} = & A_1 + A_2x + A_3y + A_4x^2 + A_5xy + A_6y^2 \\ & + A_7x^3 + A_8y^3 + A_9xy^2 \end{aligned} \quad (3.38)$$

The selection of such a function has two advantages. First, it automatically provides the continuity of deflection and slope in the vertical plane along all the boundaries. Secondly, the normal slopes vary linearly along the exterior edges ($y=0$) of the sub-element. However, the variation of normal slopes is parabolic along the interior edges of sub-elements. This means that they are discontinuous along the interior boundaries. If the normal slopes are made continuous along these boundaries the resulting displacement function will be a conforming type of function.

Two approaches are possible to achieve the continuity of these slopes. This can be accomplished either by equating the normal slopes at the mid-points of the internal boundaries or by forcing them to vary linearly along these boundaries. Clough adopted the former approach and the latter has been selected here. The method opted here requires the use of additional correction functions. These functions

have been determined independently for the sub-elements. The stiffness matrices of the sub-elements are determined in the usual manner using their corrected displacement functions. Once this is done, the stiffness matrix of the total element is obtained by summing up the individual sub-element stiffness matrices. All the steps involved are discussed in detail at a later stage and at present the method of determining suitable correction function is considered.

The steps involved in determining the correction functions are discussed in detail for the sub-element a . For the remaining two sub-elements b and c these are determined on similar lines. Before going into the mathematical formulation of the correction functions it is important to study the variation of normal slope along a boundary of the sub-element. Figure 3.5 shows the element a with its local co-ordinates (x, y, z) . The parabolic variation of normal slope along the boundary 13 is represented in Figure 3.6. At any point between the nodes 1 and 3, the normal slope is obtained by measuring the ordinates upto the curve pqr . The slope at the mid-point of the boundary is equal to f_5 as shown in the figure. If the variation is to be linear, the slope at this point should be the average value of the slopes f_1 and f_3 at the nodes, and at any other point the normal slope will be

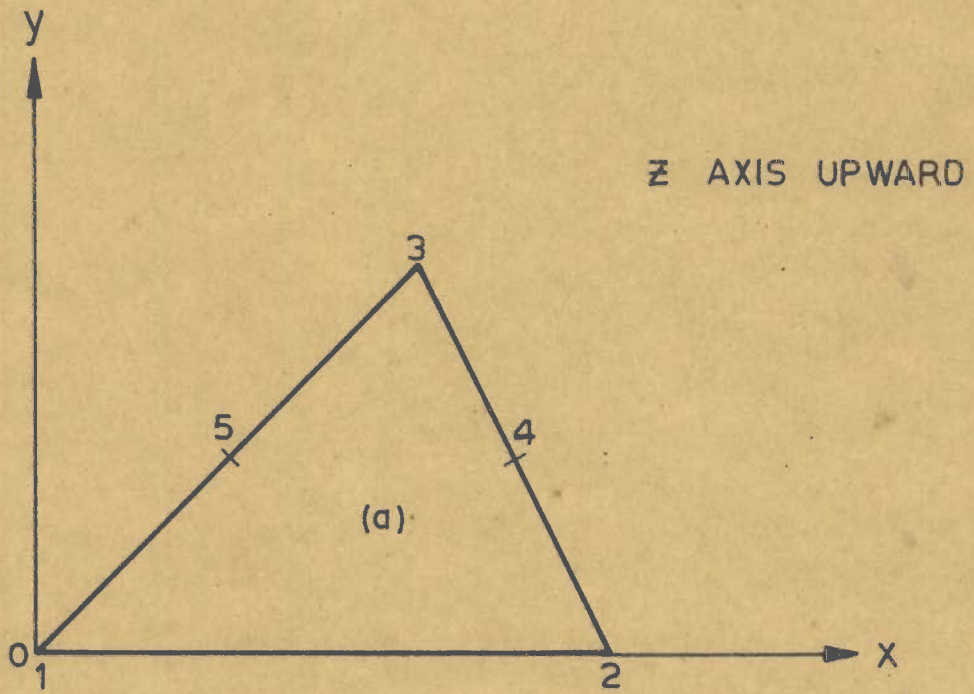


FIG. 3.5 SUB - ELEMENT (a)

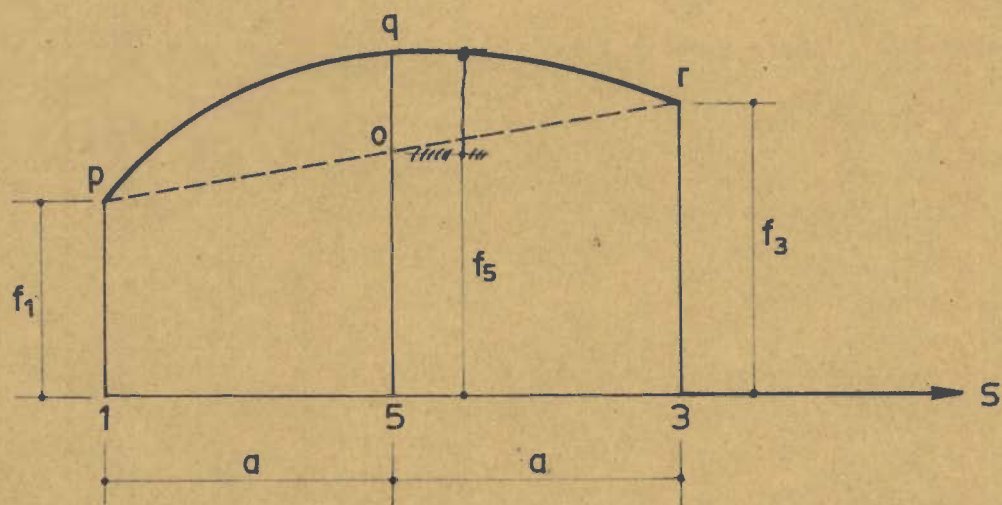


FIG. 3.6 VARIATION OF NORMAL SLOPE ALONG A BOUNDARY

obtained by measuring the ordinates upto the straight line pr, Figure 3.6. Presently, the variation is parabolic, and because of this, the deviation from linearity at the mid-point is given by

$$\delta = f_5 - (f_1 + f_3)/2 \quad (3.39)$$

At other points the deviation is obtained by measuring the difference between the ordinates upto the curve pqr and the straight line pr. It is obvious that this deviation from linearity also follows a parabolic variation. This means, it can be represented by a parabola with the rise equal to δ at the centre and zero at ends.

The aim of using correction functions is to eliminate these deviations so that the normal slopes vary linearly along the edges 13 and 23 of the sub-element a. Therefore, for each of the sides where linear variation of normal slope is to be prescribed, a function is selected such that (39):

- (i) The function itself is zero on all sides,
- (ii) The normal slope varies parabolically with a value of unity at the mid-point of the side for which it is selected,
- (iii) The first derivatives are zero on all the remaining sides,
- (iv) The function and its first derivatives are continuous within the domain.

A correction function with the above properties does not alter the conditions at the nodes of the sub-element. For the sub-elements under consideration two such functions are necessary; one of them remains operative at the edge 13 and the other at 23. These functions are added to the original displacement function (Eq. 3.38) in suitable proportions to nullify the existing deviation from linearity on the interior sides.

The steps involved in correcting the displacement function are simple. Let the selected displacement function (Eq. 3.38) be written as

$$w^{(a)} = [M(x,y)] \{A\} \quad (3.40)$$

The normal slopes at the mid-points of the sides 23 and 13 are, Figure 3.5

$$\left\{ \begin{matrix} w_{n4}^{(a)} \\ w_{n5}^{(a)} \end{matrix} \right\} = [G] \{A\} \quad (3.41)$$

For linear variation of normal slopes along these sides, the values at the mid-points should be the average of the slopes at the nodes. These can be written as

$$\left\{ w_{n(av)}^{(a)} \right\} = [H] \{A\} \quad (3.42)$$

Therefore, the deviation from linearity at these points are

$$S^{(a)} = \left\{ \begin{array}{l} S_4^{(a)} \\ S_5^{(a)} \end{array} \right\} = ([G] - [H]) \{A\} \quad (3.43)$$

If E_1 and E_2 are the correction functions for the sides 23 and 13 respectively, the corrected displacement function of the sub-element is given by

$$w^{(a)} = \left\{ [M(x,y)] - [E_1, E_2]([G] - [H]) \right\} \{A\} \quad (3.44)$$

In order to obtain a corrected displacement function the first step, therefore, is to calculate the normal slopes at the mid-points of the interior sides of the sub-elements. The normal slope along a boundary inclined at an angle γ as shown in Figure 3.7 is given by

$$w_n = -w_x \sin \gamma + w_y \cos \gamma \quad (3.45)$$

For the sub-element a, considering only the terms giving parabolic variations the normal slope is given by

$$w_n^{(a)} = -3x^2 \sin \gamma A_7 + 3y^2 \cos \gamma A_8 + (2xy \cos \gamma - y^2 \sin \gamma) A_9 \quad (3.46)$$

The deviation from linearity at the mid-points of the sides 23 and 13 are determined by considering the inward normal slopes as shown in Figure 3.8. The reason for this will be clear at a later stage.

Equation (3.46) gives inward normal slope at 5

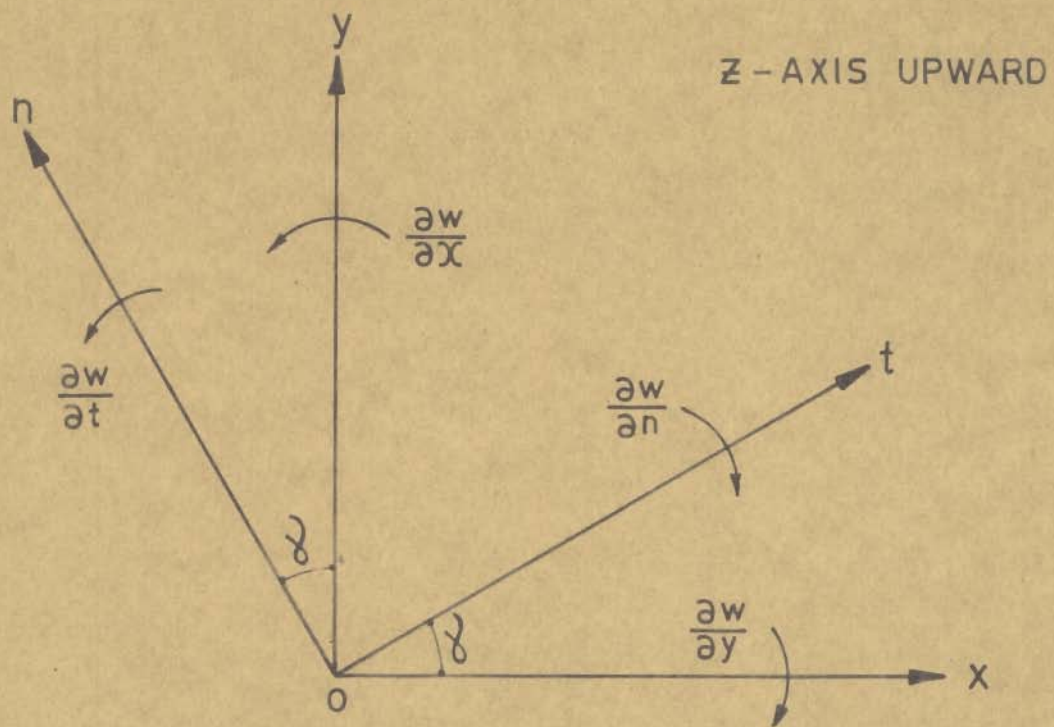


FIG. 3.7 ROTATION OF CO-ORDINATES

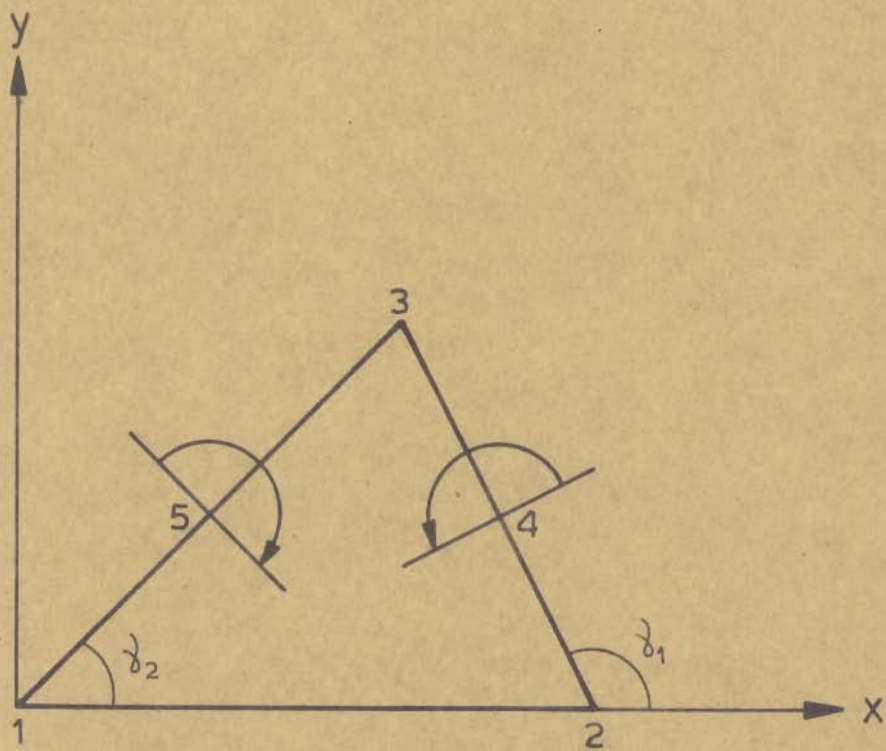


FIG. 3.8 INWARD NORMAL SLOPES

$$\begin{aligned} (a) \\ w_{n5} &= -3x_5^2 \sin \gamma_2 A_7 + 3y_5^2 \cos \gamma_2 A_8 \\ &\quad - (y_5^2 \sin \gamma_2 - 2x_5 y_5 \cos \gamma_2) A_9 \end{aligned} \quad (3.47)$$

at 3 for the side 13

$$\begin{aligned} (a) \\ w_{n3} &= -3x_3^2 \sin \gamma_2 A_7 + 3y_3^2 \cos \gamma_2 A_8 \\ &\quad - (y_3^2 \sin \gamma_2 - 2x_3 y_3 \cos \gamma_2) A_9 \end{aligned} \quad (3.48)$$

and at 1 for the same side 13

$$(a) \\ w_{n1} = 0 \quad (3.49)$$

Average value of the normal slopes at the nodes 1 and 3 is

$$(a) \\ w_{n(av)} = (w_{n1} + w_{n3})/2 \quad (3.50)$$

Therefore, the deviation from linearity at point 5 is given by

$$\delta_5^{(a)} = w_{n5}^{(a)} - w_{n(av)}^{(a)} \quad (3.51)$$

The deviation at point 4, the mid-point of the side 23 is calculated on similar lines. When this is calculated, these deviations can be expressed as

$$\begin{Bmatrix} \delta_4^{(a)} \\ \delta_5^{(a)} \end{Bmatrix} = \begin{bmatrix} a_{11} & a_{12} & a_{13} \\ a_{21} & a_{22} & a_{23} \end{bmatrix} \begin{Bmatrix} A_7 \\ A_8 \\ A_9 \end{Bmatrix} \quad (3.52)$$

where,

$$\begin{aligned} a_{11} &= -\frac{3}{4} x_{32}^2 \sin \gamma_1 \\ a_{12} &= \frac{3}{4} y_3 \cos \gamma_1 \\ a_{13} &= -\left(\frac{y_3^2}{4} \sin \gamma_1 - \frac{x_{32} y_3}{2} \cos \gamma_1\right) \end{aligned} \quad (3.53)$$

$$\begin{aligned} a_{21} &= \frac{3}{4} x_3^2 \sin \gamma_2 \\ a_{22} &= -\frac{3}{4} y_3^2 \cos \gamma_2 \\ a_{23} &= \left(\frac{y_3^2}{4} \sin \gamma_2 - \frac{x_3 y_3}{2} \cos \gamma_2\right) \end{aligned}$$

$$x_{32} = x_3 - x_2$$

Let $E_1^{(a)}$ and $E_2^{(a)}$ be

the corrective functions associated with the sides 23 and 13 respectively. Following the reasoning given in the previous paragraphs, the corrected displacement function of the sub-element a is given by

$$\begin{aligned} w^{(a)} &= A_1 + A_2 x + A_3 y + A_4 x^2 + A_5 xy + A_6 y^2 \\ &+ A_7 \left[x^3 - a_{11} E_1^{(a)} - a_{21} E_2^{(a)} \right] \\ &+ A_8 \left[y^3 - a_{12} E_1^{(a)} - a_{22} E_2^{(a)} \right] \\ &+ A_9 \left[xy^2 - a_{13} E_1^{(a)} - a_{23} E_2^{(a)} \right] \end{aligned} \quad (3.54)$$

These correction functions nullify the deviation from the linearity of the normal slopes given by the original displacement function (Eq. 3.38),

along the inner boundaries 13 and 23 (Figure 3.5) of the sub-element a. Since the normal slopes now vary linearly along the edges 13 and 23, the equation (3.54) represents a conforming displacement function for the sub-element a, because the normal slope along the exterior edge 12 has already a linear variation due to the selection of the original displacement function of equation (3.38). Such conforming functions are determined for the remaining two sub-elements. The individual stiffness matrices are then determined from their displacement functions with respect to their own local co-ordinates. Once this is done, the stiffness matrix of the total element composed of these three sub-elements is easily determined with respect to (x_0, y_0, z_0) system.

Derivation of the Correction Functions

These functions are determined such that they fulfil the requirements stated in a previous paragraph. But unfortunately it is almost impossible to derive a simple function which satisfies the conditions. Zienkiewicz (39) has suggested a few functions one of which was proposed by Irons (38). An explicit evaluation of the integrals of stiffness matrix becomes extremely involved due to the complex nature of these correction functions. Therefore, it becomes necessary to resort to numerical integration.

In this study the correction functions have been derived in a piece-wise manner. For this purpose,

the sub-element a is now divided into three zones by joining the three corners and its centre of gravity as shown in Figure 3.9. The local co-ordinates $(\bar{x}, \bar{y}, \bar{z})$ are also indicated. Let these divided zones be denoted as I, II and III. The correction functions $E_1^{(a)}$ and $E_2^{(a)}$ are defined piece-wise over the zones I, II and III as follows

$$\begin{aligned}
 E_1^{(a)}(I) &= A_{11}\bar{y}^2 + A_{12}\bar{y}^3 + A_{13}\bar{x}\bar{y}^2 \\
 E_1^{(a)}(II) &= \frac{4}{\bar{x}_2} \bar{x} (\bar{x} - \bar{x}_2)\bar{y} + B_{11}\bar{y}^2 \\
 &\quad + B_{12}\bar{y}^3 + B_{13}\bar{x}\bar{y}^2 \qquad (3.55)
 \end{aligned}$$

$$E_1^{(a)}(III) = C_{11}\bar{y}^2 + C_{12}\bar{y}^3 + C_{13}\bar{x}\bar{y}^2$$

and,

$$\begin{aligned}
 E_2^{(a)}(I) &= A_{21}\bar{y}^2 + A_{22}\bar{y}^3 + A_{23}\bar{x}\bar{y}^2 \\
 E_2^{(a)}(II) &= B_{21}\bar{y}^2 + B_{22}\bar{y}^3 + B_{23}\bar{x}\bar{y}^2 \qquad (3.56)
 \end{aligned}$$

$$\begin{aligned}
 E_2^{(a)}(III) &= \frac{4\bar{x}}{\bar{x}_2} (\bar{x} - \bar{x}_2)\bar{y} + C_{21}\bar{y}^2 \\
 &\quad + C_{22}\bar{y}^3 + C_{23}\bar{x}\bar{y}^2
 \end{aligned}$$

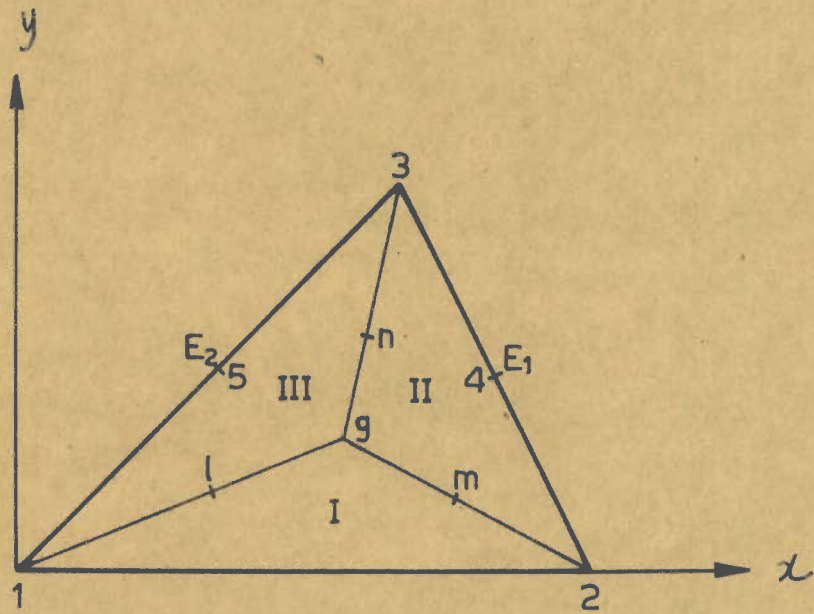
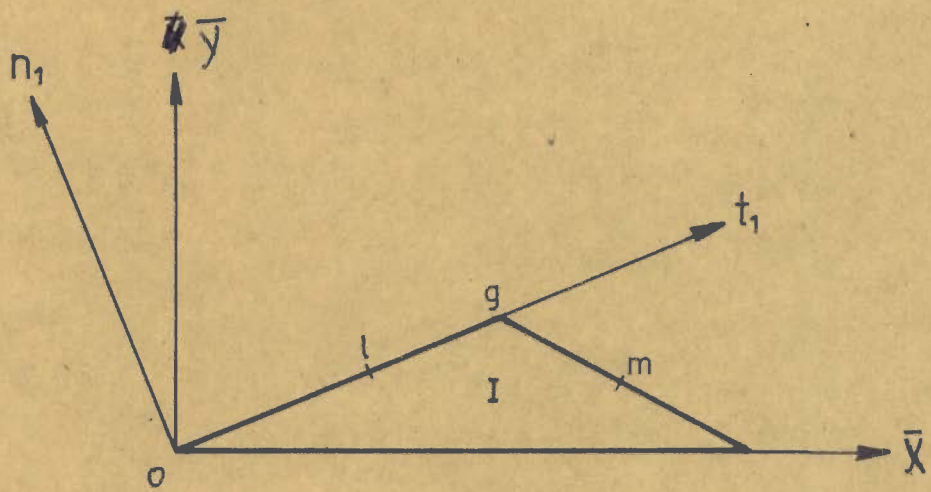
Numerical integration is avoided when the correction functions are selected in this manner. Each one of these functions involves nine undetermined constants. The terms involving no constant provide unit inward normal slopes at the mid-points of the sides $\bar{y} = 0$ of the zones II and III. Because of this reason,

the deviations $\int_4^{(a)}$ and $\int_5^{(a)}$ were determined by calculating the inward normal slopes. At this stage, few important characteristics of the selected functions are to be recognised. First, these functions become zero along the edges $\bar{y} = 0$ of the zones I, II and III. Secondly, these functions and their first derivatives vanish at the nodes of the sub-element a. Thus the ~~req~~ required correction functions are defined completely after evaluating the undetermined constants. These constants are determined by solving an equal number of simultaneous equations which are formed by observing that the correction functions defined piece-wise over the zones I, II and III, and the corresponding first derivatives, should match perfectly along the interfaces of the divided zones of the sub-element, Figure 3.9.

^F
For this purpose, continuity is considered first at the centre of gravity g of the sub-element where the zones I, II and III meet (Figure 3.9). At this point the continuity conditions are as follows:

$$\begin{aligned} \text{(I)} & & \text{(II)} \\ u_g & = & u_g \\ \text{(II)} & & \text{(III)} \\ u_g & = & u_g \end{aligned} \tag{3.57}$$

where the vector u_g denotes the function and the first derivatives with respect to the co-ordinate system (x, y, z) of the sub-element, Figure 3.9. Therefore,



\bar{x}, \bar{z} AXES UPWARD

FIG. 3.9 DIVISION OF A SUB-ELEMENT INTO ZONES

$$u_g = \left\{ \begin{array}{c} E \\ \frac{\partial E}{\partial x} \\ \frac{\partial E}{\partial y} \end{array} \right\} \quad (3.58)$$

g

where, E is a correction function. Equations (3.57) thus, provide six conditions. These conditions lead to the continuity of the corrective function and the derivative $\frac{\partial E}{\partial t_1}$ along the lines separating the zones I, II and III, Figure 3.9. However, the continuity of the derivative $\frac{\partial E}{\partial n_1}$ in the direction n_1 normal to these lines is yet to be established. These derivatives are made continuous by equating them at the mid-points of the three lines separating the above mentioned zones. This gives,

$$\begin{array}{lcl} \text{(III)} & & \text{(I)} \\ u_{n1} & = & u_{n1} \\ \text{(I)} & & \text{(II)} \\ u_{nm} & = & u_{nm} \\ \text{(II)} & & \text{(III)} \\ u_{nn} & = & u_{nn} \end{array} \quad (3.59)$$

where $u_n = \frac{\partial E}{\partial n_1}$ (3.60)

Equations (3.57) and (3.59) provide nine simultaneous equations to determine the constants of the correction functions defined piece-wise in equations (3.55) and (3.56). The conforming displacement function of the sub-element a given by the equation (3.54) is completely defined once these constants are

determined. Similar displacement functions are derived for the remaining two sub-elements b and c. When this is done, the stiffness matrices of all the three sub-elements are derived in the usual way described in section 2.6. The stiffness matrix of the total element is then derived by using the stiffness matrices of the sub-elements.

Following the steps outlined in section 2.7, the stiffness matrix of the total element composed of three sub-elements a, b and c is obtained as

$$\begin{Bmatrix} R_i \\ R_j \\ R_k \\ R_o \end{Bmatrix} = \begin{bmatrix} K \end{bmatrix} \begin{Bmatrix} r_i \\ r_j \\ r_k \\ r_o \end{Bmatrix} \quad (3.61)$$

All the above notations have the same meaning as was assigned to them when they appeared first. The stiffness matrix of equation (3.61) has the size of 12 x 12. It expresses the force-displacement relationships at the four nodes i, j, k and o. This matrix is now reduced to 9 x 9 size, expressing the force-displacement relationships at the external nodes i, j and k by observing that no forces are applied at the internal node o, Figure 3.4. For this purpose, the matrices of equation (3.61) are partitioned as below

$$\begin{Bmatrix} R \\ \bar{R}_o \end{Bmatrix} = \begin{bmatrix} K_{11} & K_{12} \\ K_{21} & K_{22} \end{bmatrix} \begin{Bmatrix} r \\ r_o \end{Bmatrix} \quad (3.62)$$

where,

$$R = \begin{Bmatrix} R_i \\ R_j \\ R_k \end{Bmatrix} \quad (3.63)$$

and,

$$r = \begin{Bmatrix} r_i \\ r_j \\ r_k \end{Bmatrix} \quad (3.64)$$

Since no external forces are applied at the node 0, the conditions of equilibrium are satisfied by writing the equation (3.6~~3~~²) as

$$\begin{Bmatrix} R \\ - \\ 0 \end{Bmatrix} = \begin{bmatrix} K_{11} & K_{12} \\ K_{21} & K_{22} \end{bmatrix} \begin{Bmatrix} r \\ - \\ r_0 \end{Bmatrix} \quad (3.65)$$

The above relations can be broken up as (omitting the brackets)

$$R = K_{11}r + K_{12}r_0 \quad (3.66)$$

$$0 = K_{21}r + K_{22}r_0 \quad (3.67)$$

From equation (3.67)

$$r_0 = -K_{22}^{-1} K_{21}r \quad (3.68)$$

Substituting r_0 in equation (3.66)

$$R = (K_{11} - K_{12}K_{22}^{-1} K_{21}) r \quad (3.69)$$

Equation (3.69) states the force-displacement relationships at the nodes i , j and k of the total

element. Therefore, the required stiffness matrix of the total element is

$$k = \begin{pmatrix} K_{11} & -K_{12} \\ K_{12} & K_{22} \end{pmatrix}^{-1} K_{21} \quad (3.70)$$

The vectors R and r denoting the forces and the displacements respectively at the nodes i , j and k are now replaced by the usual notations for the nodal forces and displacements of an element. Therefore, the stiffness matrix of the total element is

$$F = ku \quad (3.71)$$

where, k is defined in equation (3.70)

The selection of equation (3.38) as the original displacement function for a sub-element did automatically lead to the linear variation of normal slope along $y = 0$, but because of it, the symmetry in the appearance of the displacement function is lost. However, the loss is almost fully recovered by using the total element of the Figure 3.4, composed of three sub-elements. This is because the sub-elements tend to compensate for each other. Moreover, with successive refinements in the sub-divisions symmetry property will improve. Similar behaviour is to be expected of the function proposed by Clough (22).

In this study quadrilateral elements have not been considered separately. A quadrilateral can be divided into two or four sub-elements as shown in Figure 3.10. Therefore, the stiffness matrix of these elements can be very conveniently obtained by using the stiffness matrices of the triangular element discussed above.

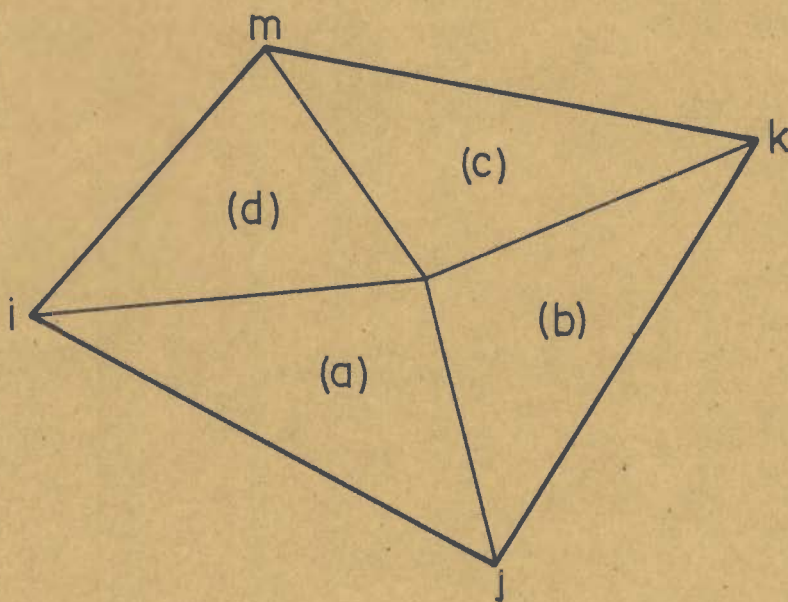
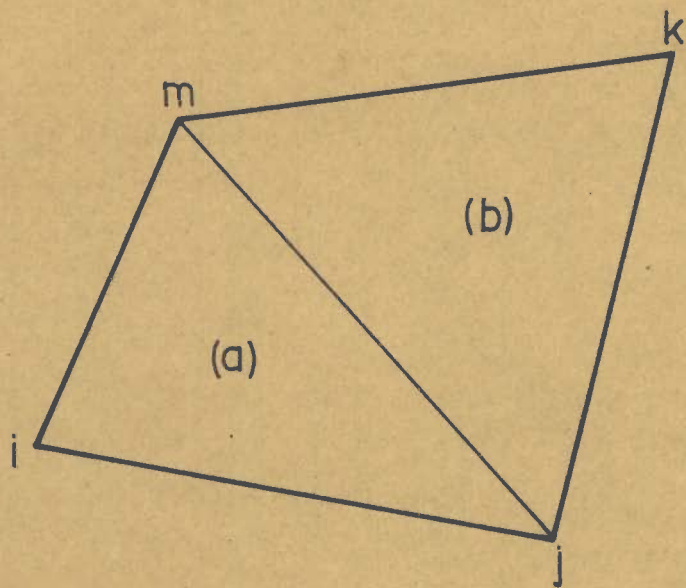


FIG. 3.10. COMPOSITE QUADRILATERAL ELEMENTS

CHAPTER FOUR

EXAMPLES AND DISCUSSION ON RESULTS

4.1 INTRODUCTION

To test the reliability of the functions proposed in the previous chapter, several plate bending problems were solved using an IBM 1620 Model I Computer. Results of the analysis are presented here for some of these problems attempted. All the examples have been selected from among the large number of problems solved by earlier investigators to demonstrate the merits of the functions proposed by them. The sources from which the problems have been selected are also indicated to facilitate comparative study. While presenting the results of the examples considered here, the results of an analysis by a standard method have also been given. This standard method is either the exact or an acceptable approximate approach that has been used for comparison to serve as a yard stick in the source reference from which the example is selected.

4.2 DISPLACEMENT FUNCTIONS TESTED

Only two functions need be considered, one for rectangular and the other for triangular elements, to test the correctness of the derivations.

However, the results are presented for four different functions; three are for rectangular elements and one for triangular elements. This has been done in order to assess the relative performance of the different functions proposed for rectangular elements. In presenting the results, the displacement functions have been identified in the following manner:

(i) TE, for triangular element,
equation (3.54)

(ii) RE-1, for rectangular element where

$$f(x) = -\frac{1}{\pi} \sin \frac{\pi x}{a}$$

$$f(y) = -\frac{1}{\pi} \sin \frac{\pi y}{b}$$

in equation (3.32)

(iii) RE-2, for rectangular element where

$$f(x) = \frac{x}{a} - \sin \frac{\pi x}{2a}$$

$$f(y) = \frac{y}{b} - \sin \frac{\pi y}{2b}$$

in equation (3.32)

(iv) RE-3, for rectangular element where

$$f(x) = \frac{1}{3} \left[2\left(\frac{x}{a}\right)^3 - 3\left(\frac{x}{a}\right) + \sin \frac{\pi x}{2a} \right]$$

$$f(y) = \frac{1}{3} \left[2\left(\frac{y}{b}\right)^3 - 3\left(\frac{y}{b}\right) + \sin \frac{\pi y}{2b} \right]$$

in equation (3.32)

4.3 EXAMPLES WORKED OUT

Study of eight different plate bending problems using the displacement functions described above, are presented in section 4.5. All the plates are assumed to be isotropic and of constant thickness. The examples are described as:

- Problem - 1 Deflection analysis of a square plate subjected to pure twist (22). The plate is considered to be simply supported at three corners and free at the fourth corner. Deflections have been determined at the centre and under the concentrated load of five pounds, acting at the free corner, Figure 4.7. This case has been studied only by using rectangular elements.
- Problem 2-7 Described in table 4.⁰7
- Problem - 8 Study of deflections in a rhombic cantilever plate subjected to uniformly distributed load (22). This example has been studied only by using triangular elements. Figure 4.9 shows the plate and the assumed finite element idealisation.

PROBLEM	GEOMETRY	EDGE CONDITIONS	LOAD	RESULTS GIVEN	ELEMENT	SOURCE
2	square	all edges (SS)	U	w, M_x, M_y	R, T	22, 26, 39
3	"	"	C	"	"	22, 26, 39
4	"	all edges (C)	U	"	"	22, 26, 39
5	"	"	C	"	"	22, 26, 39
6	"	Cantilever	U	"	R	23, 55
7	rectangle (1:2)	three adjacent edges (C), one (F)	U	M_x, M_y	"	33

(SS) = simply supported, (C) = Clamped, (F) = free
 U = uniformly distributed load, C = concentrated load at the centre,
 R = rectangular, T = triangular

TABLE 4.0 DESCRIPTION OF PLATE BENDING PROBLEMS

The results are presented in the form of tables. Tables were preferred as the results of the analysis by the displacement functions for rectangular elements are very close and become indistinguishable from each other, if plotted, even when the subdivision is coarse. However, some of the results of the analysis by the function TE have been plotted (Figures 4.10 to 4.15). The results are presented separately for rectangular and triangular elements. This is because convergence is faster when rectangular elements are used.

To investigate convergence, the problems have been studied for different sub-divisions. Figure 4.1 shows the sub-divisions used for rectangular elements. All the elements are of the same size and square in geometry. The mesh systems used for triangular elements are shown in Figure 4.2. Here also, square mesh systems have been adopted by using the built-up elements. Whenever possible, single or double symmetry has been considered.

Moments M_x and M_y are tabulated only for the finest sub-division analysis. For rectangular elements these moments have been calculated in two-ways:

- (i) from moment-curvature relations using the displacement function,
- (ii) from the element stiffness matrix $F = ku$

When more than one element meets at a node, the individual corner forces are different. Therefore, the results presented for the moments refer to their

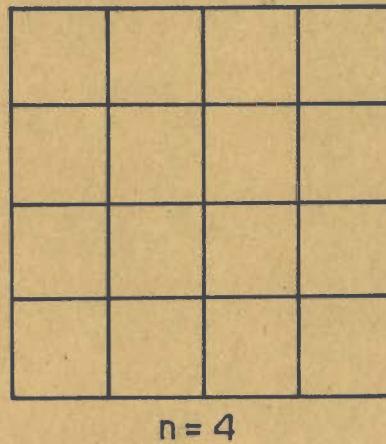
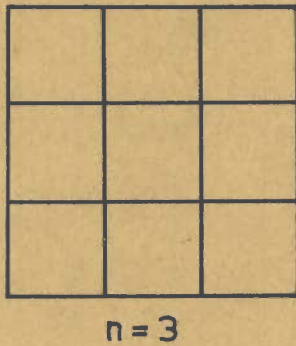
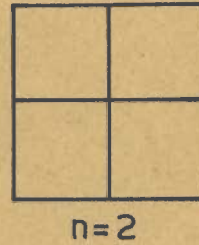
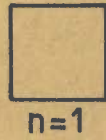


FIG. 4.1 SUB-DIVISIONS FOR RECTANGULAR ELEMENTS

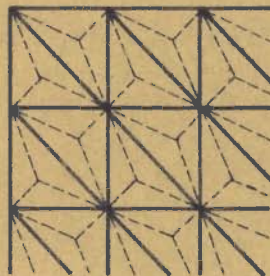
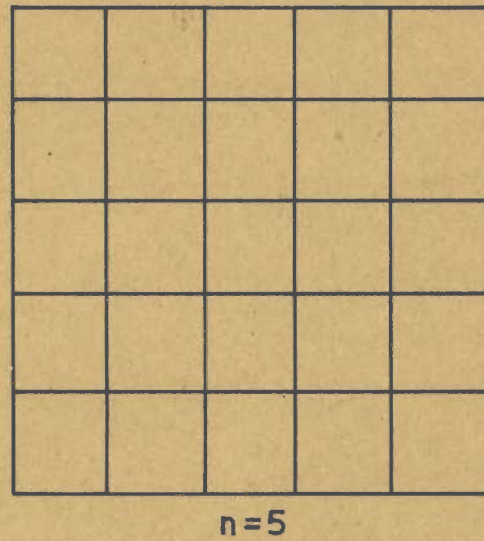
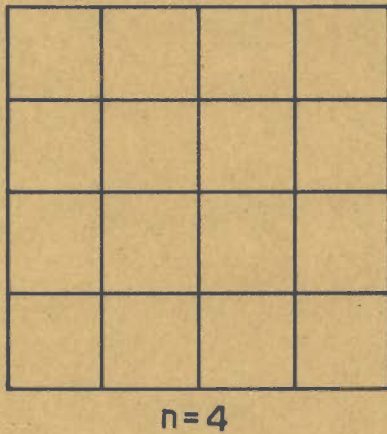
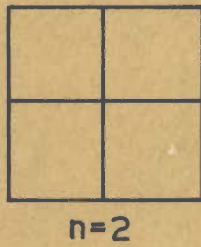
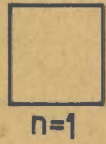


FIG. 4.2 SUB-DIVISIONS USED FOR TRIANGULAR ELEMENTS

mean values at the nodes. For triangular elements the moments have been calculated from the finite difference equations using the known values of nodal displacements.

When a plate is subjected to uniformly distributed load, the forces to be applied at the nodes of an assemblage can be,

either, simple concentrated nodal loads on the basis of the area that a node commands in the entire assemblage,
or, equivalent nodal forces determined from the principle of virtual work as discussed in section 2.7.

In all the examples, the nodal forces have been determined by the first method. However, for problem-2 the nodal forces have been calculated by both methods when rectangular elements are used. Results of analysis by using these two different nodal forces are presented side by side to facilitate easy comparison. For problem-5, both the methods give same nodal forces. Figure 4.3 shows the tributary areas for calculating the nodal loads by the first method for a 2 x 2 sub-division. For triangular elements only the first method has been used.

The sub-division analysis can be done in two ways. One way is to use the stiffness matrix of an element whose sides are successively reduced

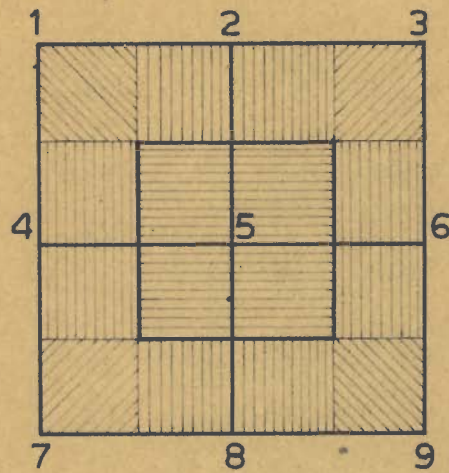
in size in linear proportion with the successive increase in the number of elements in the mesh system. For example, in the analysis of a square plate of side L the element side lengths for 1×1 sub-division should be L , $L/2$ for 2×2 , $L/3$ for 3×3 and L/n for the $n \times n$ system. Because of this the output will always be for the same plate and for each sub-division analysis a new element stiffness matrix has to be read.

Alternatively, the same element stiffness matrix can be used for each sub-division analysis. If this is done, the results for $n \times n$ system refers to the analysis of a plate of side lengths equal to n times the side lengths of the element. However, these results can be easily converted to the results for the actual plate. In this method only one element stiffness matrix is needed.

4.4 BRIEF DESCRIPTION OF COMPUTER WORK ON IBM 1620

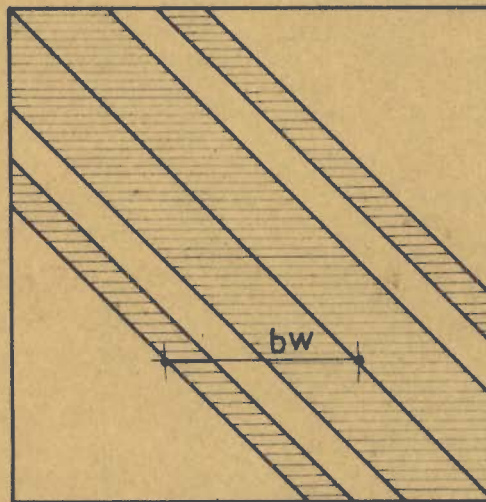
The equations of equilibrium, i.e., the stiffness matrix of the entire assemblage is generated by summing up the individual element stiffness matrices. This stiffness matrix, by suitable numbering of the nodes of the assemblage, can be represented as shown in Figure 4.4. The bandwidth depends on the numbering of the nodes.

At first a FORTRAN program was written which generates the entire stiffness matrix of the assemblage. The matrix is then condensed by



$n=2$

FIG. 4.3 NODAL LOADS FROM TRIBUTARY AREAS



bw = band-width

FIG. 4.4 STIFFNESS MATRIX [K]

applying the boundary conditions of the problem which leads to the elimination of some columns and rows of the matrix. After this the matrix is inverted by using a library sub-routine based on the Gauss elimination method. The nodal displacements are then obtained by performing the matrix multiplication operation on the inverted matrix and the load vector. This method is very simple and straight forward, but unfortunately because of the limited capacity of the available IBM 1620 computer (60,000 digit locations including additional core storage) this program could not be used beyond a very coarse sub-division. This was so even when the element stiffness matrix was obtained from a separate program and another program was written for calculating the moments. However, the program served the purpose of checking the derivations to a large extent.

The computer work was, therefore, modified so that reasonable accuracy is achieved in the analysis. These features are described below:

- (i) Separate programs have been written for generating the element stiffness matrices.
- (ii) A "MAIN PROGRAM" was written to generate half the band matrix as shown in Figure 4.4, taking advantage of the symmetry of the stiffness matrix.

In this program, the most significant

saving has been achieved by storing the nett or the effective band matrix whose size depends on the boundary conditions. Obviously, this saving has been made by ignoring the unwanted rows and columns of the stiffness matrix during its generation. To do this, one extra column matrix of size equal to total number of nodes for any sub-division times the assumed degrees of freedom at the nodes has been used for incorporating the boundary conditions. This matrix is read as data; its elements are either zero or non-zero. Whenever an element, say the i th element, is zero, the nodal displacement corresponding to the i th column of the stiffness matrix of the assemblage is considered to be zero as shown in Figure 4.5. Thus, during the generation of the stiffness matrix, the rows and oolumns corresponding to all the zero elements in the auxiliary column matrix are ignored.

The band matrix generated as above has been solved by using a library sub-routine "SYMBND". This is based on Cholesky's method. The nodal displacements are then calculated using another library sub-routine "SYMSOL" which performs the multiplication operation on the solved band matrix and the load matrix.

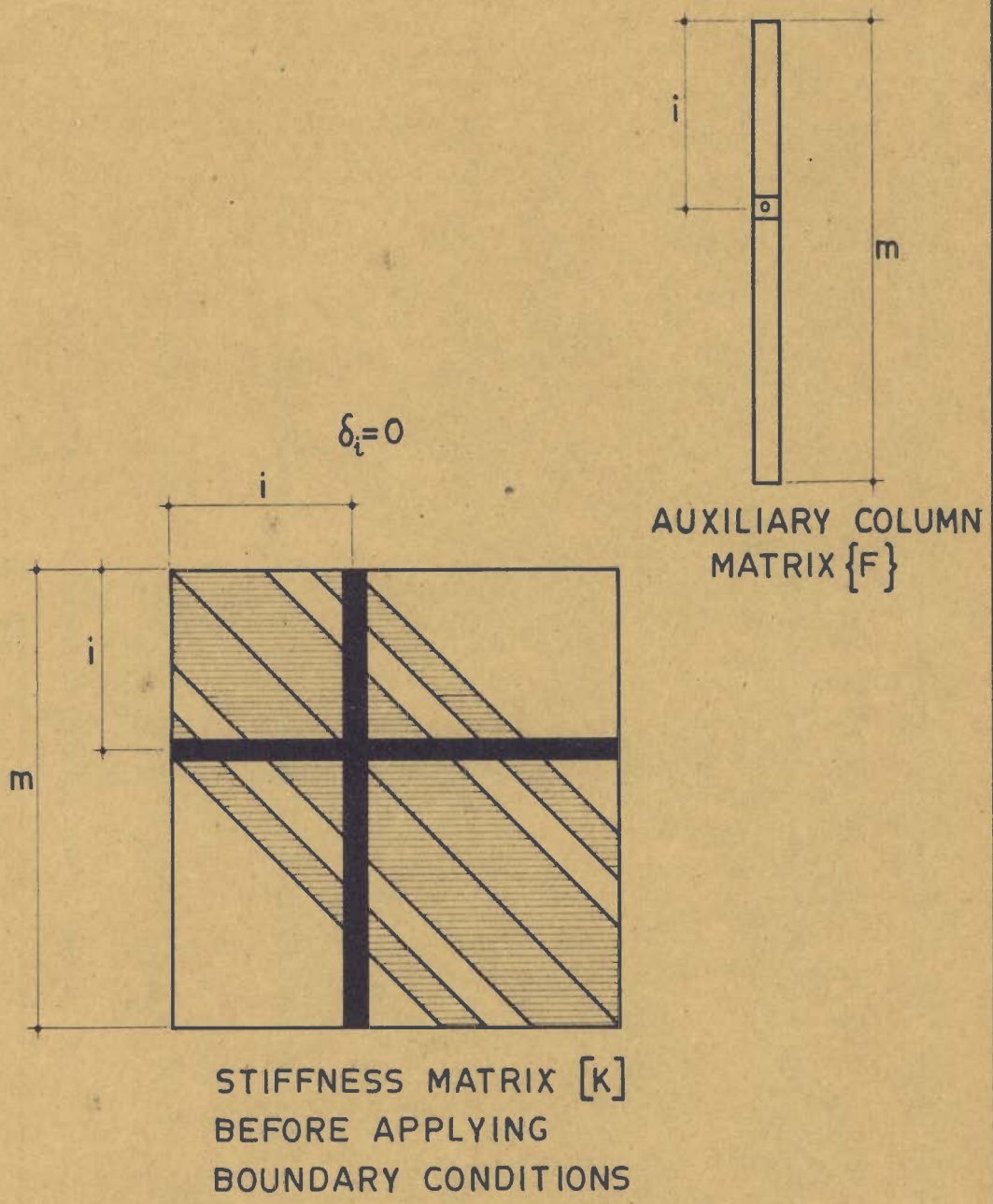


FIG. 4.5 $[K]$ AND $\{F\}$ MATRICES

The results, i.e., the nodal displacements are stored in the space used for reading the loads.

All the examples have been analysed by using elements of the same size. Therefore, to perform all the computations described upto the last paragraph only one element stiffness matrix is required. This element stiffness matrix is read in the beginning as data and stored in the memory. After determining the nodal displacements, the corner displacements of all the elements are related to them. The corner forces of all the elements are then calculated by using the element stiffness matrix stored in the beginning and the element displacements determined from the nodal displacements of the assemblage.

- (iii) A third program "STRESS" has been written to calculate the moments from the moment-curvature relations. In this program the output of displacements from the "MAIN" program is fed as input data.

The planning of the computer work as described above has taken considerable time but it has improved the computational work in two significant ways. First, more number of equations can be generated. Secondly, computation time is reduced by the use of band matrix. The size of band matrix that can be stored is 82×40 , when the nodal forces are determined in the MAIN program by using the element stiffness matrix.

The programs developed, have some limitations and the work has been divided into parts which is not ideal from the point of convenience. But all these limitations can be easily overcome by altering a few cards and the entire work can be converted into a single program by treating the first and the third parts as sub-programs of the main routine, to be used advantageously in a faster machine with larger memory space. All these space saving techniques have been adopted to suit the extremely limited memory space of IBM 1620. Moreover, the problems have been selected carefully so that reasonable accuracy is achieved within the framework of the available facilities. By assuming a uniform mesh system, wherein the elements are square and of the same size, only one element stiffness matrix need be read and stored in the machine during the execution of the MAIN program. This has helped in keeping the data preparation to a minimum. Figure 4.6 gives the flow chart of the MAIN program.

4.5 TABLES OF RESULTS

Plate geometry and the portions analysed for the various examples are shown in Figure 4.7 through 4.9. The results presented for the first and the last examples represent the actual deflections at the points mentioned in the tables. For the remaining problems the results given are the co-efficients of deflections and moments M_x and M_y .

NOTE:

$N\emptyset E$ = TOTAL
ELEMENTS

$ND\emptyset F$ = DEGREES OF
FREEDOM AT
NODE

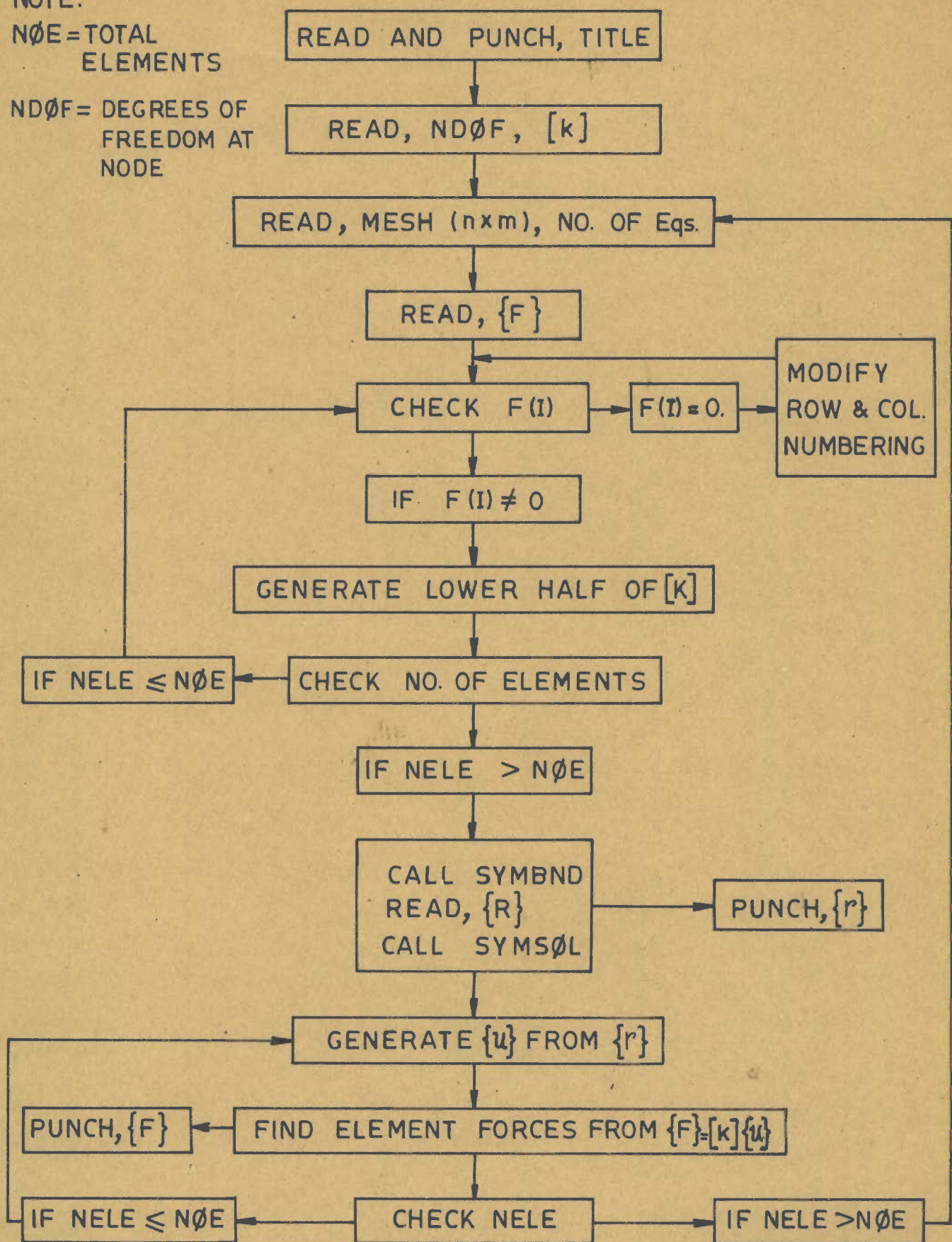


FIG. 4.6 MAIN PROGRAM FLOW CHART

The expressions for w , M_x and M_y may be obtained in each case as indicated below:

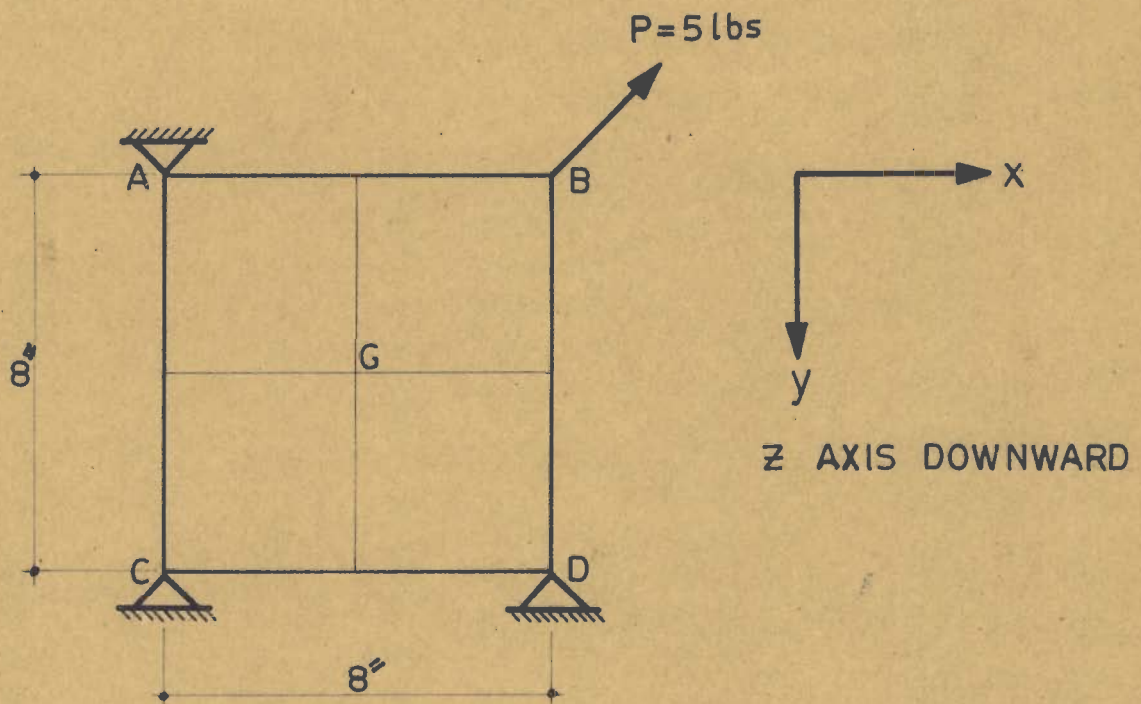
- (i) when the plate is subjected to uniformly distributed load q

$$\begin{aligned}w &= \alpha \frac{qL^4}{D} \times 10^{-3} \\M_x &= \beta_x qL^2 \times 10^{-2} \\M_y &= \beta_y qL^2 \times 10^{-2}\end{aligned}\quad (4.1)$$

- (ii) when the plate is subjected to a concentrated load P at the centre

$$\begin{aligned}w &= \alpha \frac{PL^2}{D} \times 10^{-3} \\M_x &= \beta_x P \times 10^{-2} \\M_y &= \beta_y P \times 10^{-2}\end{aligned}\quad (4.2)$$

In tables of moments for the functions RE-1, RE-2 and RE-3 two sets of results are given. The results for method (1) represent the values obtained from the element stiffness matrices (Eq. 2.26) and the results from the moment-curvature relations (Eq. 2.11) are under the heading method (2). In all the examples the nodes are to be located by counting the rows first and next the columns on which they lie. An example of numbering is shown in Figure 4.8.

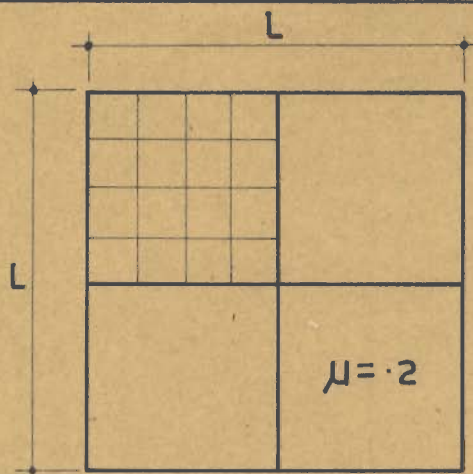


$$t = 1 \text{ in}$$

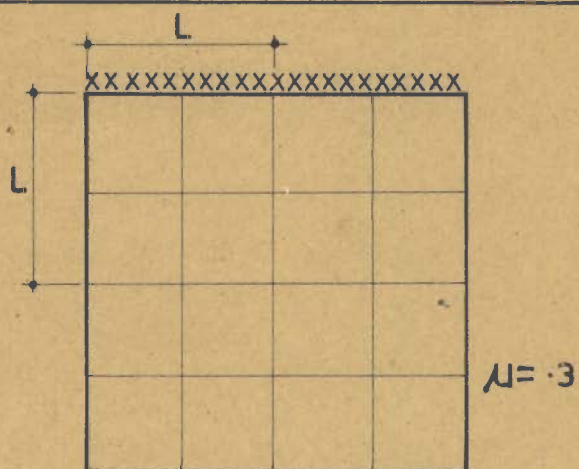
$$E = 100000 \text{ psi}$$

$$\mu = 0.3$$

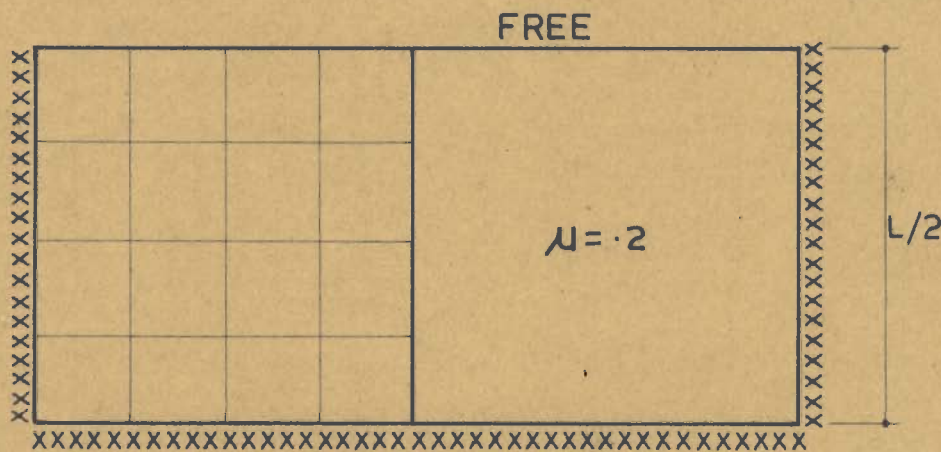
FIG. 4.7 SQUARE PLATE UNDER PURE TWIST



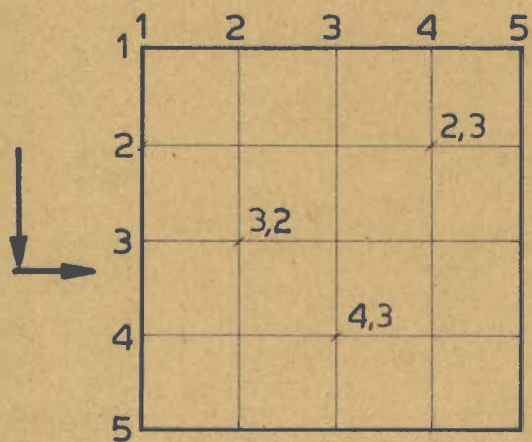
(a) EX: 2-5



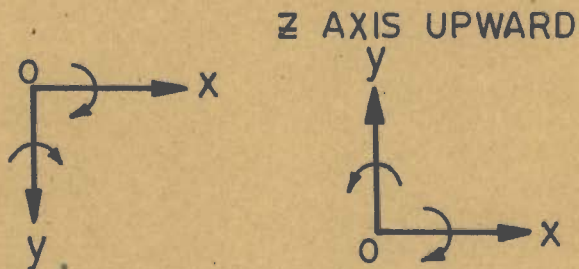
(b) EX: 6 - CANTILEVER



(c) EX: 7



(d) EXAMPLE OF NODAL NUMBERING



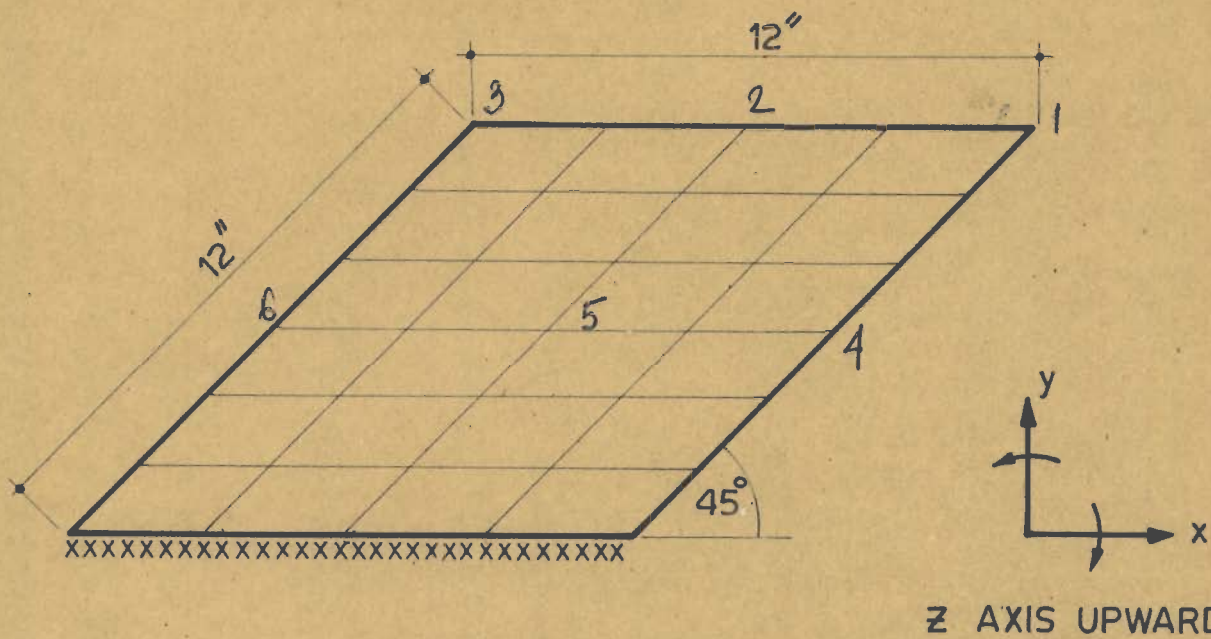
Z AXIS DOWNWARD

I. RECTANGULAR ELEMENT

II. TRIANGULAR ELEMENT

(e) CO-ORDINATES SYSTEM

FIG. 4.8 DETAILS OF EXAMPLES

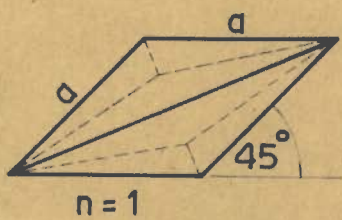


$q = 0.26066 \text{ psi}$

$E = 10.5 \times 10^6 \text{ psi}$

$t = 0.125 \text{ in}$

$\mu = 0.3$



TYPE - I

FIG. 4.9 RHOMBIC CANTILEVER

TABLE 4.1.1

DEFLECTIONS IN A SQUARE PLATE UNDER PURE TWIST WITH 2X2 MESH

FUNCTION	AT A β	AT G
RE-1	0.249595	0.062398
RE-2	0.249597	0.062399
RE-3	0.249597	0.062399
EXACT	0.2496	0.0624

TABLE 4.2.1 A

CONVERGENCE OF CENTRAL DEFLECTION , EX-2
RESULTS FOR RECTANGULAR ELEMENTS
NODAL FORCES CALCULATED FROM TRIBUTARY AREAS

MESH	RE-1	RE-2	RE-3
1X1	1.9972	2.4948	2.5300
2X2	3.4857	3.5998	3.6114
3X3	3.7993	3.8496	3.8552
4X4	3.9119	3.9402	3.9438

EXACT 4.0624

TABLE 4.2.1 B

CONVERGENCE OF CENTRAL DEFLECTION , EX-2
RESULTS FOR RECTANGULAR ELEMENTS
USING EQ. FORCES FROM VIRTUAL WORK

MESH	RE-2	RE-3
1X1	4.7217	4.7887
2X2	4.3097	4.3266
3X3	4.1780	4.1849
4X4	4.1277	4.1318

EXACT 4.0624

TABLE 4.2.2 A

DEFLECTIONS AT SEVERAL POINTS AT 4X4 SUB-DIVISION , EX-2
 NODAL FORCES CALCULATED FROM TRIBUTARY AREAS

POINTS	RE-1	RE-2	RE-3	EXACT
22	1.2668	1.2869	1.2899	0.6589
33	2.0332	2.0548	2.0573	2.1322
44	3.3746	3.4010	3.4043	3.5109
55	3.9119	3.9402	3.9438	4.0624
54	3.6332	3.6604	3.6639	3.7762
53	2.8198	2.8431	2.8460	2.9382
52	1.5510	1.5659	1.5675	1.6232

TABLE 4.2.2 B

DEFLECTIONS AT SEVERAL POINTS AT 4X4 SUB-DIVISION , EX-2
 USING EQ. FORCES FROM VIRTUAL WORK

POINTS	RE-2	RE-3	EXACT
22	0.6661	0.6680	0.6589
33	2.1697	2.1725	2.1322
44	3.5691	3.5728	3.5109
55	4.1277	4.1318	4.0624
54	3.8379	3.8418	3.7762
53	2.9891	2.9923	2.9382
52	1.6549	1.6568	1.6232

TABLE 4.2.3 A

MX AT SEVERAL POINTS AT 4X4 SUB-DIVISION , EX-2
 NODAL FORCES CALCULATED FROM TRIBUTARY AREAS

POINTS	RE-1		RE-2		RE-3		EXACT
	METHOD (1)	METHOD (2)	METHOD (1)	METHOD (2)	METHOD (1)	METHOD (2)	
55	4.4125	4.2639	4.4148	4.3344	4.4160	4.3561	4.4203
54	4.2265	4.0646	4.2314	4.1516	4.2330	4.1781	4.2411
53	3.600	3.3962	3.6092	3.5311	3.6115	3.5719	3.6272
52	2.3183	2.0375	2.3264	2.2506	2.3284	2.3154	2.3442

TABLE 4.2.3 B

MX AT SEVERAL POINTS AT 4X4 SUB-DIVISION , EX-2
USING EQ. FORCES FROM VIRTUAL WORK

POINTS	RE-2		RE-3		EXACT
	METHOD (1)	METHOD (2)	METHOD (1)	METHOD (2)	
55	4.5669	4.4866	4.5684	4.5075	4.4203
54	4.3902	4.3084	4.3922	4.3362	4.2411
53	3.7884	3.7104	3.7911	3.7504	3.6272
52	2.5405	2.4648	2.5430	2.5290	2.3442

TABLE 4.2.4 A

MY AT SEVERAL POINTS AT 4X4 SUB-DIVISION , EX-2
NODAL FORCES CALCULATED FROM TRIBUTARY AREAS

POINTS	RE-1		RE-2		RE-3		EXACT
	METHOD (1)	METHOD (2)	METHOD (1)	METHOD (2)	METHOD (1)	METHOD (2)	
55	4.4125	4.2639	4.4148	4.3344	4.4160	4.3561	4.4203
54	4.1257	3.9787	4.1272	4.0456	4.1280	4.0663	4.1254
53	3.2753	3.1327	3.2756	3.1906	3.2756	3.2088	3.253
52	1.8978	1.7552	1.9001	1.8091	1.8995	1.8258	1.8476

TABLE 4.2.4 B

MY AT SEVERAL POINTS AT 4X4 SUB-DIVISION , EX-2
USING EQ. FORCES FROM VIRTUAL WORK

POINTS	RE-2		RE-3		EXACT
	METHOD (1)	METHOD (2)	METHOD (1)	METHOD (2)	
55	4.5669	4.4866	4.5684	4.5075	4.4203
54	4.2726	4.1913	4.2737	4.2109	4.1254
53	3.4012	3.3164	3.4014	3.3335	3.253
52	1.9933	1.9024	1.9732	1.9182	1.8476

TABLE 4.3.1

CONVERGENCE OF CENTRAL DEFLECTION , EX-3
RESULTS FOR RECTANGULAR ELEMENTS

MESH	RE-1	RE-2	RE-3
1X1	7.9889	9.9792	10.1202
2X2	10.6249	11.2426	11.2927
3X3	11.1359	11.4403	11.4640
4X4	11.3232	11.5076	11.5223

EXACT 11.6

TABLE 4.3.2

DEFLECTIONS AT SEVERAL POINTS AT 4X4 SUB-DIVISION , EX-3

POINTS	RE-1	RE-2	RE-3	EXACT
22	1.2668	1.2869	1.2899	1.3167
33	4.7001	4.7258	4.7305	4.7677
44	8.8744	8.9297	8.9372	8.9864
55	11.3232	11.5076	11.5223	11.6
54	9.9217	10.001	10.008	10.066
53	7.0407	7.0907	7.0964	7.1392
52	3.6163	3.6409	3.6441	3.6684

TABLE 4.3.3

MX AT SEVERAL POINTS AT 4X4 SUB-DIVISION , EX-3

POINTS	RE-1		RE-2		RE-3		EXACT
	METHOD (1)	METHOD (2)	METHOD (1)	METHOD (2)	METHOD (1)	METHOD (2)	
55	33.5433	18.7800	32.7983	29.2737	32.6598	32.7464	55.572 (∞)
54	10.6986	12.9499	11.2230	10.1101	11.2681	12.3356	11.023
53	4.9452	5.2214	5.0281	4.9041	5.0403	4.7706	5.0564
52	1.9501	2.0725	1.9934	1.9653	1.9994	1.9265	2.0361

TABLE 4.3.4

MY AT SEVERAL POINTS AT 4X4 SUB-DIVISION , EX-3

POINTS	RE-1		RE-2		RE-3		EXACT
	METHOD (1)	METHOD (2)	METHOD (1)	METHOD (2)	METHOD (1)	METHOD (2)	
55	33.5433	18.7800	32.7983	29.2737	32.6598	32.7464	55.572 (∞)
54	17.1913	14.7959	17.3139	16.7159	17.3690	17.2089	16.897
53	9.5526	8.8284	9.6670	9.6301	9.6767	9.8539	9.5398
52	4.4672	4.2242	4.4937	4.4947	4.4964	4.5739	4.4555

TABLE 4.4.1

CONVERGENCE OF CENTRAL DEFLECTION , EX-4
RESULTS FOR RECTANGULAR ELEMENTS

MESH	RE-1	RE-2	RE-3
1X1	0.7750	1.2832	1.3319
2X2	1.1544	1.2595	1.2649
3X3	1.2161	1.2630	1.2649
4X4	1.2375	1.2640	1.2650

EXACT 1.2653

TABLE 4.4.2

DEFLECTIONS AT SEVERAL POINTS AT 4X4 SUB-DIVISION , EX-4

POINTS	RE-1	RE-2	RE-3	EXACT
22	0.0573	0.0643	0.0645	0.0645
33	0.4398	0.4593	0.4600	0.4601
44	0.9837	1.0088	1.0100	1.0102
55	1.2375	1.2640	1.2650	1.2653
54	1.1029	1.1289	1.1299	1.1302
53	0.7333	0.7572	0.7581	0.7583
52	0.2598	0.2774	0.2781	0.2783

TABLE 4.4.3

MX AT SEVERAL POINTS AT 4X4 SUB-DIVISION , EX-4

POINTS	RE-1		RE-2		RE-3		EXACT
	METHOD (1)	METHOD (2)	METHOD (1)	METHOD (2)	METHOD (1)	METHOD (2)	
55	2.2206	2.0440	2.2125	2.1323	2.2113	2.1616	2.1143
54	1.9861	1.7771	1.9765	1.8977	1.9755	1.9371	1.8738
53	1.1172	0.8045	1.1077	1.0328	1.1070	1.1044	0.9898
52	-0.9038	-1.4075	-0.8985	-0.9683	-0.8979	-0.8372	-1.0455
51	-4.9950	-2.9183	-4.9412	-4.5132	-4.9380	-5.0067	-5.1334

TABLE 4.4.4

MY AT SEVERAL POINTS AT 4X4 SUB-DIVISION , EX-4

POINTS	RE-1		RE-2		RE-3		EXACT
	METHOD (1)	METHOD (2)	METHOD (1)	METHOD (2)	METHOD (1)	METHOD (2)	
55	2.2206	2.0440	2.2125	2.1323	2.2113	2.1616	2.1143
54	1.9775	1.8040	1.9745	1.8917	1.9746	1.9199	1.8747
53	1.2778	1.1067	1.2883	1.1978	1.2877	1.2243	1.1823
52	0.2704	0.0439	0.2588	0.1547	0.2827	0.1845	0.1378
51	-1.4446	-0.5836	-1.4629	-0.9026	-1.4566	-1.0013	-1.0267

TABLE 4.5.1

CONVERGENCE OF CENTRAL DEFLECTION , EX-5
RESULTS FOR RECTANGULAR ELEMENTS

MESH	RE-1	RE-2	RE-3
1X1	3.1002	5.1329	5.3276
2X2	4.8766	5.4510	5.4865
3X3	5.2485	5.5391	5.5550
4X4	5.3925	5.5704	5.5796

EXACT 5.6

TABLE 4.5.2

DEFLECTIONS AT SEVERAL POINTS AT 4X4 SUB-DIVISION , EX-5

POINTS	RE-1	RE-2	RE-3	EXACT
22	0.1045	0.1068	0.1067	0.107
33	1.2028	1.2247	1.2256	1.23
44	3.5845	3.6360	3.638	3.64
55	5.3925	5.5704	5.5796	5.60
54	4.3199	4.3953	4.3972	4.40
53	2.4159	2.4663	2.4680	2.47
52	0.7376	0.7687	0.7699	0.77

TABLE 4.5.3

MX AT SEVERAL POINTS AT 4X4 SUB-DIVISION , EX-5

POINTS	RE-1		RE-2		RE-3		EXACT
	METHOD (1)	METHOD (2)	METHOD (1)	METHOD (2)	METHOD (1)	METHOD (2)	
55	28.6620	13.8579	27.8875	24.3653	27.7439	27.8486	36.8
54	5.7436	7.9005	6.2313	5.1232	6.2707	4.1745	5.95
53	-0.5057	-0.5025	-0.4733	-0.5832	-0.4675	-0.6359	-0.547
52	-5.3165	-5.8881	-5.3094	-5.2998	-5.3067	-5.1218	-5.41
51	-12.4161	-8.7519	-12.3124	-11.4659	-12.3001	-12.304	-12.58

TABLE 4.5.4

MY AT SEVERAL POINTS AT 4X4 SUB-DIVISION , EX-5

POINTS	RE-1		RE-2		RE-3		EXACT
	METHOD (1)	METHOD (2)	METHOD (1)	METHOD (2)	METHOD (1)	METHOD (2)	
55	28.6620	13.8579	27.8875	24.3653	27.7439	27.8486	36.8
54	12.3684	9.9377	12.4790	11.8753	12.5260	12.3775	11.8
53	4.9521	4.1983	5.0864	5.0364	5.0950	5.2689	4.88
52	0.4453	0.5185	0.5383	0.5015	0.5434	0.6030	0.433
51	-3.3612	-1.7503	-3.3646	-2.2931	-3.3452	-2.4600	2.52

TABLE 4.6.1

DEFLECTIONS AT SEVERAL POINTS AT 4X4 SUB-DIVISION , EX-6

POINTS	RE-1	RE-2	RE-3	POINT MATCHING SOLUTION	FINITE DIFFERENCE SOLUTION
23	0.2135	0.2212	0.2215	0.2191	0.1745
33	0.7257	0.7389	0.7396	0.7280	0.7291
43	1.3767	1.3939	1.3948	1.3676	1.3946
53	2.0750	2.0944	2.0955	2.0479	2.0981
52	2.0682	2.0879	2.0889	2.0385	2.0903
51	2.0516	2.0717	2.0727	2.0139	2.0701

TABLE 4.6.2

MX AT SEVERAL POINTS AT 4X4 SUB-DIVISION , EX-6

POINTS	RE-1		RE-2		RE-3		POINT MATCHING SOLUTION
	METHOD (1)	METHOD (2)	METHOD (1)	METHOD (2)	METHOD (1)	METHOD (2)	
11	-0.5867	-0.4542	-0.5519	-0.4544	-0.5346	-0.4496	0.369
12	-0.7127	-0.4764	-0.7240	-0.5905	-0.7248	-0.6258	-0.693
13	-0.6935	-0.4830	-0.7139	-0.6010	-0.7139	-0.6370	-0.699
23	-0.3200	-0.3397	-0.3127	-0.3287	-0.3129	-0.3286	-0.354
33	-0.0991	-0.1116	-0.0939	-0.0755	-0.0951	-0.1070	-0.105
43	0.0237	-0.0009	0.0240	0.0115	0.0238	0.0159	0.028

TABLE 4.6.3

MY AT SEVERAL POINTS AT 4X4 SUB-DIVISION , EX-6

POINTS	RE-1		RE-2		RE-3		POINT MATCHING SOLUTION
	METHOD (1)	METHOD (2)	METHOD (1)	METHOD (2)	METHOD (1)	METHOD (2)	
11	-1.7070	-1.5142	-1.7390	-1.5147	-1.7373	-1.4987	-1.26
12	-2.0962	-1.5883	-2.0779	-1.9685	-2.0779	-2.0836	-2.141
13	-2.0984	-1.6102	-2.1037	-2.0034	-2.1052	-2.1236	-2.11
23	-1.1278	-1.2048	-1.1274	-1.0624	-1.1273	-1.1207	-1.121
33	-0.4890	-0.5507	-0.4919	-0.4585	-0.4920	-0.4885	-0.48
43	-0.1240	-0.1835	-1.2430	-0.1358	-1.2434	-0.1209	-0.117

TABLE 4.7.1

MX AT SEVERAL POINTS AT 4X4 SUB-DIVISION , EX-7

POINTS	RE-1		RE-2		RE-3		HELLAN
	METHOD (1)	METHOD (2)	METHOD (1)	METHOD (2)	METHOD (1)	METHOD (2)	
11	-7.1510	-4.3384	-6.9717	-6.5989	-6.9456	-7.2981	-7.14
21	-5.1290	-3.1041	-5.1125	-4.6897	-5.1187	-5.1730	-5.18
31	-3.0623	-1.8594	-3.0778	-2.8587	-3.0780	-3.1616	-3.22
41	-0.9921	-0.6375	-1.0426	-1.0183	-1.0457	-1.1267	-1.15
51	0.1160	0.0	0.0694	0.0	0.0559	0.0	0.00
15	2.5804	2.5779	2.5414	2.6276	2.5388	2.6483	2.54
25	2.1098	1.8863	2.1061	2.0187	2.1053	2.0612	1.98
35	1.2764	1.0814	1.2860	1.1931	1.2856	1.2265	1.17
45	0.3762	0.0076	0.3421	0.1249	0.3119	0.1575	0.11
55	-1.4192	-0.0061	-1.4383	-0.0090	-1.4322	-1.0009	0.00

TABLE 4.7.2

MY AT SEVERAL POINTS AT 4X4 SUB-DIVISION , EX-7

POINTS	RE-1		RE-2		RE-3		HELLAN
	METHOD (1)	METHOD (2)	METHOD (1)	METHOD (2)	METHOD (1)	METHOD (2)	
51	0.1160	0.00	0.0694	0.00	0.0558	0.00	0.0
52	-0.9955	-0.6386	-1.0451	-1.0143	-1.0483	-1.1208	-1.13
53	-3.0015	-1.8039	-3.0036	-2.7696	-3.0023	-3.0615	-3.17
54	-4.4711	-2.7178	-4.4444	-4.0800	-4.4421	-4.4968	-4.64
55	-4.9874	-3.0504	-4.9522	-4.5459	-4.9496	-5.0047	-5.16
44	-1.1810	-1.1710	-1.1900	-1.2592	-1.1899	-1.1203	-1.32
35	0.4441	0.0849	0.4231	0.3487	0.4222	0.4344	0.35
25	0.7249	0.4248	0.7079	0.6297	0.7069	0.6965	0.68
15	0.00	0.3782	0.00	0.0431	0.00	-0.0545	0.00

TABLE 4.8.1

DEFLECTIONS AT SEVERAL POINTS IN A RHOMBIC CANTILEVER PLATE						
POINTS	1	2	3	4	5	6
TE	0.21155	0.14867	0.09910	0.11280	0.07195	0.04129
EXP.(22)	0.297	0.204	0.121	0.129	0.056	0.022

TABLE 4.9.1

CONVERGENCE OF CENTRAL DEFLECTION IN EX-2 TO EX-5

MESH	RESULTS FOR FUNCTION TE			
	EX-2	EX-3	EX-4	EX-5
1X1	1.3130	5.2520	0.2758	1.1032
2X2	3.1156	9.2843	0.8968	3.7269
3X3	3.5624	10.3071	1.0721	4.5691
4X4	3.7243	10.6983	1.1367	4.9105
5X5	3.8014	10.8924	1.1667	5.0815
EXACT	4.0624	11.6	1.2653	5.6

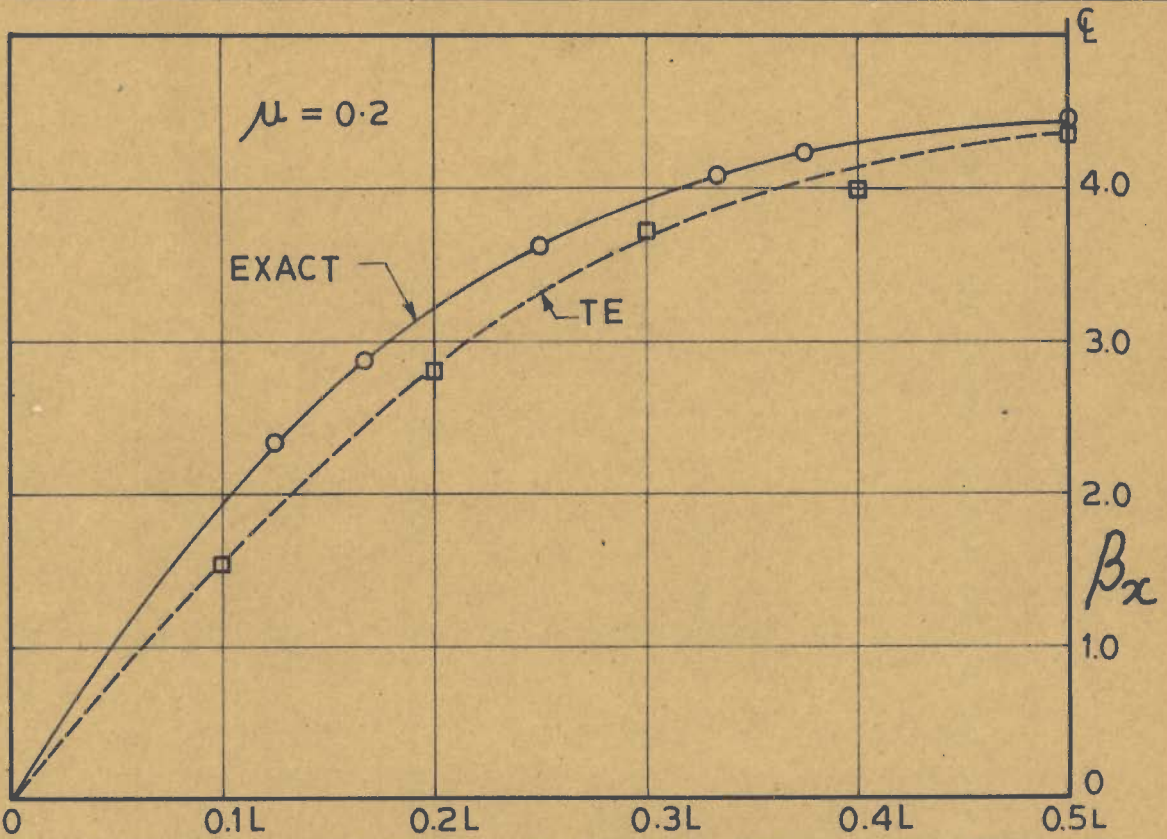


FIG. 4.10 M_x ALONG ξ ($y=0$) AT 5x5, EX-2

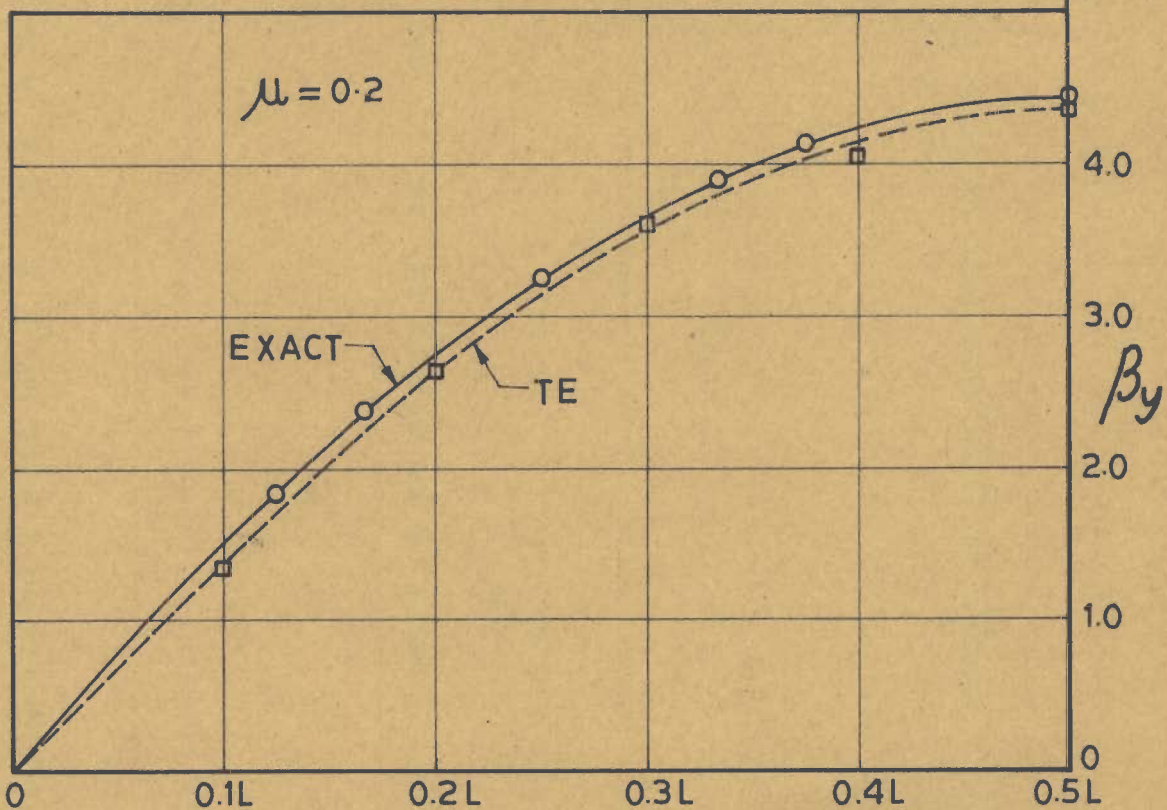


FIG. 4.11 M_y ALONG ξ ($y=0$) AT 5x5, EX-2

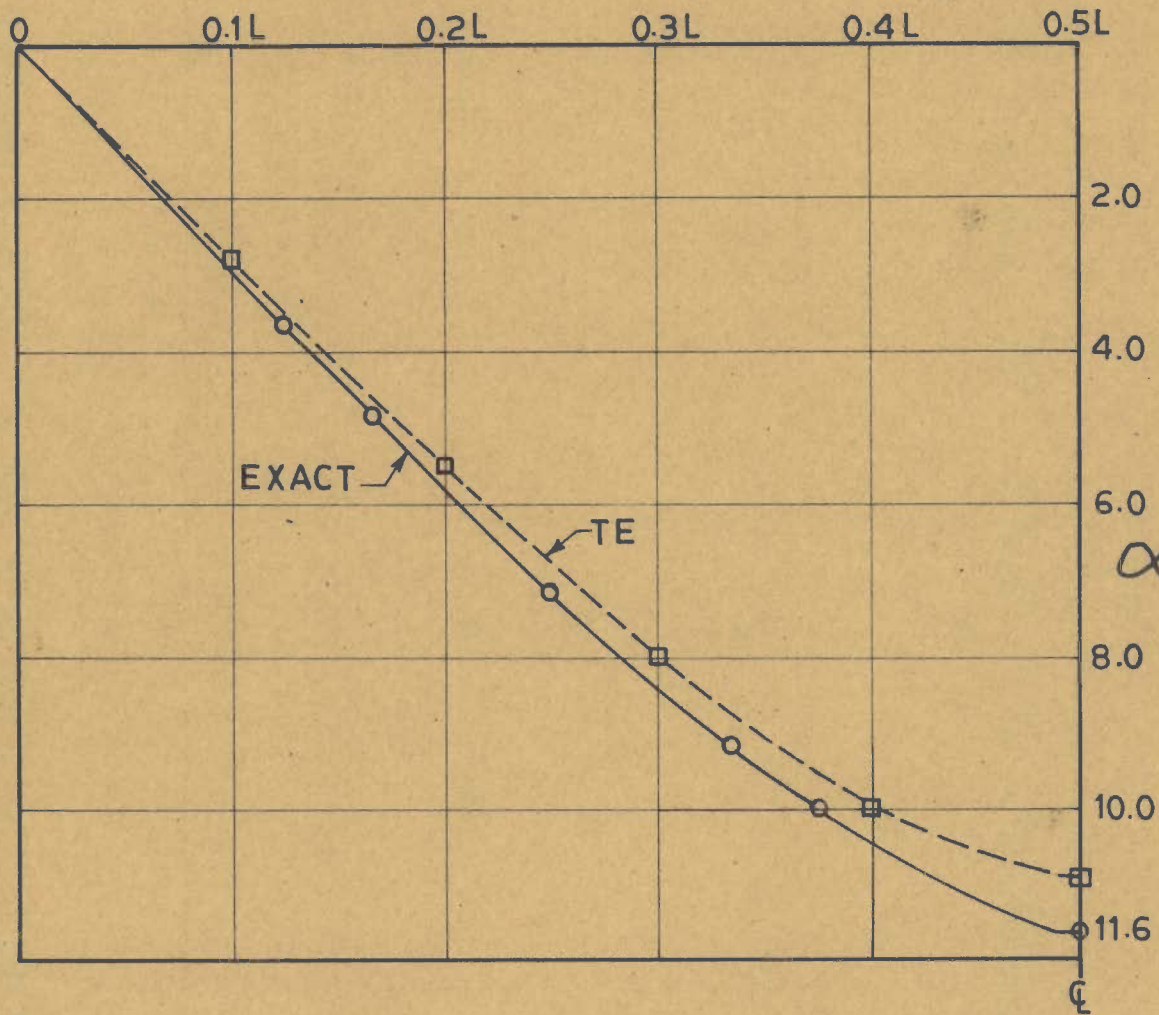


FIG. 4.12 DEFLECTION ALONG ξ ($y=0$) AT 5x5, EX-3

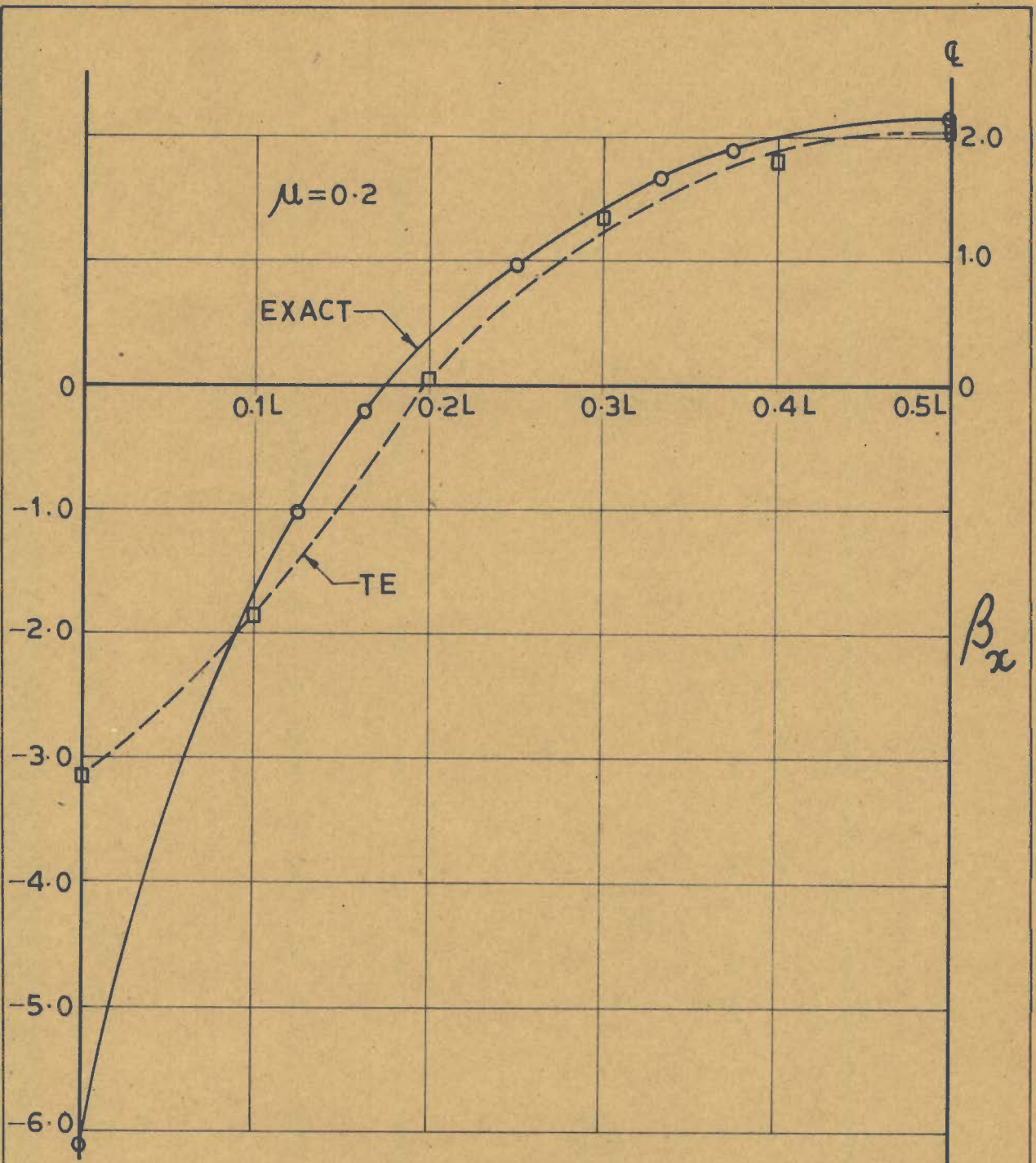


FIG. 4.13 M_x ALONG ζ ($Y=0$) AT 5×5 , EX-4

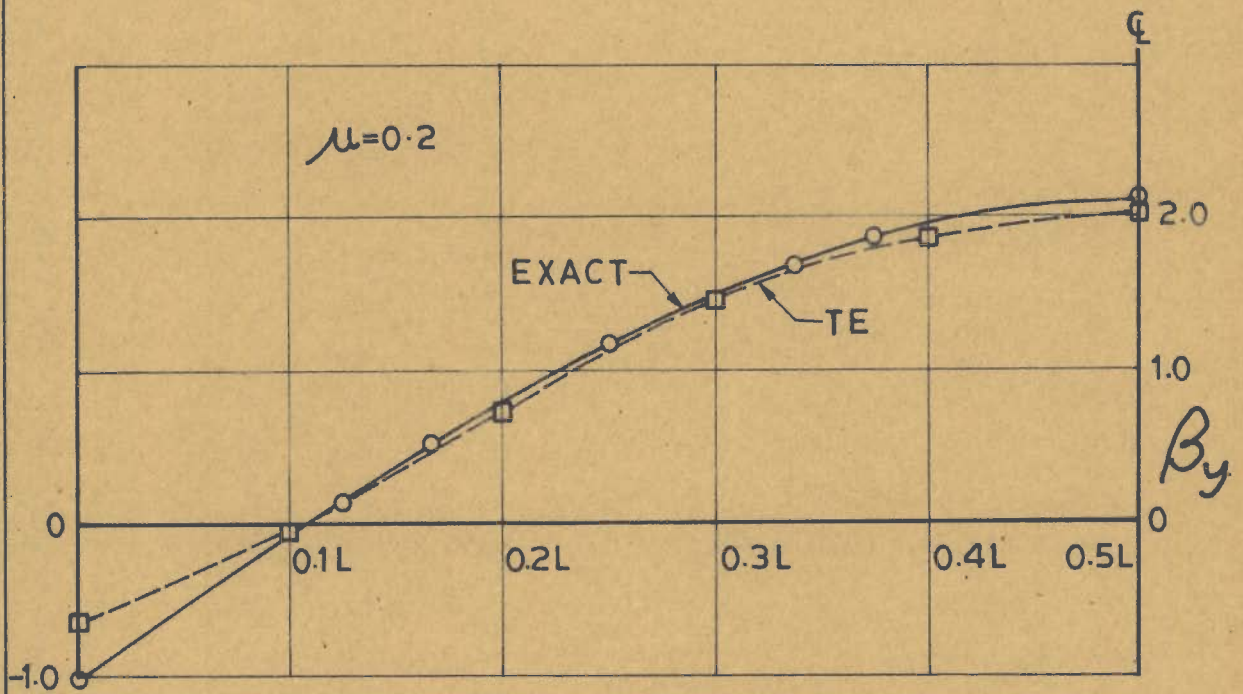


FIG. 4.14 M_y ALONG ξ ($y=0$) AT 5x5, EX-4

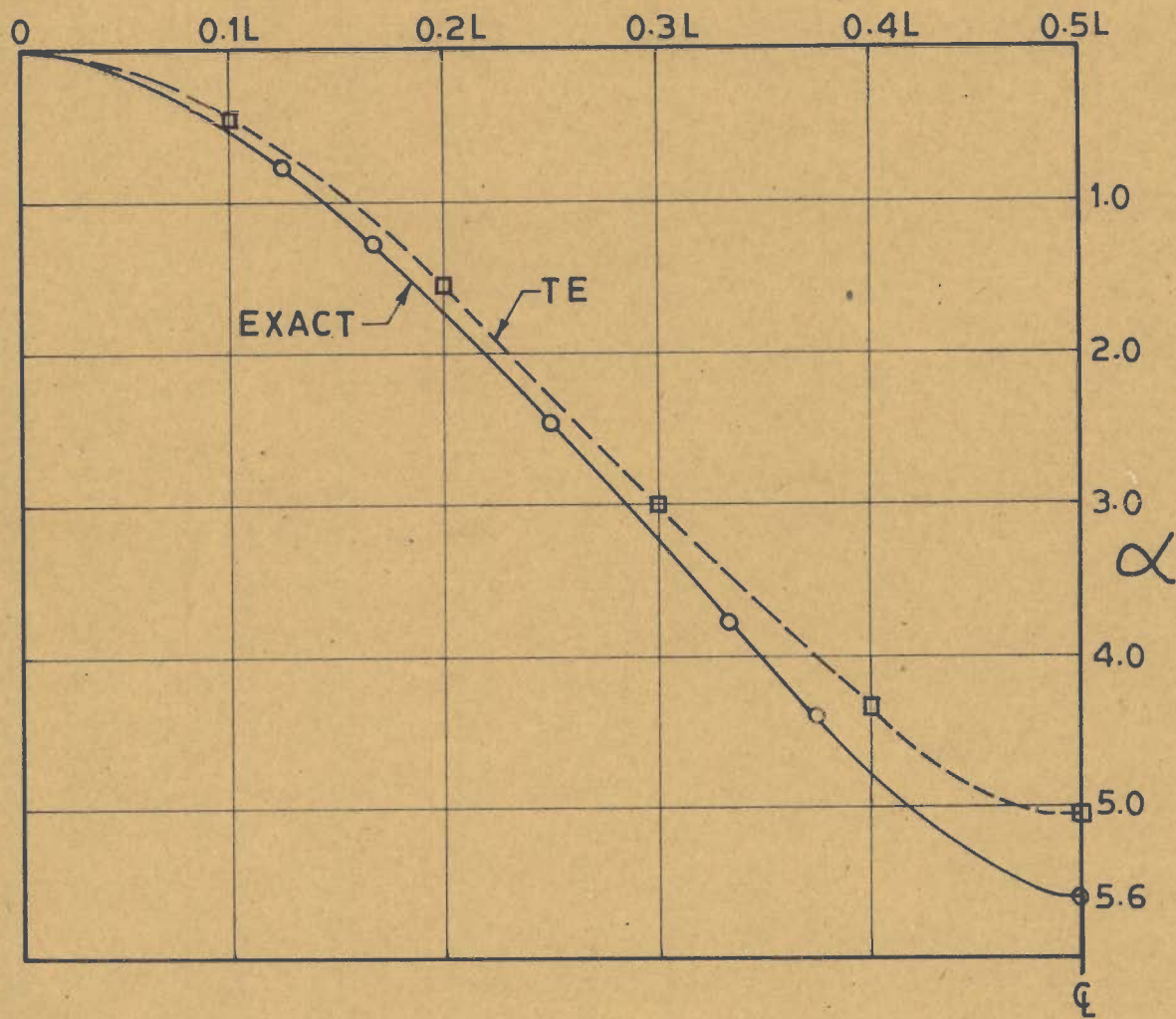


FIG. 4.15 DEFLECTION ALONG ξ ($y=0$) AT 5x5, EX-5

4.6 DISCUSSION ON RESULTS

General observations

A study of the tables brings out certain interesting features of the analysis.

- (i) All the new displacement functions investigated show convergence towards the true answers. The convergence is monotonic in all the cases. This, however, is to be expected because all the displacement functions considered are of the conforming type.
- (ii) The convergence is fast when rectangular element functions RE-1, RE-2 and RE-3 are used and slow when function TE, for the triangular elements, is used. In triangular elements the normal slopes have been forced to vary linearly along the boundaries. This artifice did help in developing the conforming function TE, but because of it the elements have become stiff. Absence of such restraint in the displacement functions RE-1, RE-2 and RE-3 for rectangular elements have made these elements relatively more flexible and this makes for faster convergence. Besides, these elements possess greater degrees of freedom.

- (iii) The results of the analysis by the functions RE-1, RE-2 and RE-3 are almost the same particularly for deflections, for the finest sub-division used; although for coarser sub-divisions the results given by the functions do not agree so very closely. The function RE-3 gives the best results.
- (iv) Function TE shows very reasonable accuracy for the deflections. Still further improvement is expected by using finer sub-divisions.

Detailed Discussion of Examples

(i) Deflections

Example - 1 has been analysed by using rectangular element functions RE-1, RE-2 and RE-3. All the three functions give same results upto the 5th place of decimals and the accuracy is practically 100% compared with the exact solution even when a very coarse 2 x 2 sub-division is used.

Convergence has been studied by observing the variation of the central deflection in examples 2 to 5. In example - 2, the nodal forces have been calculated by two methods when the functions RE-2 and RE-3 have been used; first, considering the tributary areas and secondly, using the method of virtual work. It is observed that the distributed load is overestimated when the equivalent nodal forces are calculated from

the principle of virtual displacements. On the other hand, the load is underestimated in the first approach. This is, of course, obvious as the loads assigned to the nodes which lie on boundaries are directly transmitted to the supports. Thus, in example - 2, the functions RE-2 and RE-3 overestimate the central deflection for the equivalent nodal forces and underestimate for the loads calculated from the tributary areas. However, the discrepancy gets reduced with finer sub-divisions and with a 4 x 4 grid, the maximum error in the central deflection is about 3 % when the nodal forces are calculated by the first approach for the function RE-2. For the same type of nodal forces, RE-3 gives result which is 97.09 % of the exact answer. With successive increase in the number of elements, the results converge towards the exact answer. This indicates that the errors in estimating the nodal forces decrease, as one may expect, for both the methods by increasing the fineness of the sub-division and at some stage both types of nodal forces will give practically the same results. Function TE gives very reasonable accuracy for central deflection. For 5 x 5 sub-division the error is about 6.42 %.

Better accuracy in central deflection is obtained in example - 3 by all the functions for rectangular elements. Maximum error for the 4 x 4 sub-division is given by RE-1 which is 2.38 %.

Errors for RE-2 and RE-3 are less than 1 %. In this example TE also gives reasonable results. For the finest sub-division the error is 6.09 %.

RE-1, RE-2 and RE-3 again yield the best results in example - 4. Functions RE-2 and RE-3 give almost the exact value for the central deflection even for the 2 x 2 coarse sub-division. With 4 x 4 sub-division RE-3 shows practically 100% accuracy compared with the exact answer, while RE-1 and RE-2 results reach an accuracy of 97.81 % and 99.8 % respectively. At other points, RE-3 gives deflections which are indential with the exact values upto three places of decimals, for the finest (4 x 4) sub-division (Table 4.4.2). Results from RE-1 and RE-2 for these deflections are extremely satisfactory although they do not match the remarkable accuracy of RE-3. Results from TE are not so accurate. For 5 x 5 sub-division, the error in central deflection is 7.79 %.

In example - 5, the errors in the central deflection are negligible for RE-2 and RE-3 at 4 x 4 sub-division. RE-3 gives better results right from the beginning followed by RE-2 and RE-1 in that order. Function RE-2 and RE-3 give the same deflections upto the second place of decimals at several other points. These results very closely agree with the exact answers. As before, TE is less accurate.

In example - 4, RE-2 and RE-3 give deflections higher than the exact answer only for the 1 x 1 sub-division and the results for all the three functions are four times the values given by the same functions for the same 1 x 1 sub-division in example - 5. This is obvious because the nodal load applied at the centre in example - 4 is four times the load taken in example - 5. In both the examples double symmetry has been used. The nodal load for the concentrated load is 0.25 and for the distributed load it is 1.0, as the area of one square element is 4 unit sq.

Results of deflections at several points in the cantilever plate (Table 4.6.1) are extremely satisfactory for all the functions RE-1, RE-2 and RE-3 when compared with those given by Point-Matching and Finite Difference solutions (55)...

Deflections at several points in the rhombic cantilever plate computed by using triangular elements (TE) are presented in Table 4.8.1. The results for 4 x 6 sub-division analysis are very reasonable.

In examples 2 to 5 where the second quadrant of the plate (Figure 4.8) was analysed (by using the mesh systems shown for triangular elements in Figure 4.2), the results of the displacements showed extremely good symmetry properties at 5 x 5 sub-division.

(ii) Moments

Moments M_x and M_y have been studied in all the examples excepting the first and the last. The figures in the tables represent the mean values of the moments M_x and M_y at the nodes.

For the functions RE-1, RE-2 and RE-3, the maximum moments as well as the moments at several other points agree very satisfactorily with the results obtained by the exact and other approximate methods used for comparison and indicated in tables. Function TE does not give satisfactory accuracy with 5 x 5 sub-divisions. However, similar behaviour is observed in several other displacement functions proposed for triangular elements (22,39). Finer sub-divisions are necessary to obtain better results with these elements.

It is observed that the results of M_x and M_y calculated by the first method (from the element stiffness matrices) agree closely with those obtained by the second method (from the moment-curvature relations given by a displacement function). The above statement refers to the results obtained by using the functions RE-1, RE-2 and RE-3. The moments calculated by the first method are the concentrated moments at the nodes, which in some way represent the forces distributed along the element boundaries; whereas

the second method gives the moments at a point. It is observed in the tables that the moments calculated by the first method are generally a little higher than those obtained by the second method.

For triangular elements the moments were calculated by using the finite difference formulae. Therefore, these results once again demonstrate the accuracy of deflections.

CHAPTER FIVE

APPLICATION OF THE METHOD TO SHELL STRUCTURES

5.1 INTRODUCTION

Shells support applied loads by developing both bending and membrane (in-plane) forces. The latter contributes significantly to the overall strength of a shell structure. For several shapes, such as shells of revolution, the in-plane forces are predominant. In such shells, bending forces develop near the supports and penetrate into the body of the shell only to a short distance before they completely die down. A mathematical analysis of a shell problem is obtained by solving the governing differential equations and satisfying the boundary conditions. Because this process can become quite involved, several simplified methods of analysis have been proposed from time to time. A detailed discussion on the methods is beyond the scope of this study and interested reader may refer to a number of available books and publications on the subject (44-46).

5.2 ANALYSIS BY THE FINITE ELEMENT METHOD

In the finite element method, the shell structure is idealised as an assemblage of finite elements interconnected at a finite number of points (47-52). Obviously, curved elements are ideal

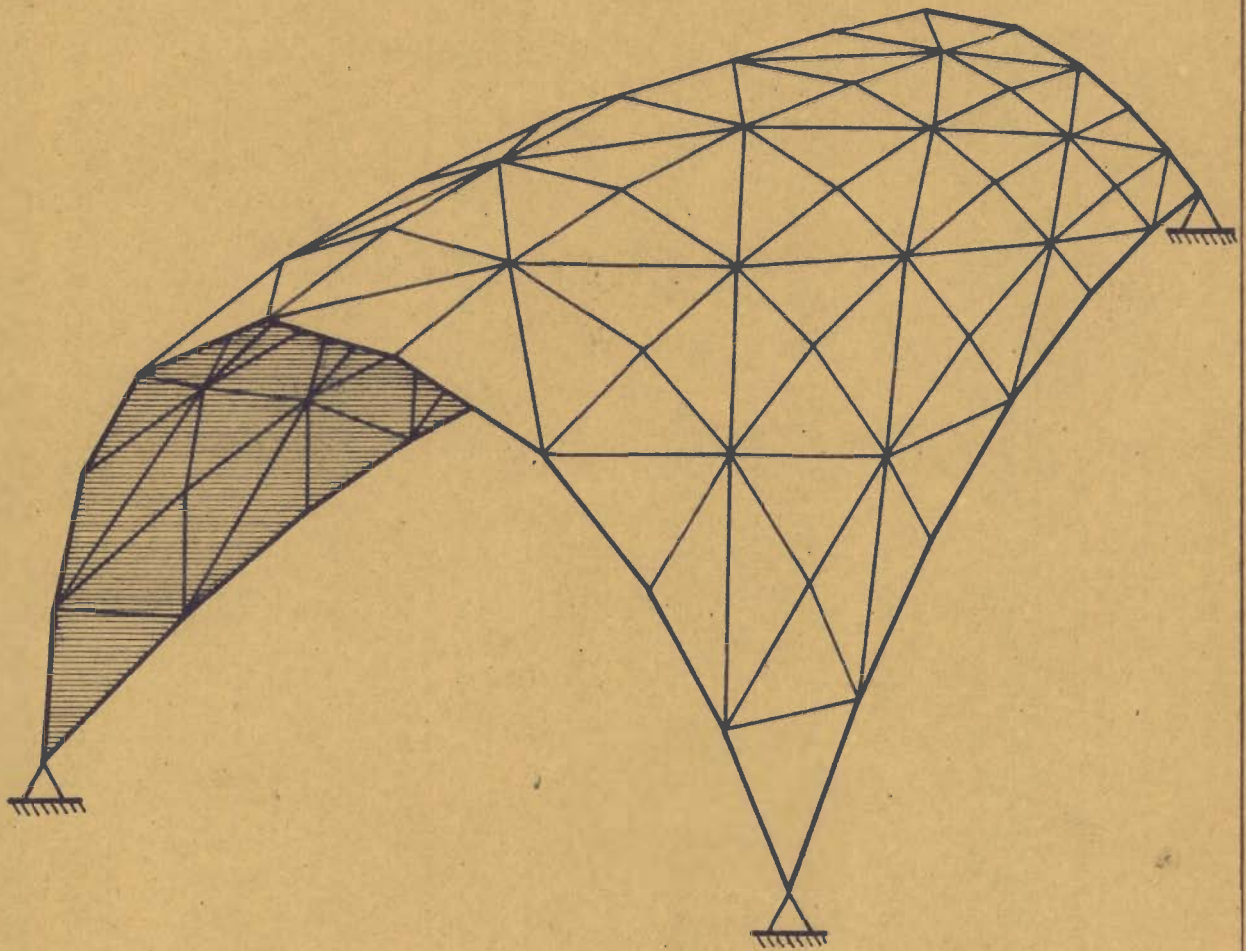


FIG. 5.1 A SHELL IDEALISED BY FLAT ELEMENTS.

for representing a shell surface, but their analysis is extremely difficult. Therefore, as a further simplification, flat elements are used. With the introduction of flat elements, a physical error creeps into the analysis. This error, however, gets reduced as more elements are employed in approximating a curved surface. Figure 5.1 shows a shell idealised by means of flat elements. It is obvious that triangular elements are ideal for approximating a shell of arbitrary shape. Rectangular elements have been employed for cylindrical shells. This is possible because the surface is developable.

The elements chosen to represent a shell should have both membrane and bending characteristics. It is assumed that the bending and membrane actions do not interact with each other, i.e., they are independent actions. Thus the total stiffness matrix of a element is obtained by summing up its bending and membrane stiffness matrices which are formed separately.

If the bending stiffness is given by,

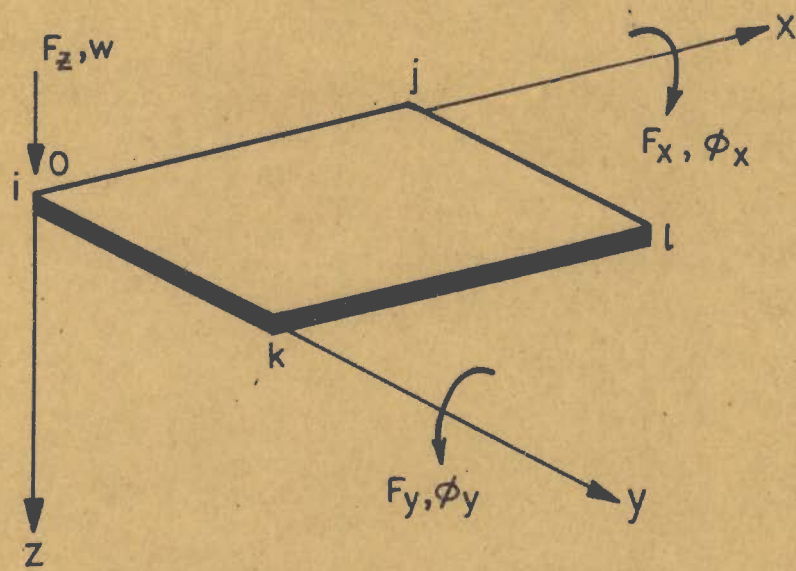
$$F^b = k^b u^b \quad (5.1)$$

and membrane stiffness by

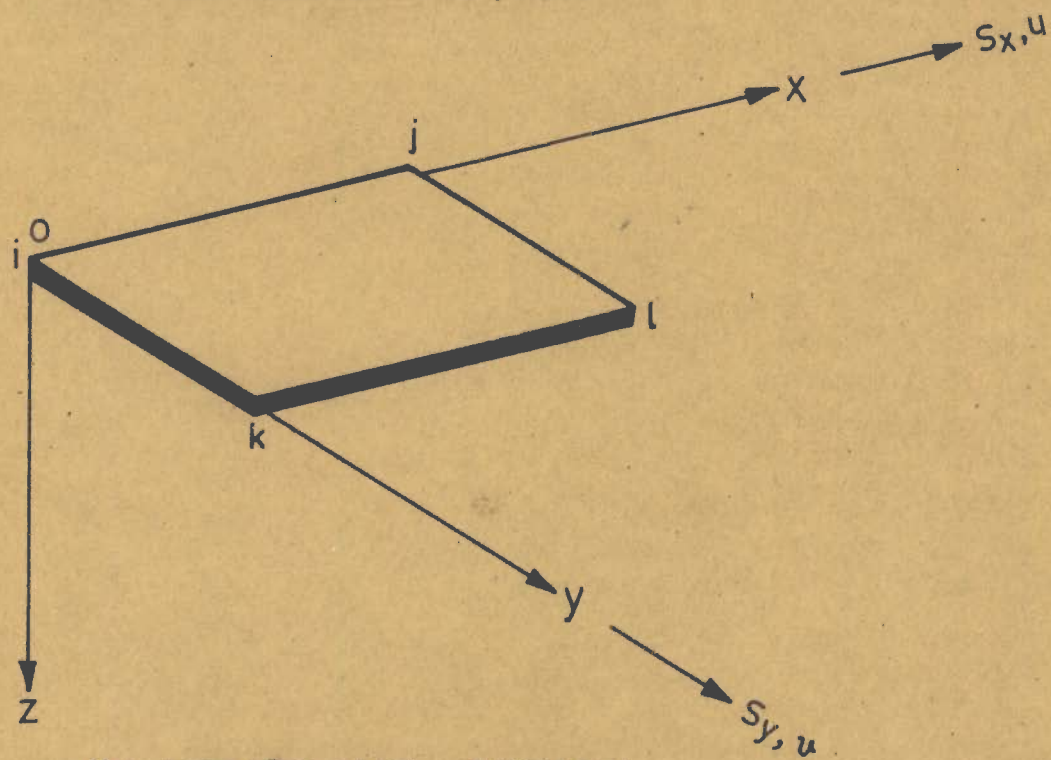
$$F^m = k^m u^m \quad (5.2)$$

the total stiffness matrix of the element is obtained as

$$\begin{Bmatrix} F^b \\ F^m \end{Bmatrix} = \begin{bmatrix} k^b & \\ & k^m \end{bmatrix} \begin{Bmatrix} u^b \\ u^m \end{Bmatrix} \quad (5.3)$$



(a) BENDING ACTION



(b) MEMBRANE ACTION

FIG. 5.2 FORCES AND DISPLACEMENTS IN AN ELEMENT USED IN SHELL ANALYSIS.

The superscripts b and m refer to bending and membrane actions respectively.

Of the two actions, the bending part is already discussed in previous chapters. For the membrane action, the derivation of the element stiffness matrix follows the same steps outlined in section 2.6, by selecting suitable displacement functions. The only difference is that the deformations now occur in the plane of the flat elements. Also, the stress-strain relations are now different. However, the convergence requirements remain the same as stated in section 2.3. The problem of selecting a displacement function for membrane action is much simpler. A function is easily obtained by prescribing a linear variation of the nodal deformations. Moreover, such an assumption leads to a conforming type of displacement function. Thus, for example, the displacement u along x -axis, for a rectangular element may be taken as

$$u = A_1 + A_2x + A_3y + A_4xy \quad (5.4)$$

A similar expression is taken for the displacement v along the y -axis. For other shapes such as triangles and quadrilateral elements, functions which provide linear variation of edge displacements are available (39).

When a conforming type of displacement function is used, the displacements are continuous along the boundaries of the elements. The continuity

of displacements is preserved when all the elements lie in a single plane; generally it will be violated if the elements are oriented in different planes. Thus for shell analysis simple non-conforming functions are used. For an arbitrary configuration, the elements of the idealised system will be in different planes. The stiffness matrix of the entire assemblage is obtained in the usual manner, using appropriate co-ordinate transformation matrices. Number of equations for an average analysis will now be very large because of the greater number of degrees of freedom prescribed for a shell element. Therefore, in order to obtain a fairly good approximation, a fast computer with large memory space is essential.

CHAPTER SIX

CONCLUSIONS

Conclusions derived from the present study may be summarised as follows:

- (1) All new functions proposed in this study converge towards the exact answers. Convergence is monotonic with successive refinements in the sub-division analysis.
- (2) The method developed for deriving the displacement functions for rectangular elements proves that many more suitable conforming type of displacement functions can be easily found. In fact, the number of such functions is practically unlimited and all of them satisfy the convergence criteria.
- (3) Trigonometric functions can be suitably used along with polynomial terms to derive displacement functions for rectangular elements as shown in the method developed for these elements.
- (4) The displacement function using polynomial functions proposed for triangular elements has very satisfactory accuracy and can be used for plates of arbitrary shapes.
- (5) Convergence is rapid for the rectangular element displacement functions and little slow for the triangular element function.

- (6) The results for displacements are more accurate than for the stress resultants.
- (7) The comparative study of the performance of the three different compatible displacement functions proposed for rectangular elements shows that all of them have almost the same accuracy at 4 x 4 sub-division although they exhibit different degrees of accuracy for coarser sub-divisions. The function RE-3 gives the best results and it is recommended for the analysis of rectangular plates.
- (8) For all practical purposes, uniformly distributed loads can be represented by sets of concentrated loads calculated from the tributary areas.
- (9) Mean values of bending moments at the joints in an assemblage represent the actual values with extremely good accuracy.
- (10) Moments computed from the stiffness matrices of the rectangular elements may be employed in practical designs as they are generally a little higher than those obtained by using the moment curvature relations.

REFERENCES

1. Timoshenko, S.P. and Woinowsky-Kriger, S Theory of Plates and Shells, Second Edition International Students Edition, Mc Graw Hill Inc., New York, 1965
2. Kantorovich, L.V. and Krylov, V.I Approximate Methods of Higher Analysis, Translated by C.D. Benster, P. Noordhoff Ltd., Netherlands, 1964.
3. Allen, D.N. de G. and Windle, D.W. In Stress Analysis, ed. Zienkiewicz and Holister, Chapter 1, John Wiley, New York, 1965.
4. Hrennikoff, A. Solutions of Problems of Elasticity by the Framework Method, J. Appl. Mech., 8, A 169-A 175, 1941.
5. Parikh, K.S. Analysis of Shells using framework analogy, Ph. D dissertation, M.I.T., Boston, 1962.

6. Argyris, J.H. and Kelsey, S. Energy theorems and Structural Analysis, Butterworths Scientific Publications, London, 1960
(Reprinted from Aircraft Engineering, 1954-55).
7. Argyris, J.H. Recent Advances in Matrix Methods of Structural Analysis Pergamon Press, London, 1964.
8. Argyris, J.H. and Kelsey, S. Modern Fuselage Analysis and Elastic Aircraft, Butterworths, London, 1963.
9. Clough, R.W. The Finite Element Method in Plane Stress Analysis, Proc. Second Conf. on Electronic Computation, ASCE, 1960.
10. Clough, R.W. In Stress Analysis, ed. Zienkiewicz and Holister, Chapter 7, John Wiley, New York, 1965.
11. Clough, R.W. and Rashid, Y. Finite Element Analysis of Axi-symmetric Solids, J. ASCE, Engg. Mech. Div., Vol. 91, EM-1, 1965.
12. Melosh, R.J. Structural Analysis of Solids, J. ASCE, Struct. Div., Vol. 89, ST-4, 1963

13. Swako, F.
and Cope, R.J. Use of Finite Element Method for the analysis of Right Bridge Decks, Conf. on use of Digital Computer in Struct. Engg., University of Newcastle, England, July, 1966.
14. Dawe, D.J. A Finite Element Approach to Plate Vibration Problems, J. Mech. Engg. Sci., 7, 1965.
15. Zienkiewicz, O.C. The Finite Element Methods and its Application in Vibration Analysis, Symposium on Numerical Methods for Vibration Research, University of Southampton, Vol.3, July 1966.
16. Pestle, E.C.
and Lakie, F.A. Matrix Methods in Elastomechanics, Mc Graw Hill Inc., New York, 1963.
17. Livesley, R.K. Matrix Methods of Structural Analysis, Pergamon Press, London, 1959.
18. Fraeijs de Veubeke, B. In Stress Analysis ed Zienkiewicz and Holister Chapter 9, John Wiley, New York, 1965.

19. Gallagher, R.H. A Correlation Study of Methods of Matrix Structural Analysis, *AgarDograph* 69, 1962.
20. Turner, M.J.,
Clough, R.W.,
Martin, H.C.,
and Topp, L.J. Stiffness and Deflection Analysis of Complex Structures, *J. Aero. Sci.*, Vol.23, 1956.
21. Irons, B.M.
and Draper, K. On the Inadequacy of Nodal Connections in a Stiffness Solution for a Plate in Bending, *J. AIAA*, 3, July 1965.
22. Clough, R.W.
and Tocher, J.L. Finite Element Stiffness Matrices for Analysis of Plate Bending.
(Through private communication).
23. Zienkiewicz, O.C.
and Cheung, Y.K. The Finite Element Method for Analysis of Elastic Isotropic and Orthotropic Slabs, *Proc. Inst. Civil Engrs. (London)*, 28, August 1964.
24. West, P.E. A Finite Element Solution to Skew Slab Problems, *Civil Engg. and Pub. Works Review*, Vol. 61, 718, May 1966.

25. Ramstad, H.
and Holland, I. The Finite Element Method
for Analysis of Skew Plates
in Bending by use of
Parallelogram Elements, Conf.
on use of Digital Computers
in Struct. Engg., University
of New-Castle, England,
July 1966.
26. Ramstad, H. Parallelogram Elements in
Bending Accuracy and
Convergence of Results, Report,
Div. of Struct. Mech., The
Technical University of Norway,
Trondheim, Norway, October 1967.
27. Melosh, R.J. A Stiffness Matrix for the
Analysis of Thin Plates in
Bending, J. Aero-Sci.,
January 1961.
28. Melosh, R.J. Basis for Derivation of
Matrices for the Direct
Stiffness Methods, J. AIAA,
1, July 1963.
29. Argyris, J.H. Matrix Displacement Method of
Plates and Shells, Ingenieur -
Archiv, XXXV Band, ZWEITES HEFT,
1966.

30. Papenfuss, S.W "Lateral Plate Bending by Stiffness Matrix Method with Application to a Marquee", M.S. Thesis, Department of Civil Engineering, University of Washington, Seattle, December 1959.
31. Butlin, G.A. and Lekie, F.A. A study of Finite Elements Applied to Plate Flexure, Symposium on Numerical Methods for Vibration Problems, The Inst. of Sound and Vibration Research, University of Southampton, Vol.3, July 1966.
32. Butlin, G.A. "On the Finite Element Technique in Plate Bending Analysis; A Derivation of Basic Stiffness Matrix", Internal Report, Engineering Department, Churchill College, Cambridge, England, 1965.
33. Hansteen, H. Finite Element Displacement Analysis of Plate Bending based on Rectangular Elements. Conf. on use of Digital Computers in Struct. Engg., University of New-Castle, England, July 1966.

34. Bogner, F.K.,
Fox, R.L., and
Sohmit, L.A. The Generation of Inter
Element, Computable, Stiff-
ness and Mass Matrices
by the use of Interpolation
Formulae, Proc. Conf. on
Matrix Methods in Struct.
Mech., Wright Patterson Air
Force Base, Ohio,
October 1965.
35. Adini, A. "Analysis of Shell Structures
by Finite Element Method",
Ph.D. Dissertation, Depart-
ment of Civil Engineering,
University of California,
Berkeley, 1961.
36. Tocher, J.L. "Analysis of Plate Bending
using Triangular Elements",
Ph.D. Dissertation, Depart-
ment of Civil Engineering,
University of California,
Berkeley, 1961.
37. Zienkiewicz, O.C.
and Cheung, Y.K. Plate and Shell Problems
Finite Element-Displacement
Approach. Conf. on use
Digital Computers in Struct.
Engg., University of New-Castle
England, July 1966.

38. ----- Discussion on Reference 23
cited above.
39. Zienkiewicz, O.C. The Finite Element Method
and Cheung, Y.K. in Structural and Continuum
Mechanics, Mc Graw Hill Inc.,
New York, 1967.
40. Beseley, G.P., Triangular Elements in
Cheung, Y.K., Bending - Conforming and
Irons, B.M. and Non-Conforming Solutions,
Zienkiewicz, O.C. Proc. Conf. Matrix Methods
in Struct. Mech., Wright
Patterson Air Force Base,
Ohio, October, 1965.
41. Sander, C. Bornes Superieures et
Inferieures dans l'analyse
Matricielle des Plaques
en Flexion-Torsion, Bull. Soc.
Royale des Sc. de Liege, 33,
1964.
42. Fraeijs de Veubeke, B. Bending and Stretching of
Plates, Proc. Conf. Matrix
Methods in Struct. Mech.
Wright Patterson Air Force
Base, Ohio, October 1965.

43. Henshell, R.D. and Warburton, G.B. Finite Element Technique Applied to the Vibration of Plate systems, Symposium on Numerical Methods for Vibration Problems, The Institute of Sound and Vibration Research, University of Southampton, Vol.3, July 1966.
44. Flugge, W. Stresses in Shells, Springer - Verlag Berlin, 1960.
45. Goldenveizer, A.L. Theory of Elastic Thin Shells, Translated by G. Herrmann, Pergamon Press, New York, 1961.
46. Ramaswamy, G.S. Design and Construction of Concrete Shell Roofs, Mc Graw Hill Inc., New York 1968.
47. Argyris, J.H. Matrix Displacement Analysis of Anisotropic Shells by Triangular Elements, J. Roy. Aero-Soc., 69, November 1965.

48. Clough, R.W.
and Tocher, J.L. Analysis of Thin Arch Dams
by the Finite Element Method,
Proc. International
Symposium on the Theory of
Arch Dams, Southampton
University, England, April
1964, (Pergamon Press)
49. Zienkiewicz, O.C.
and Cheung, Y.K. Finite Element Method of
Analysis of Arch Dams and
Comparison with Finite
Difference, Procedures. Proc.
International Symposium on
the Theory of Arch Dams,
Southampton University,
England, April 1964
(Pergamon Press)
50. Zienkiewicz, O.C.
and Cheung, Y.K. In Stress Analysis, ed
Zienkiewicz and Holister,
Chapter 8, John Wiley,
New York, 1965.
51. Grafton, P.E.
and Strome, D.R. Analysis of Axi-Symmetric
Shells by the Direct
Stiffness Method, J. AIAA,
1, 1963.

52. Lu, Z.A.,
Penzien, J
and Popov, E.P. Finite Element Solution for
Thin Shells of Revolution,
Institute of Engg. Research
Report SESM 63-3, University
of California, Berkeley,
September, 1963.
53. Irons, B.M.
and Barlow, J. Comment on Reference 28,
J. AIAA, 2, 1964.
54. Tocher, J.L.
and Kapur, K.K. Comment on Reference 28,
J. AIAA, 3, 1965.
55. Leissa, A.W., and
Niederfuhr, F.W. A Study of Cantilever Plate
subjected to a uniform load,
J. Aero Sci., Vol. 29, 1962.

APPENDIX - 1

GENERATION OF K MATRIX IN THE COMPUTER

The programming logic for generating K for regular mesh systems is illustrated in Figures A-1 and A-2 which are self-explanatory.

Stage I: Only individual element stiffness matrices k are involved. In all the sub-divisions reported earlier the elements used are of the same shape and size. Thus a sub-division analysis involves the use of only one k matrix.

Stage II: This is a summing-up operation in the horizontal direction. The operation is continued for n elements in the horizontal direction. Result is shown for 2 elements in Figure A.

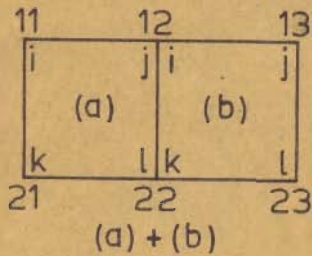
Stage III: This is summing-up in the vertical direction using the results of stage II. The operation is continued for m sets of n horizontal elements. Generation of the K matrix completes with this operation.

The main program thus generates the stiffness matrix for $n \times m$ sub-divisions.

i	j
(a)	
k	l

$$\begin{Bmatrix} F_i \\ F_j \\ F_k \\ F_l \end{Bmatrix} = \begin{bmatrix} k_{ii} & k_{ij} & k_{ik} & k_{il} \\ k_{ji} & k_{jj} & k_{jk} & k_{jl} \\ k_{ki} & k_{kj} & k_{kk} & k_{kl} \\ k_{li} & k_{lj} & k_{lk} & k_{ll} \end{bmatrix} \begin{Bmatrix} u_i \\ u_j \\ u_k \\ u_l \end{Bmatrix}$$

STAGE I, ELEMENT [k] MATRIX.

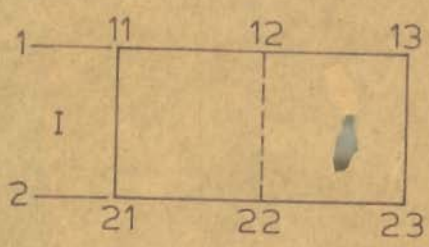


R_{11}	(a) k_{ii}	Symmetrical				r_{11}
R_{12}	(a) k_{ji}					(a) (b) $k_{jj} + k_{ii}$
R_{13}	0	(b) k_{ji}	(b) k_{jj}	r_{13}		
R_{21}	(a) k_{ki}	(a) k_{kj}	0	(a) k_{kk}	r_{21}	
R_{22}	(a) k_{li}	(a) (b) $k_{lj} + k_{ki}$	(b) k_{kj}	(a) k_{lk}	(a) (b) $k_{ll} + k_{kk}$	r_{22}
R_{23}	0	(b) k_{ii}	(b) k_{ij}	(b) k_{ik}	(b) k_{ll}	r_{23}

[K] matrix for (a)+(b)

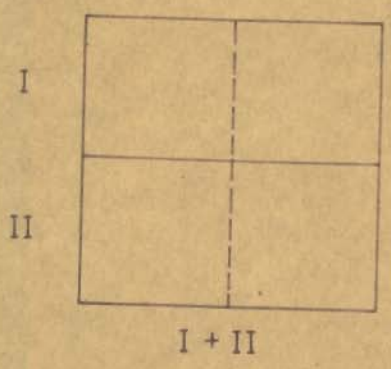
STAGE -II, BUILDING UP IN HORIZONTAL DIRECTION

FIG. A1 GENERATION OF [K]



$$\begin{Bmatrix} R_1 \\ R_2 \end{Bmatrix} = \begin{bmatrix} k_{11} & k_{12} \\ k_{21} & k_{22} \end{bmatrix} \begin{Bmatrix} \Delta_1 \\ \Delta_2 \end{Bmatrix}$$

RESULTS OF STAGE II



I k_{11}	II k_{12}	
I k_{21}	I II $k_{22} + k_{11}$	II k_{12}
	I k_{21}	II k_{22}

[K] FOR I+II

STAGE III BUILDING UP IN VERTICAL DIRECTION



FIG. A2 GENERATION OF [K]